Modeling and Simulation of a Photovoltaic Assisted Single-Slope Solar Still

by

Hashim Migaybil

B.Sc., King Abdul-Aziz University, 2011

A THESIS SUBMITTED IN PARTIAL FULFILLMENT OF THE REQUIREMENTS FOR THE DEGREE OF

MASTER OF APPLIED SCIENCE

in
The Faculty of Graduate and Postdoctoral Studies

(Chemical and Biological Engineering)

THE UNIVERSITY OF BRITISH COLUMBIA

(Vancouver)

December 2020

The following individuals certify that they have read, and recommend to the Faculty of Graduate and Postdoctoral Studies for acceptance, the thesis entitled:

Modeling and Simulation of a Photovoltaic Assisted Single-Slope Solar Still

submitted by Hashim Migaybil in partial fulfillment of the requirements for

the degree of Master of Applied Science

in Chemical and Biological Engineering

Examining Committee:

Bhushan Gopaluni, Chemical and Biological Engineering

Supervisor

Ryozo Nagamune, Mechanical Engineering

Supervisory Committee Member

Yankai Cao, Chemical and Biological Engineering

Supervisory Committee Member

Abstract

Water is crucial and very important to our lives needs such as human needs, artificial needs and agriculture's needs. Seawater desalination process in industrial applications plays a primarily role in meeting the demands for fresh water. The energy of desalination process can be obtained from fossil fuel or from a renewable source of energies such as solar, wind and geothermal energy. Nowadays, Solar energy can be utilized in water production by evaporating saline water in order to produce fresh water. Solar still desalination is considered as one of the emerging processes among other different methods that employs renewable source of energy. This technology has multiple advantages comprising simplicity, ease of maintenance, low cost and low environmental impact. Solar still is a renowned technology for water desalination, impurities and contaminants removal and high-quality water production. Scientists have to illustrate the applications of the solar desalination system based on energy, exergy, thermo dynamic properties and cost analysis. The design analysis should consider the technique and types of the desalination system. It is necessary to model a flexible visualized computer program in order to design/or perform a reliable analysis for a widespread range of solar desalination processes with different structures. The proposed topic claims for modeling and simulation of an integrated solar cell heating element (photovoltaic cell) system accompanied with a single slope solar still for performance improvement, process optimization and efficiency enhancement. The main objective of this study is to develop a software using SIMULINK in order to design and simulate solar desalination systems single slope solar still with a photovoltaic Cell. The study results reveal that solar desalination technique without a photovoltaic cell is astonishing with lower efficiency and performance, while comparing with solar desalination technique assisted with a photovoltaic cell (heating coil) that improve the efficiency by 45% and enhance the performance of the entire system.

Lay Summary

Water is a very important and essential component in our lives that is necessary for covering our agricultural, industrial, and leisure needs. Seawater desalination in industrial applications plays a primarily role in meeting the demands for freshwater. However, the required energy in such a desalination process is either obtained from fossil fuel and/or from a renewable energy source including solar, wind, and geothermal energy. Solar still desalination is considered as one of the potential emerging technologies that employs renewable source of energy. Herein, we study the potential of a design modification to further utilize solar energy in accelerating saline water evaporation via integrating a photovoltaic cell in a single-slope solar still for freshwater production. The key objective is to develop a software using SIMULINK in order to design and simulate an integrated solar cell heating element (photovoltaic cell) system coupled with a single-slope solar still for performance enhancement and increased freshwater productivity. The results reveal that solar desalination systems without a photovoltaic cell and heating coil had much lower efficiency, as compared to solar stills assisted with a photovoltaic cell (connected to a heating coil) that improve the efficiency more than 45% at peak time and improve the performance of the entire system.

Preface

All the work narrated in this thesis was performed in the Department of Chemical and Biological Engineering at the University of British Colombia, Vancouver campus. I, Hashim Migaybil, was the investigator of this research and responsible for selecting the proposed topic, designing the entire model system with coding, simulating and running the designed system, obtaining/discussing the results and figures, and stating the major findings as well as comparing the results of solar still performance, thermodynamic properties and efficiency. Prof. Bhushan Gopaluni supervised the research, providing instructions, guidance, approving the topic and work, and editing this thesis.

Table of Contents

List of Tables

List of Figures

List of Abbreviations

MOEP	Ministry of Economics and Planing
GCC	Gulf Cooperation Council
GUI	Graphical User Interface
KSA	Kingdom of Saudi Arabia
RO	Reverse Osmosis
GHG	Greenhouse Gases
MED	Multi Effect Distillation
MSF	Multi Stage Flash
SWCC	Saline Water Conversion Corporation
RE	Renewable Resources
SWRO	Seawater Reverse Osmosis
PV	Photovoltaic
Cp	Heat capacity at constant pressure
DC	Direct Current
NOM	Number of Modules
NOB	Number of Batteries
SSSBS	Single slope single basin
DSSBSMR	Double slope single basin with mirrors
DSSBS	Double slope single basin without outer mirrors
SSDBS	Single slope double basin
SSTBS	Single slope triple basin solar stills

Nomenclature

Q_{ev}	Evaporation Energy, kW
Q_{rw-g}	Heat transfer between brine water and glass cover by radiation, kW.
Q_{rg-amb}	Heat transfer between glass cover and the ambient, kW
Q_{load}	Thermal Load inside the still, kW
Q_r	Radiative heat transfer energy, kW
h_c	Convective heat transfer coefficient between water and cover, $W/m^2\ ^oC$
h_{evp}	Evaporative convective heat transfer coefficient between water and cover, $W/m^2\ ^oC$
Exev	Evaporation exergy, kW
I_{total}	Total exergy destruction rate, kW
dH	Water level inside the tanks, m
V	Open circuit voltage, V
A	Short circuit currents, A
Vm	Maximum voltage, V
Im	Maximum current, A
Effst	Solar still efficiency, %
FOB	Full overboard price, $/watt/module
PVCt	Total photovoltaic cost, $
A_{st}	Solar still area, m^2
At	Total Photovoltaic system area, m^2
A_g	Glass cover area, m^2
Ac	Cell area, m^2
Am	Module area, m^2

a	Cover tilted angle degree, ^{o}
t	Insulation thickness, cm
d	Brine depth, cm
Pstd	Solar still productivity per unit area, kg/m^2.day
Pdye	Solar still productivity with black dye per unit area, kg/m^2.day
Tw	Basin water temperature, ^{o}C
Tg	Glass Cover Temperature, ^{o}C
BS	Battery storage, Wh
I(t)	Solar flux on an inclined collector, W/m^2

List of Subscripts

c	Convective
e	Evaporative
r	Radiative
b-w	Basin to water
w-g	Water to glass
ft	Feed tank
Ht	Feed tank total height, m
amb	Ambient

Greeks

$\propto$	Absorptivity
τ	Transmissivity
ε	Emissivity
σ	Stephen-Boltzmann constant ($W/m^2 K^4$)
η	Efficiency, %

Acknowledgments

In the name of Allah, the most merciful, decent and the most graceful, I start this thesis. Recognitions, and glorification to you my lord for your guidance, generous and support in every step of the way.

I would like to share this accomplishment and success with the people who helped me a lot to make it possible. First, I would like to express my sincere gratitude and appreciation to Prof. Bhushan Gopaluni who gave me the opportunity to work in his research group. Also, for his remarkable and endless support and guidance throughout this project, and for sharing his knowledge and experience with me. Prof. Gopaluni faithfully expanded my knowledge in the area of Modeling, Simulation and Optimization in chemical engineering applications.

Also, I would like to thank and appreciate the Royal Saudi Government including the Ministry of Education for the scholarship that they have granted me. They fulfilled my desire to pursue my graduate studies at UBC and to adapt to a new environment. I would like to recognize the financial support of my sponsor King Abdulaziz University as well. In addition, I would like to thank Dr. Hisham Maddah for sharing his knowledge, skills and expertise with me in the field of solar energy, and for his guidance and his time throughout my research.

Finally, I also would like to pay very special gratefulness to my loving and kind parents for their continuous support, and for being on my side through their heart-felt words at the times of difficulty despite being thousands of miles away from me. It is their encouragement that made challenges and uncertainty look easygoing. I wish this achievement would make them happy and proud. Without the help of the aforementioned people and parties, this work would have not been possible.

Chapter 1: Introduction & Literature Review

1.1 Water Shortage Problem:

Water is the most essential fluid on the Earth and the main source of life, since it is required for all biological process. It is considered as the main component of Earth's hydrosphere and the fluid of all living organisms. Water is vital to our lives needs such as human needs, artificial needs and agriculture's needs. As shown in figure 1, water forms enormous area of the Earth, since it covers around 71% of Earth's surface area, mostly in Oceans and seas. Only small percentages (1.7%) of water occurs as a groundwater. The ice caps of Antarctica and Greenland forms 1.7%; whereas, in the air it can be formed as vapor or clouds. Very small portions around 0.001% can be formed as precipitation. Only 2.5% of this water of freshwater. In addition to that, just 0.3 % of this freshwater can be considered fit for human consumption [2].

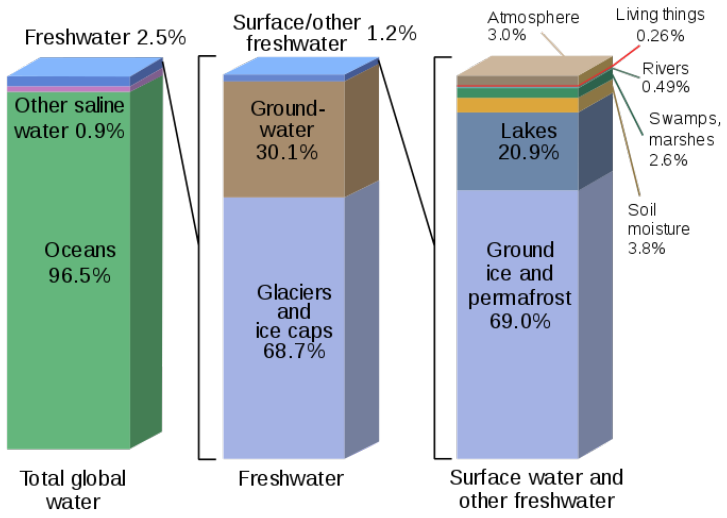

Figure 1: A graphical distribution of the locations of water on Earth, adopted from [3]

Only 3% of the Earth's water is fresh water. Most of it is in icecaps and glaciers (69%) and groundwater (30%), while all lakes, rivers and swamps combined only account for a small fraction (0.3%) of the Earth's total freshwater reserves [3].

Water has a steadying effect on earthly and interplanetary processes, since it has the physiochemical characteristics and profuse nature. Nowadays, survival without water is impossible. Water scarcity is a major global challenge. Yet, globally, 2.2 billion people lack access to safe fresh and drinking water. Also, 4.2 billion people lack safely managed sanitation services. Moreover, there are three billion people who do not have sufficient handwashing facilities.

Water stress applies to conditions wherever there is no sufficient water for all practices such as domestic, industrial or agricultural uses. It has been proposed that when renewable freshwater availability annual per capita is less than 1,700 cubic meters, subject countries commence to experience regular water stress. In contrast, water scarcity starts to hinder economic development and human health and well-being when the availability of fresh water is less than 1,000 cubic meters (refer to figure 2) [4].

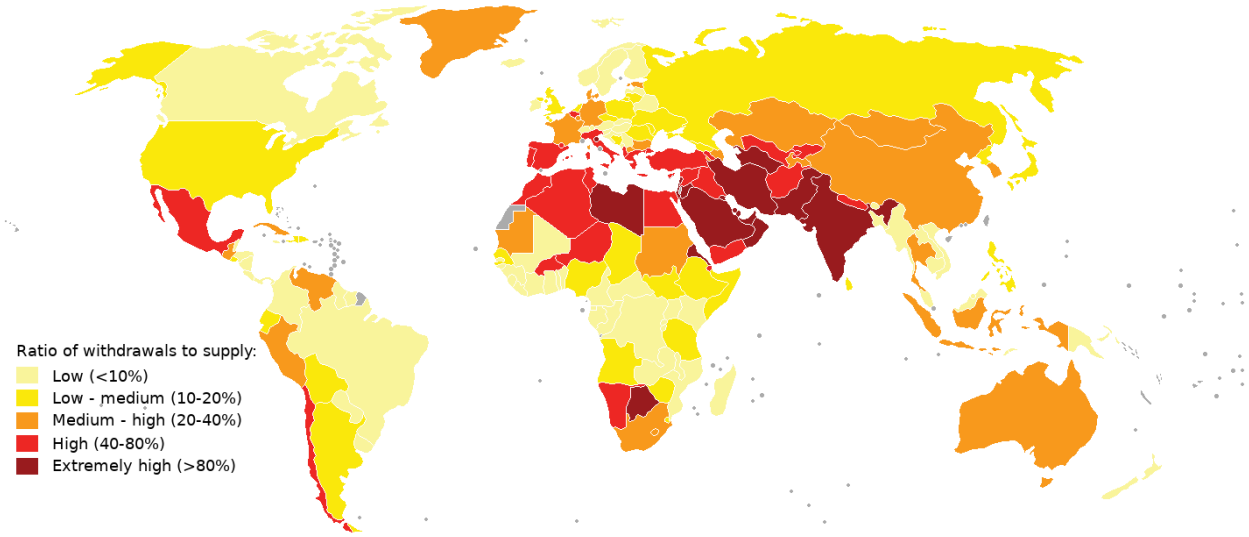

Figure 2: Global Water Stress Map [1]

Over the last decades, the approach to safe fresh drinking water has improved gradually and significantly in almost every part of the world. However, some experts have estimated that by 2025 more than half of the world population will be facing water-based vulnerability, a situation which has been called a water crisis by the United Nations.

Desalination Process provides such an alternative resource, providing water for industrial, irrigational and municipal use. Solar desalination technology is one of the trusted methods to produce fresh water in a sustainable way [5].

1.2 Water Scarcity in Saudi Arabia:

Saudi Arabia is an arid country which lacking permeant water recourses such as rivers and water bodies. It is considered as one of the driest countries in the world. The only water recourses that supply water needs in Saudi Arabia are desalinated water, groundwater and surface water. The reason that the Kingdom suffers from a scarcity of water with limited water recourses, which cause a serious problem, is that its climate is desert.

It is worth to mention that, the freshwater demand over the past twenty years has increased significantly. Also, the average evolution rate in Saudi Arabia is 3% per year with a population growth from 25 million in 2007 to around 33 million in 2018 [6].

As a result, wastewater treatment, water conservation, and water desalination process have to be taking into account especially for desert countries like Saudi Arabia and Gulf countries.

Additionally, climate change has an undesirable effect on water resources and soil moisture in Saudi Arabia which is intensely connected with the increase of temperature (Global Warming). There are many pros in reusing wastewater and treating desalinated water such as minimizing brine groundwater demand in addition to diminishing the environmental pollution [7]. Table 1 illustrates major dams in Saudi Arabia. These dams can be classified based on purposes into Ground water

recharge, Water supply, Irrigation and Flood control. MEWA specified that, the total numbers of Ground water recharge, Water supply, Irrigation and Flood control dams are 344, 63, 2 and 99 respectively.

Table 1: Major dams in Saudi Arabia [8]

Name of dam	Completed	Dam height (m)	Reservoir capacity (million m^3)	purpose
King Fahd	1998	103	325	Ground water recharge
Wadi Abha	1974	33	213	Water supply
Wadi Jazan	1970	35	51	Irrigation
Wadi najran	1980	73	86	Flood control
Qaa hathutha-Madinah	2001	7	40	Ground water recharge
Wadi Alaquiqu-Baha	1988	31	22.5	Water supply
Tarba- Tayif	1984	15	21.8	Water supply
Arda- Tayif	1984	24	21	Water supply
Tarabah- Tayif	1981	21	20	unknown
Fareah- Madinah	1982	13.5	20	Flood control
Wadi Alfaraah-Madinah	1982	13.5	20	Flood control

The quantity of water that may be depleted from reservoirs and surface during the evaporation process will increase. This is caused by the average temperature increase in the range of 1.8- 4.1

°C which is predicted between 2011-2050 [9]. Figure 3 exhibits the increase in population and water consumption in the Kingdom between 2007 to 2050.

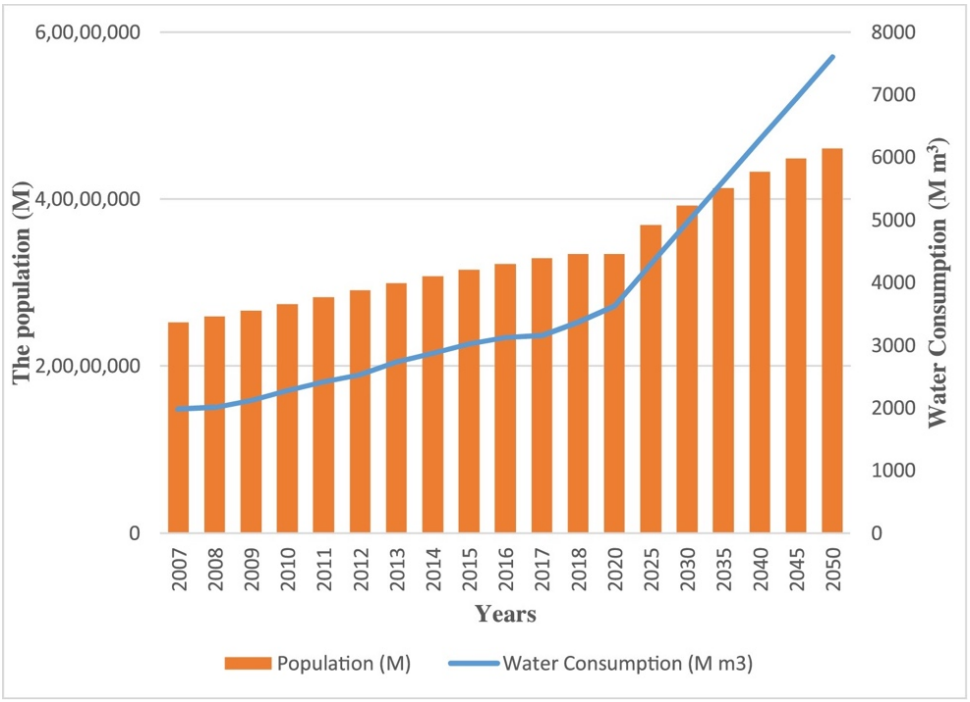

Figure 3: The increase in population & water consumption between 2007 to 2050, adopted from [10]

For example, in the southwestern region, the water surface of dam reservoir is decreasing by five meters/ year. In addition, the amount of ground water to be revived might be reduced by 91.4 million m^3 per year resulted from the increase of temperature by 5 °C. Furthermore, the agricultural water need will raise by approximately 10% in the summer and 18% in winter. Consequently, water treatment and desalination costs could be increased due to rapid climate change and temperature increase. Thus, water specifications and quality would be affected such as salinity, pH, impurities, dissolved oxygen and microorganisms.

It is worth mentioning that around 70% of the total population in Saudi Arabia is concentrated in six major cities which are Riyadh, Jeddah, Makkah, Dammam, Taif, and Madinah. Despite the fact that water consumption between 2007 and 2018 was so significant, it is likely to be abruptly raised from about 3600 million m^3 in 2020 to more than 7600 million m^3 in 2050 in the coming 30

years. The drinking water consumption in 2018 was about 3360 million m^3, which is higher than it was in 2007. Similarly, the population grow from 25.2 to 33.5 million by almost 30% between 2007 and 2018. The following table expresses the total drinking water quantity distributed in 2016 through the country [11].

Table 2: Total drinking water quantity distributed in 2016 through Saudi Arabia [11]

Region	Percentage of ground water	Percentage of desalinated water	Total percentage of distributed water
Riyadh	41%	28%	33%
Makkah	1%	36%	23%
Madinah	2%	8%	6%
Qassim	10%	0%	4%
East Province	25%	19%	21%
Asir	1%	5%	3%
Tabuk	5%	1%	2%
Hail	5%	0%	2%
Jazan	1%	3%	2%

1.3 Industrial Water Demand:

In the industrial environment, the industrial water is a noteworthy requirement. Normally, in the industrial field, treated water can be availed for three main purposes such as manufacturing process, cooling and steam generation (boiler feed water system). Treated water quality control and specifications are crucial to prevent corrosion, scaling and microbial formation.

Generally, the industrialization growth is resulted from the presence of organic and inorganic compounds in industrial wastewater. Therefore, water treatment in the such units for industrial influent is vital prior discharge to the main wastewater line.

According to the Ministry of Economy and Planning (MOEP), the industrial water demand is less than half of the domestic water demand. The treated water demands for industrial sector were increasing to reach 550, 710, 713 and 900 million m^3 in 2000, 2006, 2009 and 2014 respectively. Moreover, the industrial water demand has been rising since 1980 to reach 56 million m^3. The MOEP specified that the industrial water demand was developed by 2.2% per year between 2004-2009 and about 5% per year between 2009 and 2014. MOEP also has shown that, the demand of industrial water is expected to exceed 1000 million m^3in 2020 [8].

Figure 5 illustrates the increase of industrial water demand over a forty-year period from 2010 to 2050. As shown in the period between 2010 and 2018, the industrial water demand was annually developed by 3%. In contrast, the industrial water demand in the future will go up by 5% per year because of the growth of industrial sector.

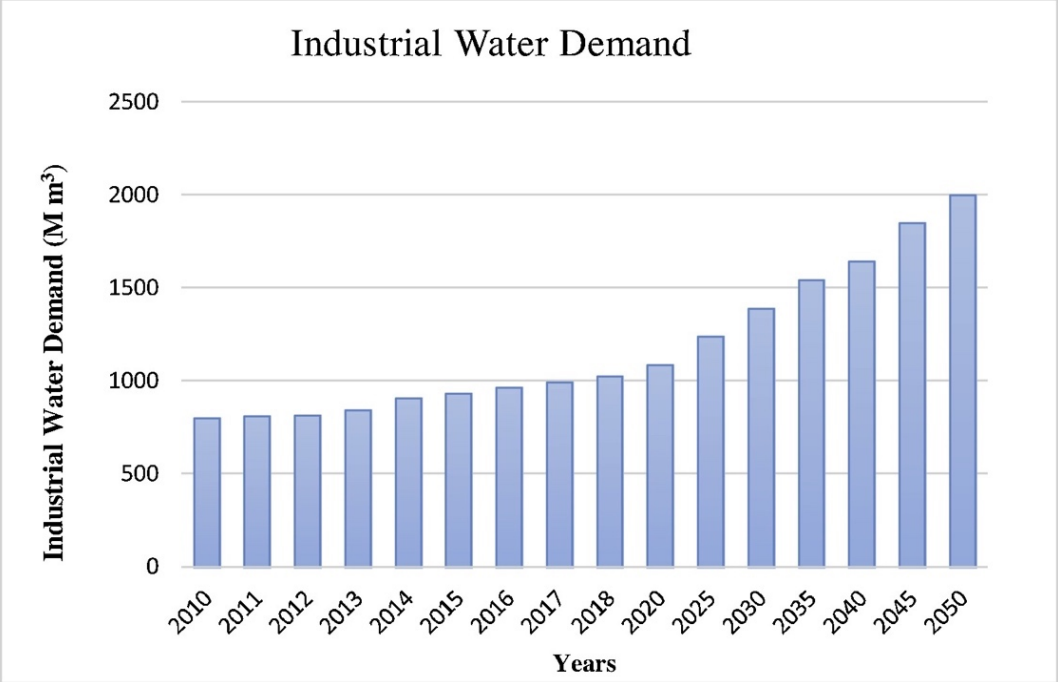

Figure 4: Industrial water demand over a forty-year period, adopted from [12]

The water treatment cost varies according to the type of technology, usually ranging from US$ 0.34 –0.75/m^3 for secondary treatment and US$ 1.19 –2.03/m^3 for tertiary treatment. Also, the total cost of industrial water involving treated water production and transportation is estimated to be about $ 3.0. Hence, treated water can be applied to cover the water demand in the industrial sector. Industrial water management is a serious issue to minimize water use. Recognizing water quality and water recycle is considered as a cost-effective method for the industrial site [8].

1.4 Water Desalination in Saudi Arabia:

In Saudi Arabia, desalination Process is considered to be a proper and strategic solution for water shortage. Figure 6 depicts a general process for the desalination process in the Kingdom. Moreover, figure 6 depicts the desalination capacity and technologies which are employed in Gulf Cooperation Council (GCC).

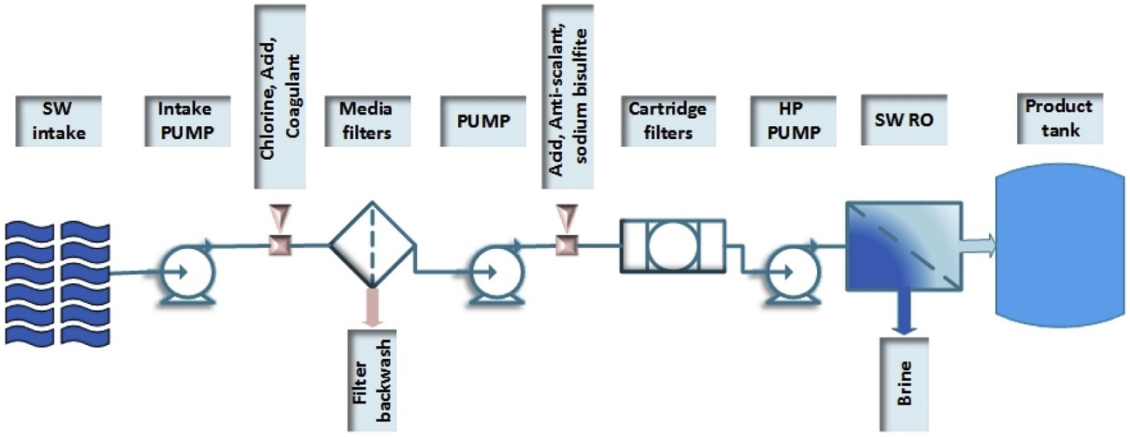

Figure 5: General process for desalination in Saudi Arabia, adopted from [13]

Saudi Arabia accounting for 18 % of total global output of desalinated water, and 41 % of the total production capacity of GCC states. The desalination capacity in KSA is approaching a daily water production of 10 million cubic meters per day (Mm^3/day), see table 3. Furthermore, the prevailing capacity of 9.8 Mm^3/day, an additional 1.6 Mm^3/day is under consideration [14].

Table 3: Desalination Capacity in m^3/day in KSA, adopted from [15]

	MED	MSF	RO	Total
Gulf coast	833,844	3,140,459	923,020	4,897,323
Red Sea coast	324,780	2,446,478	1,707,012	4,478,270
Inland locations/inland	19,173	12,491	359,425	391,089
Total	1,177,797	5,599,428	2,989,457	9,766,682

Most of the desalinated water in the KSA is still produced by thermal-based desalination processes, mainly the MSF process (5.6 Mm3/d), but less energy-intensive processes such as MED and reverse osmosis (RO) are gaining ground [16]. Moreover, figure 7 presents the desalination technologies and capacities that are availed in GCC.

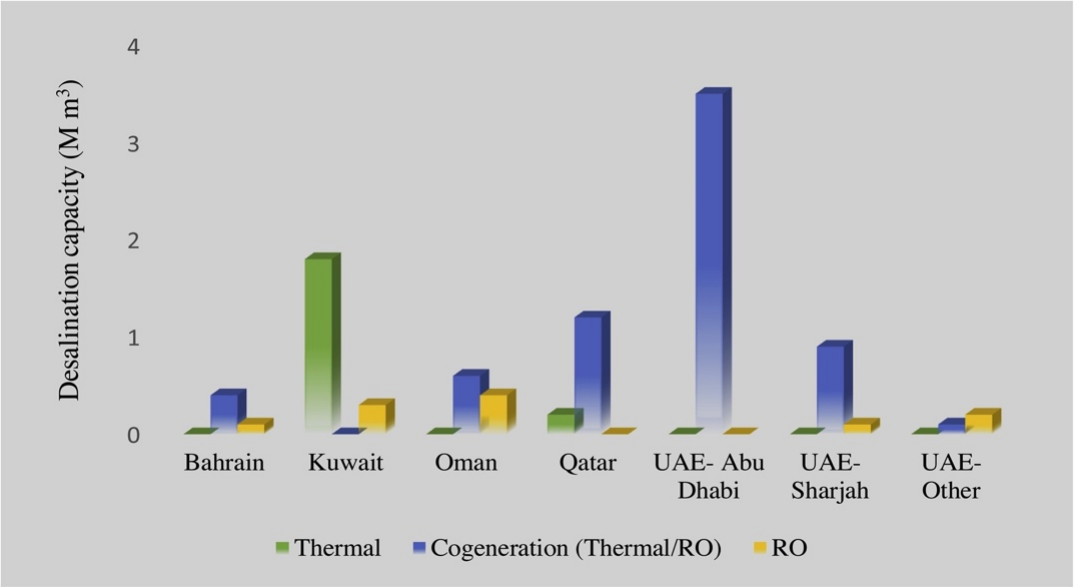

Figure 6: Installed desalination capacity by type for GCC in 2017, adopted from [13]

The largest desalinated water production in the Kingdom is Saline Water Conversion Corporation (SWCC). It produces a total of 5.2 million m^3/day of desalted water in 2018 and managed thirty desalination plants. In addition, SWCC constructed thirty-five pump station and 286 water reservoirs with total capacity of 16.8 million m^3. It built 7700 km of pipes which changing in diameters from 200 to 2000 mm to transport the desalinated water to the capital city Riyadh. Annual desalinated water (production) and consumption for GCC in 2017 are showed in table 4 [16].

Table 4: Annual desalination production and consumption for GCC in 2017 [17]

Country	Production (Million m3)	Consumption (Million m3)
Bahrain	174.9	174.4
Kuwait	562.1	533.2
Oman	228.6	222
Qatar	495	595
UAE- Abu Dhabi	1170.5	1154
UAE- Dubai	404.1	358.6
UAE- Sharjah	115.3	90.5
UAE- Other	66.5	90.5
Total	5486.6	4717.9

The average cost of desalinated water for long-term is roughly 0.8 US $/m^3. Besides, the water tariff that include the sewage cost represents almost 50% of the water production cost for moderate water consumption. Figure 7 describes the total electric power export and desalinated water export in 2016 for the Kingdom [16]. SWCC annual report declared that the long-term average cost of water desalination is about 0.8 US $/ m^3. On the other hand, the water tariff which involved sewage cost is equivalent to 50% of the water production cost. Figure 8 showed the total desalinated water export (Mm3) and electric power export (MM.W.h) by SWCC in 2016.

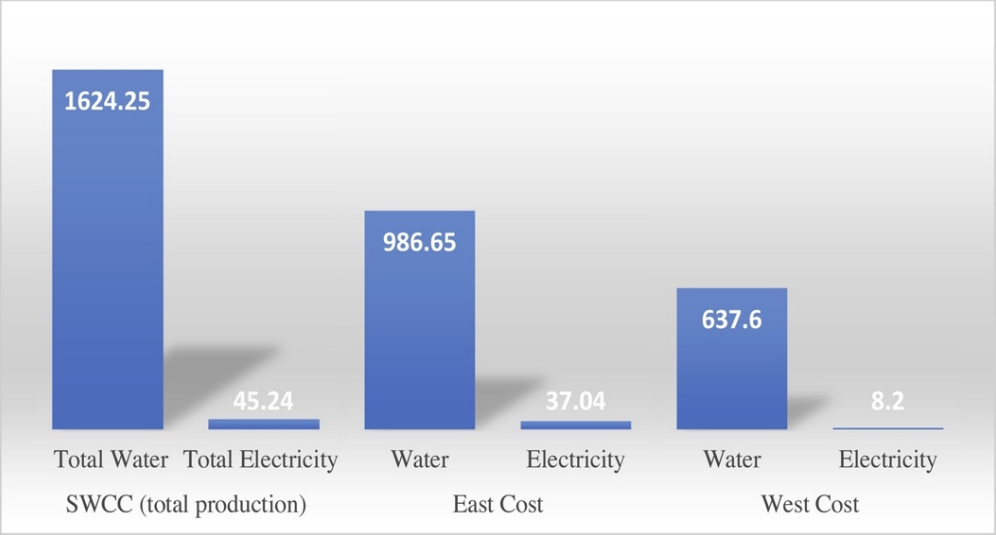

Figure 7: Total desalinated water export (Mm^3) and electric power export (MM.W.h) by SWCC in 2016, [15]

It is worth mentioning that desalination industries encounter many challenges. The main one is that the crude oil dependence for energy. It has been reported that 1.5 million barrel/day which is nearby 12% of the crude oil production used to power the desalination plants [15].

1.4 Solar Desalination System in Saudi Arabia as a Choice:

As the kingdom desalinates the largest capacity of seawater through energy-intensive thermal processes such as multi-stage flash (MSF) distillation and seawater reverse osmosis (SWRO), it is still energy-intensive (3-4 kWh/m^3). Therefore, these types of processes lead to the emission of significant amounts of greenhouse gases (GHGs) mainly CO_2. Additionally, these kinds of processes most often are limited to serving urban centers with centralized systems because of their need for on-grid power [18], [19].

As depicted in figure 9, renewable sources (RE) of energy such as solar, geothermal, and wind can operate centralized systems in urban centers with no direct GHG emissions. Likewise, they provide a chance to make desalination greener and serve countryside communities off of the grid. Currently, there are no existing desalination plants being driven by renewable energy, instead there

are some stand-alone systems. Only about 1% of total desalinated water is currently based on energy from renewable sources. Regarding domestic conditions in the Kingdom, solar and geothermal energy are the most significance. In that, solar energy can be utilized for operating seawater reverse osmosis (SWRO) plant assisted with photovoltaic cells (PV), that exploit and harness solar radiation [20], [21].

Alternatively, solar energy in the form of heat energy can be collected by collectors either concentrating collectors such as parabolic mirrors, or non-concentrating collectors such as solar ponds for operating distillation processes. Generally, the main issue that confront PV operation is the variable daytime pattern of sunlight, hence it is desirable to acquire and consider an integrated system, which requires an energy (heating coil) storage component for operating/ powering desalination system (solar still) during periods of low performance or nocturnal time. As electricity storage is still a challenge, combining power generation and water desalination can also be a cost-effective option for electricity storage when generation exceeds demand. Renewable technologies that are suited to desalination processes include but not limited to solar thermal, Photovoltaic, wind, and geothermal energy [22].

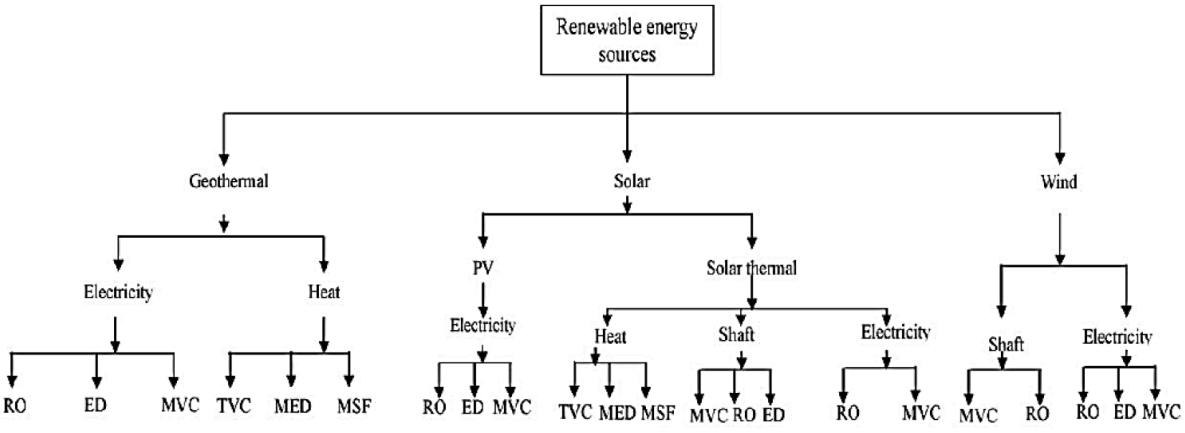

PV= Photovoltaic, RO= Reverse osmosis, ED= Electrodialysis, MVC= Mechanical vapor compression, MED= Multi effect distillation, MSF= Multi stage flash distillation, TVC= Thermal vapor compression

Figure 8: Flow chart of renewable energies powered desalination processes [22]

Saudi Arabia is endowed with a vast expanse of arid desert; thus, solar energy is available in profusion with a typical solar radiation from 2,200 to 2,400 kWh/m^2.year. The absorbed amount of energy of the collectors that collect solar thermal energy from sunlit might differ from 600 to 1,500 kWh/m^2.year. This amount of collectable heat energy corresponds to efficiencies from 25% to 60%. For instance, in an equatorial area, a stationary thermal collector and selectively coated flat plate may have a solar thermal energy rating of 925 kW/m^2.year with a thermal collection efficiency of 45% at 80 ^{o}C of application temperature, when compared with 1,100 to 1,200 kWh/m^2.year for the desert states. Solar thermal energies values depend on the application temperatures and the type of receiver devices. Figure 9 shows the good presence of the solar radiation in Saudi Arabia, which is considered to be one of the highest solar insolation energies in the world [23].

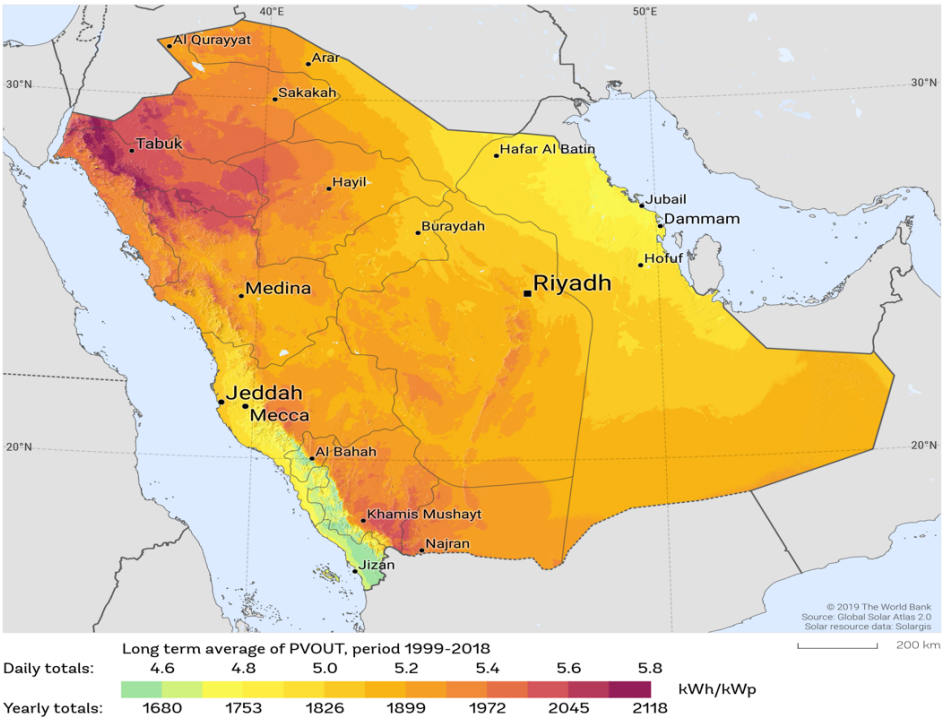

Figure 9: Solar resource maps of Saudi Arabia, adopted from Solar GIS [24]

One intrinsic drawback factor of solar collectors in desert regions is the dust cover, which could lower the rate of thermal solar energy drastically. This disadvantage factor can be avoided when the collectors are periodically checked for preventive maintenance. The other disadvantage factor of a solar powered system is that it can only provide energy input during day light hours. As it is well known that large capacity of thermal storage is needed, the desalination facility necessities to operate continuously [25].

1.5 Solar Still:

A solar still is a simple device that distills and purifies the brackish or saline water by utilizing solar energy through evaporation and condensation processes to produce drinking water. Solar stills can provide a solution for some areas, that features an abundant solar energy, nevertheless water quality and quantity may not be appropriate for human use. Water that looks purified may include some toxic and contaminated elements such as metals, which may cause infection or death if drunk. Solar desalination is considered as the best method for purifying the impure water, but in a small scale. Solar stills are self-dependence water supplying systems that can be used for low production capacity. They generally produce fresh water utilizing renewable source of energy such as solar thermal energy. These types of devices do not rely on non-renewable energy sources such as fossil fuels or electricity [26], [27]. Figure 11 showed a simple prototype of solar still.

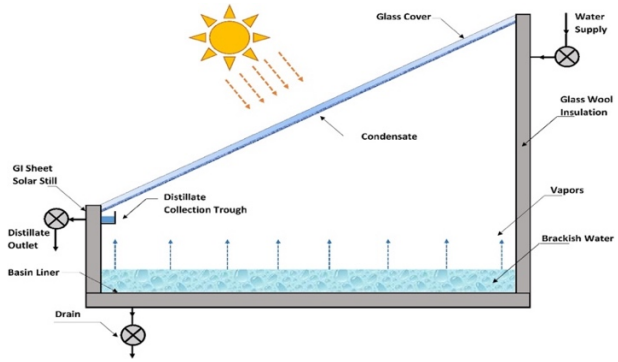

Figure 10: A simple prototype of solar still

1.6 Solar Stills Classifications:

As depicted in figure 12, the functioning of water desalination units can be broadly classified into active and passive solar stills according to the solar energy modes of operations.

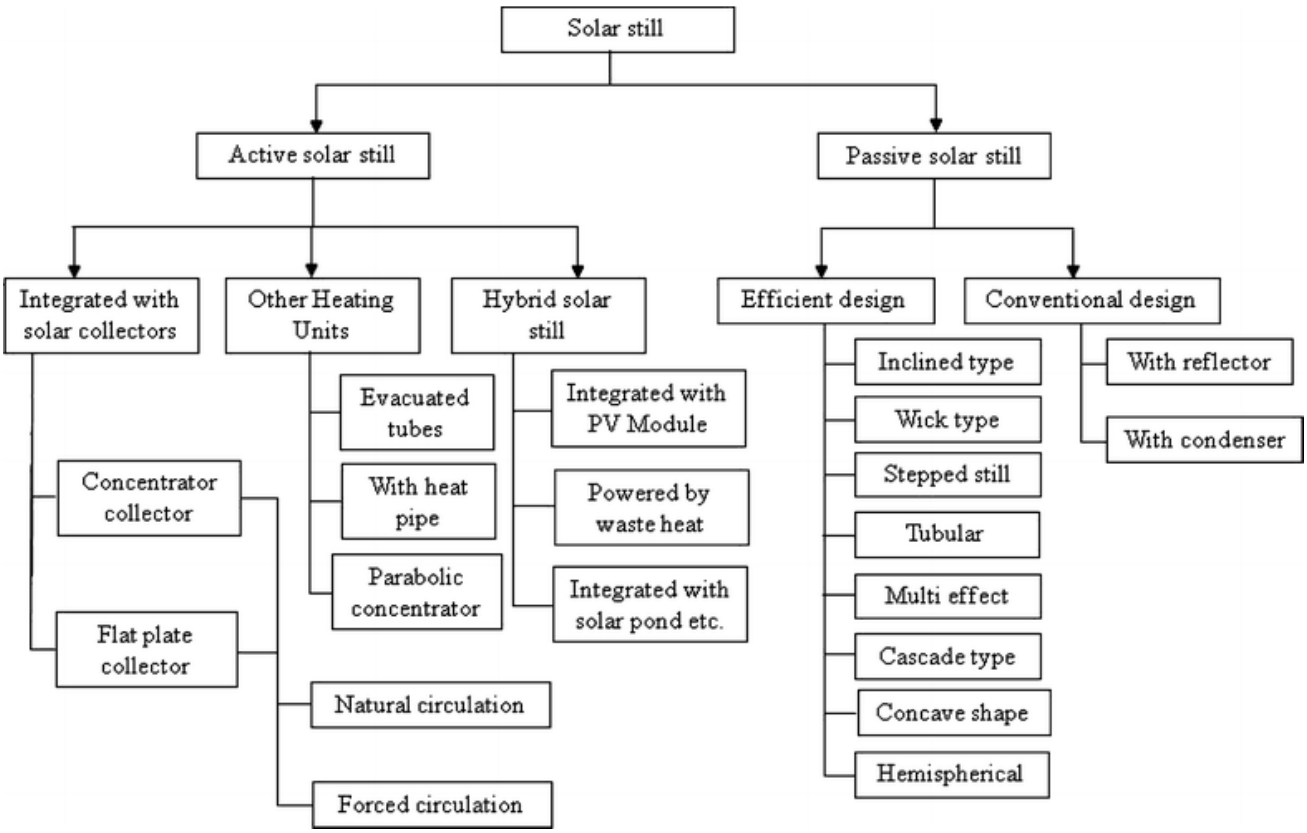

Figure 11: Solar stills classifications, adopted from ResearchGate

1.7 Passive Solar Still:

The simplest unit of solar distillation is known as the conventional single slope solar still. The simple passive solar still structure comprises of a sealed basin, which made of cement, concrete, or galvanized iron sheet. The basin contains brackish/ saline water. The inner surface/wall of the basin is coated with a black color which is essential to maximize the solar radiation/ incident absorption. While, the upper side of the still is normally covered with a transparent material such as glass or plastic. When the sun rays (solar radiations) break through the enclosed basin, heat is

generated (solar thermal energy). The entire basin is preferred to be well insulated to prevent the heat losses. Following absorbing an ample amount of heat, water temperature inside the basin will rise which causes its evaporation process. Thus, the quantity of evaporated water vapor will condense on the inclined glass cover and eventually gets accumulated in the collection chamber (trough) [28].The following are the main types of passive solar still along with their figures 13,14:

- Single slope single basin (SSSBS).
- Double slope single basin with (DSSBSMR) and without (DSSBS) outer mirrors.
- Single slope double basin (SSDBS) and single slope triple basin (SSTBS) solar stills.

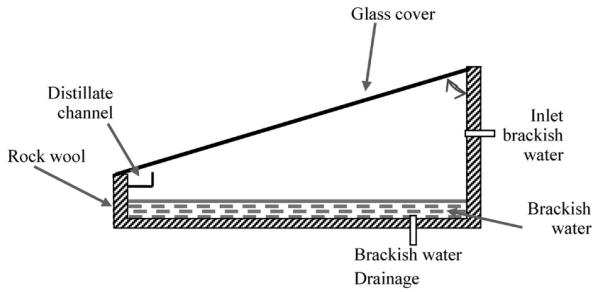

Figure 12: Schematic of the solar stills under study: SSSBS, adopted from [29]

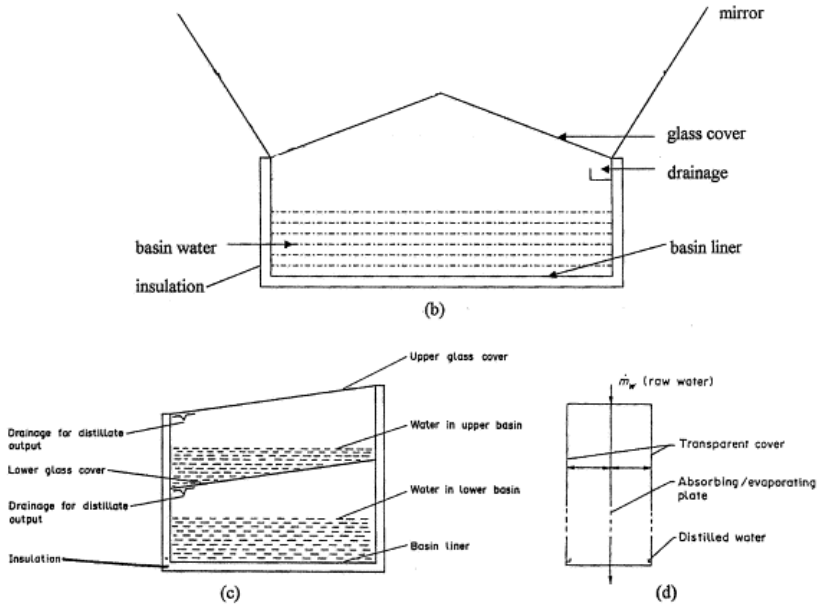

Figure 13: Schematic of the solar stills under study: (b) DSSBSMR; (c) SSDBS; (d) VS [29]

1.7.1 Basin Solar Stills Classifications:

- Single-slope and double-slope basin stills configurations:

Based on the motion of the sun in different locations and seasons, the two configurations of basin type stills, single slope and double slope illustrates that the maximum radiation is higher in double slope stills, in addition to better performance than in single slope stills. Nevertheless, single slope basin stills have less solar radiation and convective heat transfer losses. Also, as depicted in figure 15, the shaded area can be utilized for an extra condensation. Based on the yearly performance data for Delhi climatic conditions, it is determined that a single slope still presents better performance for cold climatic condition than a double slope. However, the double slope still gives better performance than single slope in summer climatic conditions [30].

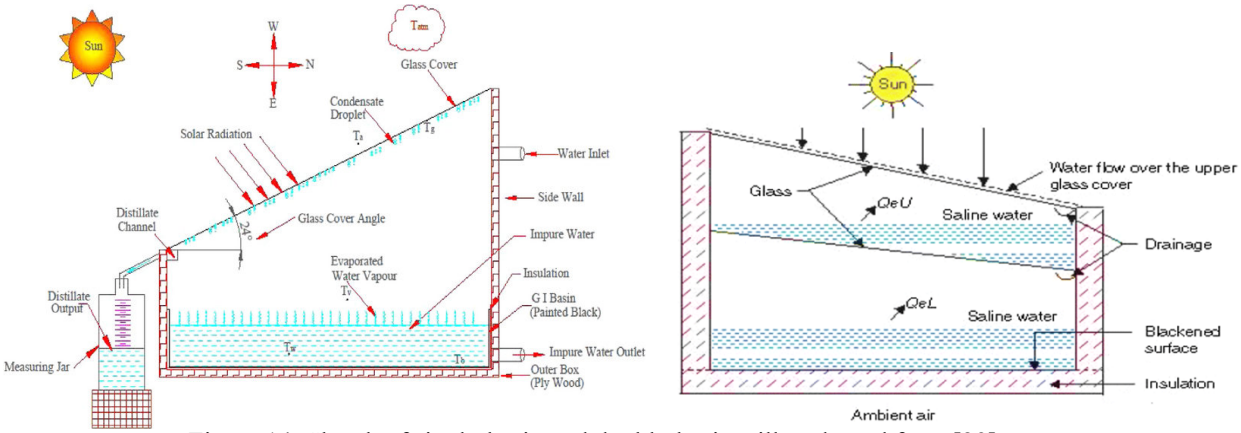

Figure 14: Sketch of single-basin and double-basin stills, adopted from [29]

1.7.2 Passive Solar Stills Advantages and Drawbacks:

There are several advantages of passive solar distillers:

- Wasted solar energy can be well employed, hence the usage of fossil fuels will be significantly reduced.

- These types of solar stills do not contain any moving part; therefore, power generation is no required.
- Solar energy classified under renewable source, and it is pollution free and eco-friendly.
- Purified water can be produced in house with a small investment and low maintenance cost for domestic and commercial purposes.

Some of the drawbacks of passive solar stills are:

- The distill water output affects during winter days.
- It should be inclined towards the sun's orientation.
- Passive stills need to be protected during whether conditions such as rain, high wind blowing, clouds etc. [29].

1.7.3 Multiple Effect Diffusion Solar Stills:

Multiple effect diffusion type solar stills mainly involve number of parallel partitions linked with saline-soaked wicks with narrow air gaps between partitions, and to increase the productivity of distillate water, the evaporation and condensation processes are recurring in all partitions. According to many researchers' findings [31], the productivity of the diffusion still can be seriously increased by reducing the diffusion gaps between partitions, and by increasing the number of partitions. The still comprises a flat plate reflector, casters for manual azimuth tracking and a vertical multiple-effect diffusion type still, which contains a glass cover and a number of parallel and vertical partitions with narrow air gaps between partitions. All fixed partitions except for the outer one is directly connected to saline-soaked wicks.

Brackish water is fed to the wicks constantly. In terms of locations and seasons, the azimuth angle of the still and of the flat plate reflector can be manually aligned in order to effectively absorb solar radiation on the first partition [32].

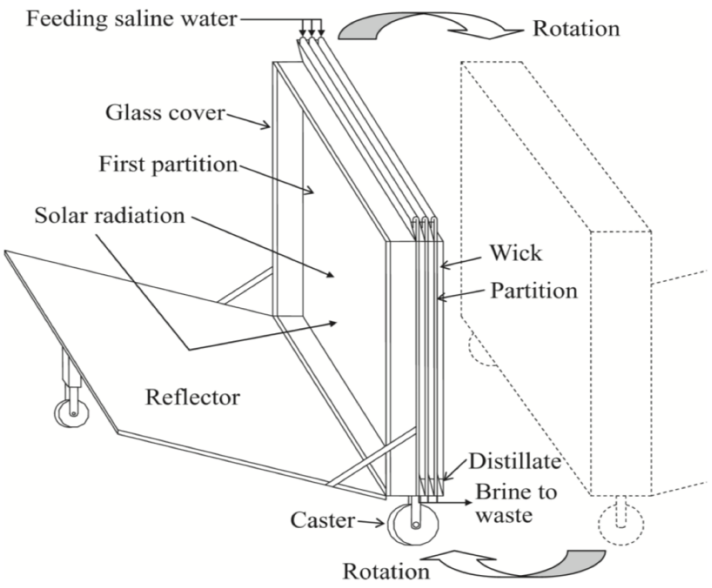

Figure 15: Schematic diagram of a multiple effect diffusion solar still, adopted from [29]

As shown in figure 16, the water vapor diffuses through a humid air layers between partitions then it condenses on the front surface of the next partition. Latent heat from condensation is recovered to cause further evaporation from the saline-soaked wick of the second partition. Likewise, the solar energy is recovered and recycled, and the evaporation and condensation processes are repeated on all partitions in the still to increase the productivity of distillate water.

Direct solar radiation, diffuse solar radiation and the solar radiation reflected by the flat plate reflector can transmit through the glass cover and are absorbed on the front surface of the first partition. The absorbed solar thermal energy causes saline water to evaporate which fed to the wick and attached to the rear surface of the first partition [32]–[34].

1.7.4 Wick Solar Stills:

The reduction in the depth of brine inside the still improves the distillate water productivity. This behavior has been founded basically because of the higher basin temperature. The benefit of selecting wick stills type is to keep the brine as shallow as possible (with low heat capacity) while

avoiding dry spots. The obtained results of a single wick still using a plastic cover which located in Valparaiso, Chile, indicated a production rate of 3.8 to 4.4 l/m^2/day with an operational efficiency roughly between 40 - 46 %. An improved design for the wick-type collector- evaporator still was established by Moustafa et al. [35]. The results of this design imply a development in the productivity and in the operation efficiency. Figure 17 showed a wick type collector-evaporator still.

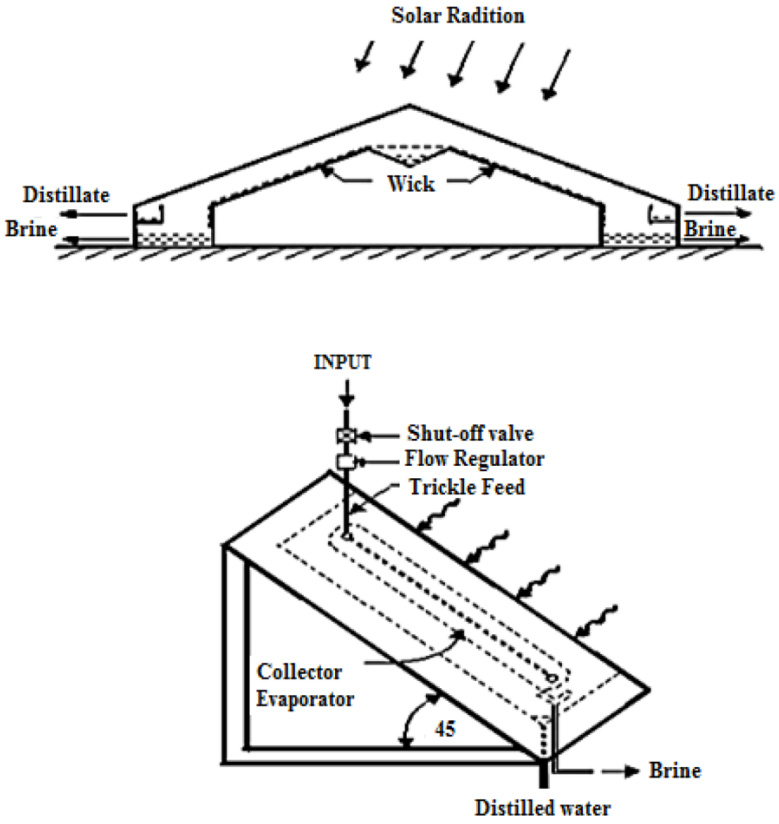

Figure 16: Wick type collector-evaporator still & Modified wick-type collector-evaporator still [35]

Multi-wick stills: Tiwari et al. [36] proposed a double-condensing, multi-wick still. Excess vapor can then be condensed on the additional surface and reduce the heat load on the glass cover, reduces class cover temperature, which in turn enhances evaporation rate. The experimental results showed a 20 % increase in the still productivity over the simple multi-wick still. Figure 18

illustrates a cross-sectional view of a double-slope multi-wick solar distillation unit with a capacity of 85 l/day [29], [35]that was installed in Delhi, India, in 1981.

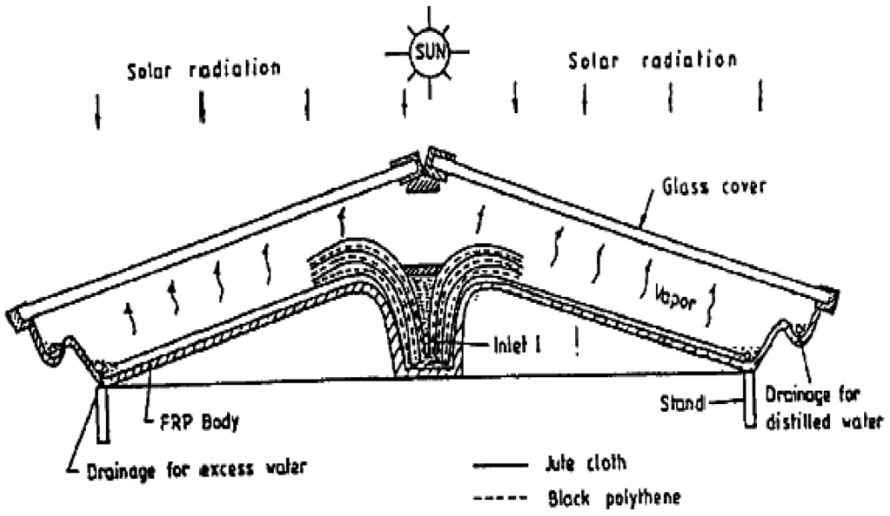

Figure 17: Double-slope multi-wick solar still (Cross Sectional View) [35]

1.7.5 Comparison between Wick and Basin Stills:

The heat capacity of the water mass in multi wicks stills is negligible. In contrast, the heat capacity in conventional basin stills is considered. Therefore, the productivity of the multi wick stills is always higher than in conventional basin stills.

Furthermore, Tiwari and Yadav [28] designated that for a medium scale installation, the multi wick solar distillation plant is more cost-effective. Nonetheless, basin stills type is preferred for larger scale supply of distilled water, because of its low cost and simplicity. Minasian and Al-Karaghoul coupled a conventional basin type solar still with a wick-type solar still. The hot brine water outlet from the wick-type will directly feed into the basin-type still, and the cover will be cooled with the basin still. It is worth to mention, the combined stills exhibited higher efficiency than the two separated subject stills. Moreover, the amount of distilled water is 85 % which is more than the basin type still and 43 % more than the wick type stand-alone still [28].

1.7.6 Hemispherical Solar stills:

As depicted in Figure 19. Arunkumar proposed a new design for a solar still for water desalination with a hemispherical top cover with and without flowing water over the cover. The daily effluent of distillate water is enlarged by decreasing the cover temperature through water flowing over it. The efficiency was 34 %, and with the effect of the top cover cooling, it is increased up to 42 %. During the conduction of different experiments, such operational parameters were measured; for example, solar radiation incident on a solar still, water temperature, cover temperature, air temperature, ambient temperature and distillate water output [37].

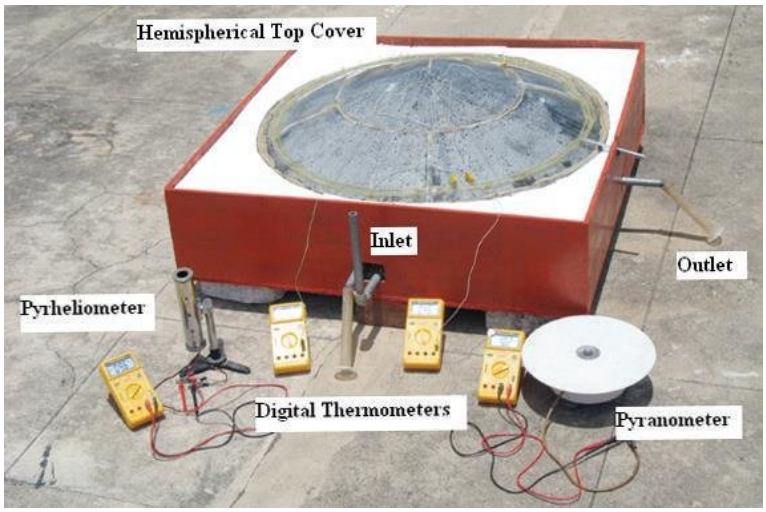

Figure 18: Hemispherical solar still, adopted from [37]

1.7.7 Concave Surface Solar still:

It is considered as a new design of a solar still with wicked concave surface. The objective of using wick surface is to increase the absorption, and evaporation areas of solar radiation (incident) to further increase the distillate water productivity of the still. As shown in figure 20, The rate of evaporation is increased because the water surface level is lower than the upper limit of the wick surface. Similarly, this concave surface design decreases the shading effect unlike the conventional type still since all sides are made of glass.

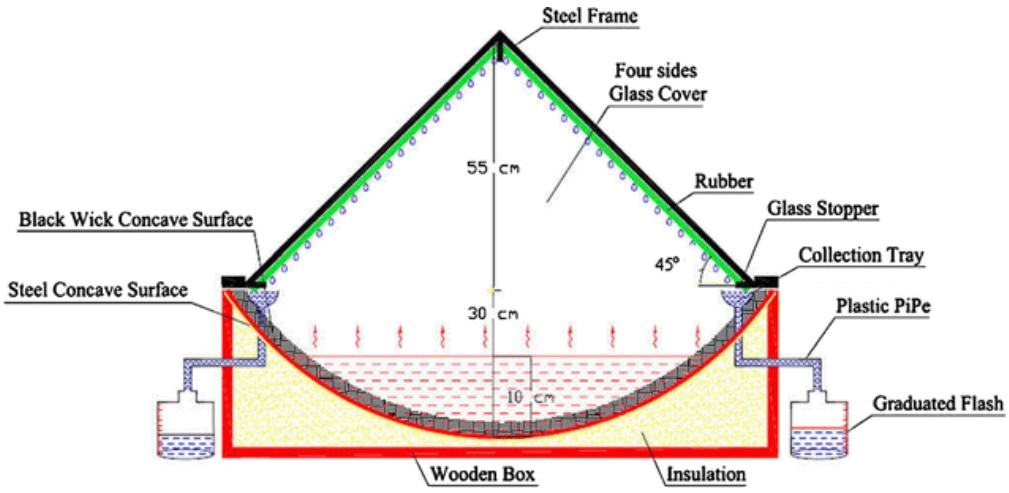

Figure 19: Concave wick solar still, adopted from [38]

Referring to a conducted experiment at Tanta University in Egypt, results show that average distillate water production in a daytime is 4.1 L/m^2. The maximum efficiency of the system is found to be 45 % and the daily efficiency of the still is 30 %. Also, the maximum hourly yield is found to be 0.5 L/hr.m^2 in the nocturnal period [38].

1.7.8 Solar Still with Cover Cooling:

This solar still type is designed by installing two cooling arrangements and both are using a double glass cover. It is aimed to increase the rate of evaporation by increasing the temperature gradient between the basin (heat source) and glass cover (heat sink). This process can be attained by either increasing the basin temperature or decreasing the cover temperature or both. These two processes are presented in Figure 21 and are labeled as feedback flow and counter flow.

Obtained results have revealed that utilizing cover cooling yields an increase in the still productivity with a significant improvement when operating the feedback flow and is greater than when using the counter flow. It worth to mention, part of the sensible heat gained by cooling the glass cover is utilized in the feed [35].

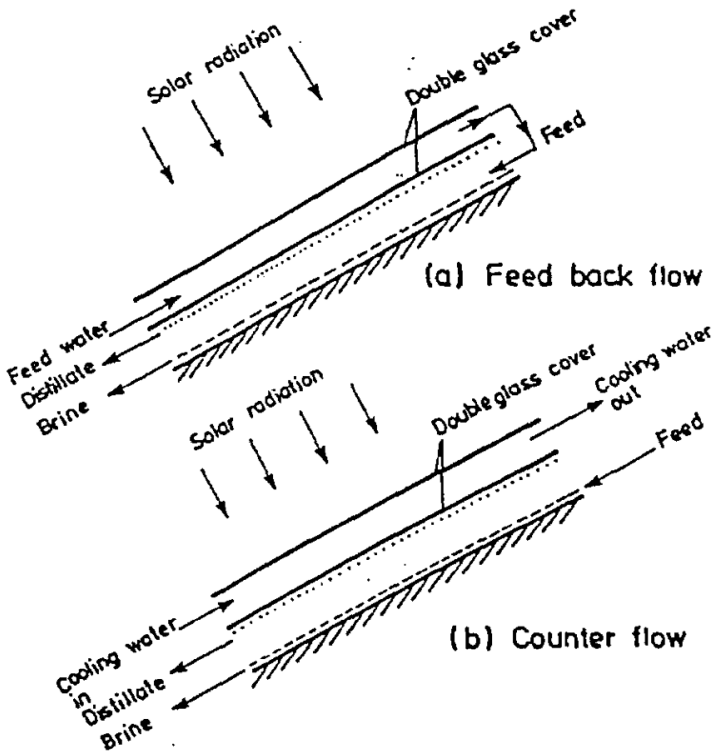

Figure 20: Cooling of glass covers by (a) feedback flow, and (b) counter flow [35]

1.7.8 The Effects of Adding Black Dyes on The Still:

Lawrence et al. [39] specified that there is a substantial effect of adding dye on still performance for large water depth in particular. In addition, black dye provides a better performance than other dye such as violet and red dyes. The presence of dye inside the still enhances the rate of water distillation because solar radiation incident is absorbed in a very thin upper layer (2 cm), hence increasing the surface temperature of the brine, and the rate of water evaporation will be promoted. Consequently, the productivity of the distillate water will definitely rise. Likewise, the salt and impurities build up issue is reduced. The reason behind that salt can settle on the bottom of the basin still without interfering in the solar radiation absorption close to the surface [40].

The reduction in the water emissivity will decrease the heat transfer by radiation from water to glass cover. This resulted in a substantial improvement in still efficiency and offers great potential

for solar still usage. Muddy water is opaque; thus, the solar radiation incident commonly becomes absorbed nearby the top layer. The daily results for distillation of muddy pond water showed that the muddy and clear water samples produced the same distillate water output [28]. It is worth to mention, not much information is available on muddy and contaminated water, which in some states of the world may be the only source of feed water.

1.8 Active Solar Stills:

The majority of researchers used a lot of techniques to design a new combined system between the solar water heater and solar still as presented in Figure 22. The purpose of modeling these types of stills is to improve the distillate water productivity and still's performance. Saline water is circulated to solar collector in order to be preheated before introducing to the solar still. Brine water becomes evaporated due to solar radiation then it condensed and collected on glass cover from where it flows towards distillate channel. It can be concluded that passive solar stills can be economical to produce potable or distilled water. However, active solar still can be economical from a commercial point of view [41].

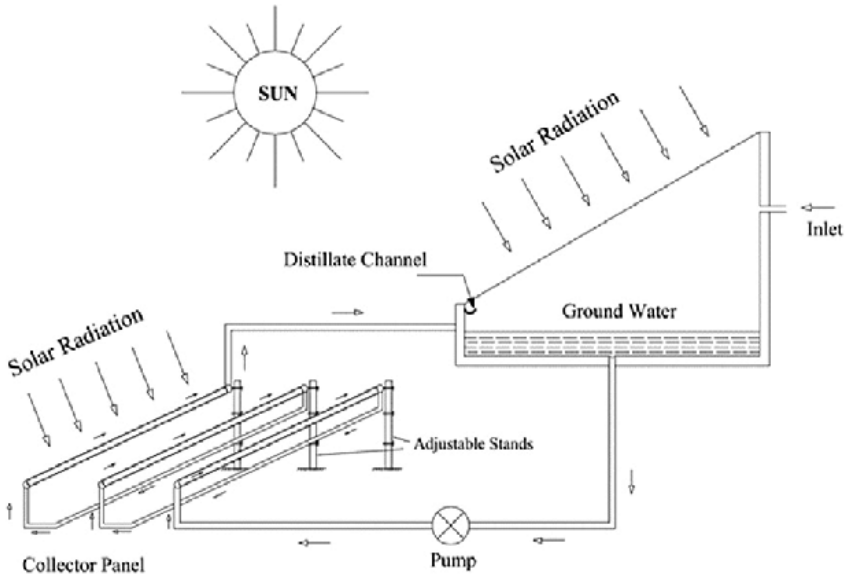

Figure 21: Active solar still coupled with flat plate collector, adopted from [41]

1.9 Analysis of Factors Affecting The production of Solar Stills:

1.9.1 The Effect of Solar Radiation:

Solar radiation energy is considered as the most critical and key factor to produce distilled water. It is obvious that the more solar incident received from the sun light, the greater the amount of distilled water yielded from the still and vice versa. Though, the greater the solar radiation, the greater the heat loss of the solar still. Consequently, the insulation of the still basin needs to be carefully studied to maintain distillate water production.

1.9.2 The Effect of Wind Speed:

The higher wind speed contributes to more output of distillate water. It can be concluded that exposing the still to a high wind speed will cool the glass cover faster. This behavior leads to an improved in the temperature difference between the water inside the basin and the cover glass layer. In contrast, the distilled water production increased only by 1.6% when the wind speed increased from 3 to 6 m/s [42]. It is notable that, when the wind speed is too high, it may cause a heat loss, therefore that the amount of distillate water is practically negligible. It is worth to mention that, this result is consistent with Cooper's survey [16]. In his research study, while Cooper increased wind speed from 0 to 2.15 m/s, the still production increased by 11.5%. Though, when he increased wind speed from 2.15 to 8.81 m/s, the output of fresh water increased by only 1.5%.

1.9.3 Effects of Ambient Temperature:

The impact of ambient temperature as an input on insulated distillation components and uninsulated distillation devices has been considered, and the results are shown in figure 23. In case the still is well insulated, the decrease in ambient temperature may leads to a higher production of distilled water, whereas in the case the still is not insulated, the reverse behavior is detected. This

phenomenon can be clarified as follow: for the distillation equipment with a good insulation, lower temperature will assist to cool the glass cover faster, thus increasing the temperature difference between the brine water layer and glass cover. In contrast, when the distillation equipment is not well insulated, low ambient temperature leads to rise heat loss of the still device, thus a reduction in water temperature in the equipment will take place accordingly. The glass cover cools down when the still temperature is low; however, the results in figure 23 showed that the impact of increased heat loss is more vital than the impact of lower glass cover temperature [42].

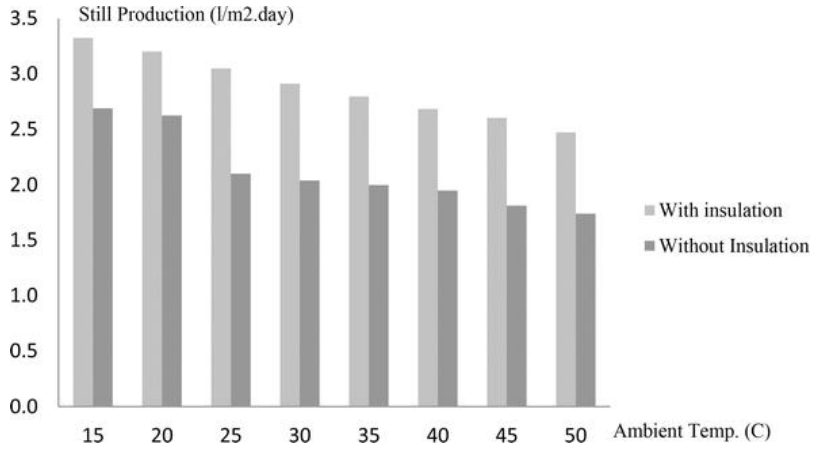

Figure 22: Effect of temperature on the output of solar stills, adopted from [42]

According to the results published by Khalifa and Hamood [30], the change of ±5°C in well-insulated distillation devices will make the average distilled water production change by ±4.5%.. Their research has revealed that when the ambient temperature increased from 26.7 to 37.8°C, the distillate outputs may increase by 11% and when temperatures are decreased from 26.7 to 15.6°C, the productions fall by 14%. As a result of SOLSTILL [42], the variation of ±5°C ambient temperature for insulated distillation systems make the distilled water output ±2.5% change.

1.9.4 Effects of The Haze and Dust:

This impact diminishes the coefficient of solar radiation intensity, thus reducing the efficiency of the distillation devices. Moreover, if dust introduces the inside surface of the glass cover, it can adversely impact the condensation flow down to the collecting trough with the distilled water dripping halfway down the glass. Consequently, it is necessary to frequently check and clean the inside and outside of the glass cover to accomplish the highest efficiency as possible [42].

1.9.5 Effects of Glass Cover's Tilt:

The effluent of freshwater relies vastly on the elements of the cover's angle and tilt direction. In order to ensure the distilled water will not drip halfway down to the collecting trough, the tilt and angle of the glass cover must be more than 15°. Additionally, it is necessary to reduce the average distance between the water surface and the tilted glass cover, and the tilt of the glass cover must be not more than 20° [30].

1.9.6 Effects of Glass Cover Temperature:

Cooper, Khalifa and Hamood, Garg and Mann [43], [44] exhibited that the glass cover can absorb around 4.75% of solar incident from the sun light, results in an increase of the cover's temperature. Moreover, the condensation of water beneath the glass cover builds a condensation water film, resulted in a partially opaque glass cover and an increase in the glass cover's temperature. Consequently, the temperature difference between the surface of the brine water in the still and condensed water in glass cover will be reduced. Hence, it is crucial to lower the surface temperature of the glass cover in order to improve the distillate water production of the still [30].

1.9.7 Effects of The Distance Between the Brine Water Level and Glass Cover:

The distance between the brine water level and the glass cover can impact the effectiveness of the solar desalination systems. As previously discussed in section 1.9.5, if the distance between the

water level and glass cover is minor, then the convective resistance of wet air flow inside the still is smaller, thus that efficiency of the system will be improved. However, this gap is subjective to the inclination of coated glass cover. If the tilt of the glass cover is increased, then the average distance between the brine water surface and glass cover is expanded, so the still output will be reduced [45].

1.9.8 The Effect of Water Temperature in the Still:

The still water temperature significantly affects the output of fresh water. As illustrated in Section 1.9.6, water film on the cover cools down the glass before running into the still. When the latent heat of steam in the steam condensation under the glass covers is employed, water can be heated and fed directly into the still. This process is applicable to both passive and active solar stills [45].

1.9.9 The Effect of Water Depth in The Still:

The water depth in the still really affects the production of distilled water. The deep-water layers lead the absorption process of solar energy take longer due to thermal inertia, hence reducing the increase of water temperature and affecting the amount of distilled water yield. As depicted in figure 24, the experimental results of a single basin solar still accompanied with evacuated glass tubes demonstrate that a test with a 1 cm depth of water inside the basin yields 5.265 l/m^2, which is 13.4% higher than a test using a 2 cm depth of water which yields only 4.555 l/m^2. It can be concluded that, these results match with the theoretical and experimental results in other researches [30], [45].

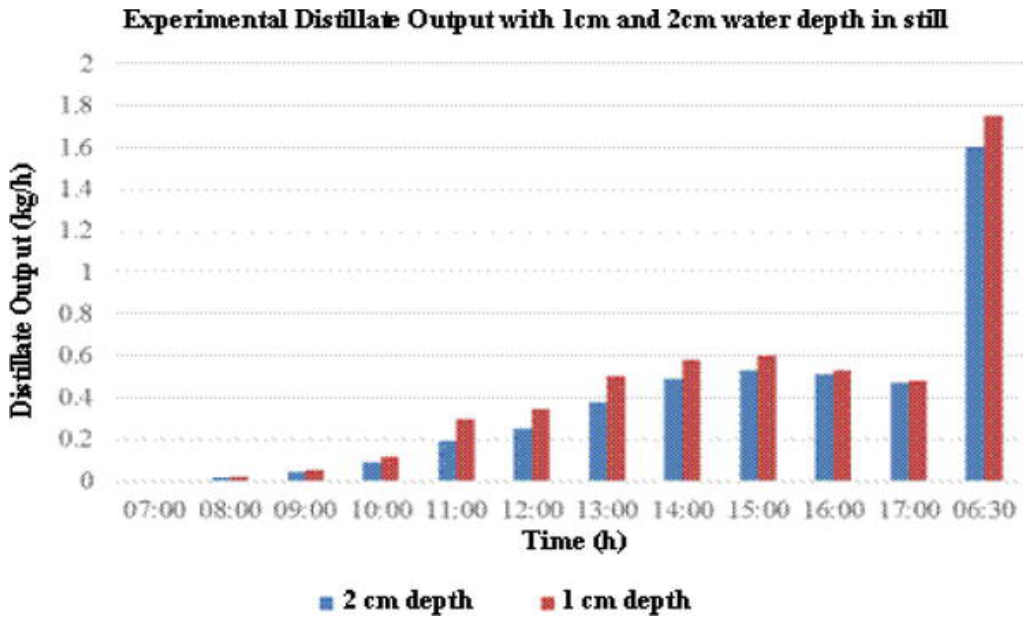

Figure 23: Experimental distillate output with different water depths in an active still [30]

2.1 Study Highlights and Novelty:

Solar still desalination is considered as one of the emerging processes among other different methods that employs renewable source of energy. This technology has multiple advantages comprising simplicity, ease of maintenance, low cost and low environmental impact. Solar still is a renowned technology for water desalination, impurities and contaminants removal and high-quality water production. Engineers and scientists have to illustrate the applications of the solar desalination system based on energy, exergy, thermo dynamic properties and cost analysis. The design analysis should consider the technique and types of the desalination system. It is necessary to model a flexible visualized computer program in order to design/or perform a reliable analysis for a widespread range of solar desalination processes with different structures.

Consequently, it is required and important to design and simulate solar desalination systems. The proposed topic claims for modeling and simulation of an integrated solar cell heating element (photovoltaic cell) system accompanied with a single slope solar still for performance improvement, process optimization and efficiency enhancement. The main objective of this study

is to develop a software using SIMULINK in order to design and simulate solar desalination systems single slope solar still with a photovoltaic Cell.

The developed software (SIMULINK) is designed for different analysis including different modifications, and comparisons. It has some features in that it has the quality of being logically, very flexible to use and easy to handle. In this work, designing a survey about the significance of utilizing a photovoltaic cell assisted with a single slope solar still for saline water desalination process is made.

Setting up and designing the required software for the proposed model system is performed. Carrying out the validation results is accomplished based on different techniques. As a result, a developed software package (a photovoltaic cell assisted with Single Slope Solar Still) is established to model/design and simulate an active single slope solar still accompanied with a photovoltaic cell. Also, a comparison between the design system areas and cost analysis for solar desalination accompanied with a photovoltaic cell.

2.2 Specific Contributions for the Study:

The step by step contributions for the proposed study are summarized as follow:

1- Select and utilize MATLAB/SIMULINK software tool to do the task of solar desalination modelling and simulation.

2- Insert the visual library into the SIMULINK browser by the aid of a graphical user interface (GUI) feature for building models as block diagrams, using click and drag mouse operations.

3- Create and set up such flow sheet program for input and output relation and design analysis using signal builder tool extracted from library browser.

4- Employ a polynomial lookup-table correlation method to construct model browser of the PV cell. It plots inputs to an output value by looking up or interpolating a table of values that is defined

with block parameters. The key specifications can be simply calculated based on the identification of module power (one parameter) to drive out many parameters of PV cell.

4- Run the design model of the whole solar still system after simulation has established to generate output figures and results through data inspector feature.

5- Evaluate and analyze output data including design areas, thermodynamic properties, heat transfer energies and costs ratios of the system.

6- The model system can achieve more than 45% efficiency with a relatively high distillate water production rate, unlike a conventional and passive solar still system with a maximum efficiency 20%.

Chapter 2: Theoretical Analysis and Modeling Equations

2.1 Flow Sheet Programs for Solar Systems:

Solar desalination processes contain a number of interactive units. A large scale of processes types and configurations can be generated by utilizing these units. A flexible computer programs are really essential to understand, design and perform the behavior of these process under various operational conditions. Using such software/programs, many flow sheeting problems can be deployed and manipulated (see figure 24). Generally, these problems can be classified into three classes as follow: (I) performance problems, (II) design problems, and (III) optimization problems [46]. Presently, with the rapid revolution of the personal computer hardware, computational and graphics mathematical software, the third generation of modeling and simulation programs for desalination processes is launched. These types of programs are based on the mathematical computations and modeling capabilities for some available commercial programs. It is worth to mention that, MATLAB/Simulink browser is one of the best and powerful tool software that introduced in the last decades. For instance, Gambier [47] demonstrated the ability of MATLAB/SIMULINK to design library for multistage flash (MSF) components. In Gamier validation, the physical properties and heat transfer correlations, were simulated individually embedded with MATLAB/ SIMULINK blocks.

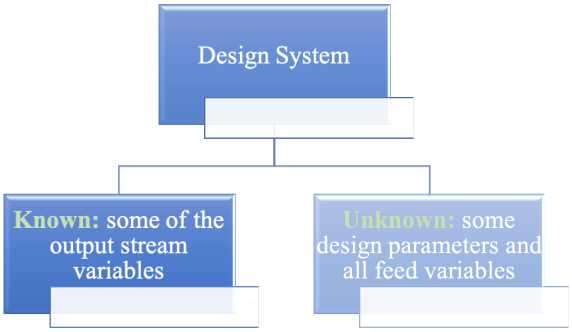

Figure 24: Design characteristics for common flow sheeting programs

The objective of this chapter is to introduce the developed modular computer program using MATLAB/ SIMULINK environments for a proposed configuration of a solar desalination process. This modular program has numerous capabilities to overcome previous programming problems and limitations such as the recycle streams. Some units are modeled to present a good example of the proposed modular program.

2.2 MATLAB/SIMULINK Software Tool:

SIMULINK associated with MATLAB is considered as a general-purpose software program that normally used for dynamic systems. This great software provides excellent performance qualities for designing regulation algorithms. Consequently, this program has been selected to do the task of solar desalination modeling and simulation. SIMULINK supports users who can undoubtedly build models from scratch or modifying an existing model. For designing a model, SIMULINK provides a graphical user interface (GUI) for building models as block diagrams, using click and drag mouse operations [48].

With this interface, users will have the ability to draw the models just as it would be with pencil and paper (or as most textbooks illustrate them). SIMULINK software can utilize many MATLAB features that includes a comprehensive block library including sinks, sources, linear and nonlinear components, and connectors. The Library Browser displays the SIMULINK block libraries installed on the user system. The user can customize and create his own blocks and builds models by copying blocks from a library into a model window.

MATLAB is a high-performance language for technical computing. It integrates computation, visualization, and programming in an easy to use environment where problems and solutions are expressed in a familiar mathematical scheme. Typical MATLAB practice include Math and computation algorithm development data which accomplish modeling, simulation, and

prototyping data analysis, exploration, and visualization scientific and engineering graphics application development, including graphical user interface building.

MATLAB is an interactive system whose basic data element is an array that does not require dimensioning. In industry, MATLAB is the tool of choice for high-productivity research, development, and analysis. It supports linear and nonlinear systems, modeled in continuous time, sampled time, or a hybrid of the two. Systems can also be multi-rate which have different parts that are sampled or updated at different rates [48].

2.3 Proposed System:

The proposed topic claims for modeling and simulation an integrated solar cell heating element (photovoltaic cell) system accompanied with a single slope solar still for performance improvement, process optimization and efficiency enhancement (refer to figure 25).

Theoretical study is made to develop a mathematical model in order to be able to predict thermal performance and efficiency of a photovoltaic cell assisted with a single slope solar still.

A schematic diagram for the proposed system is shown in figure 27. The system consists of solar still including the basin connected with a photovoltaic cell and heating coil that utilize solar thermal energy as a DC current transformed by the photovoltaic cell. The solar distillation process consists of three modes of heat transfer. There is heat transfer by conduction through the transparent cover glass, side and bottom walls that can be reduced by using an insulation material with a high thickness with a relatively low thermal conductivity value k-value. The insulation material is essential to be considered while designing such processes in order to reduce the heat loss from the solar still to ambient [49]. As exhibited in figure 26, heat from the basin liner is transferred to the saline water by convection, whereas the thermal energy from the hot saline water layer is transferred through evaporation process, convection and radiation modes into the

condensed glass cover. When water inside the still evaporates, the water vapor condenses on the glass cover yielding distillate water and latent heat of condensation. Also, the glass cover in turn dissipates and scatters the heat transfer to the ambient by convective and radiative heat transfer. The mode of heat transfers inside the solar still also incorporate mass transfer. Subsequently, the convective and evaporative heat transfer coefficients from hot water to a transparent glass cover correlation have been developed and demonstrated in the design code along with energy balance analysis equations in the next chapter. A resistance network for a proposed solar still system is depicted in figure 26 [50]:

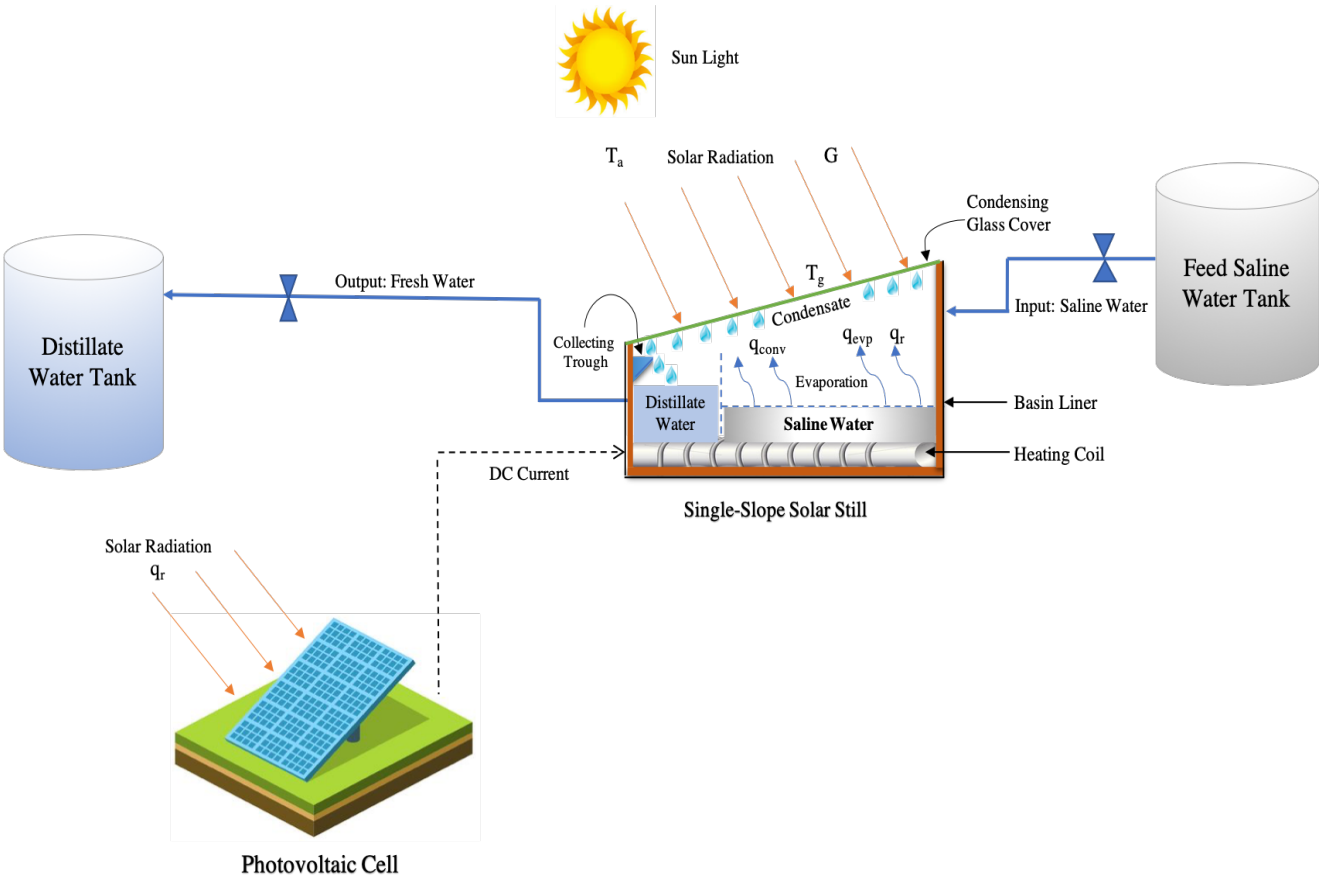

Figure 25: Proposed simple schematic diagram for a photovoltaic cell assisted single slope solar still

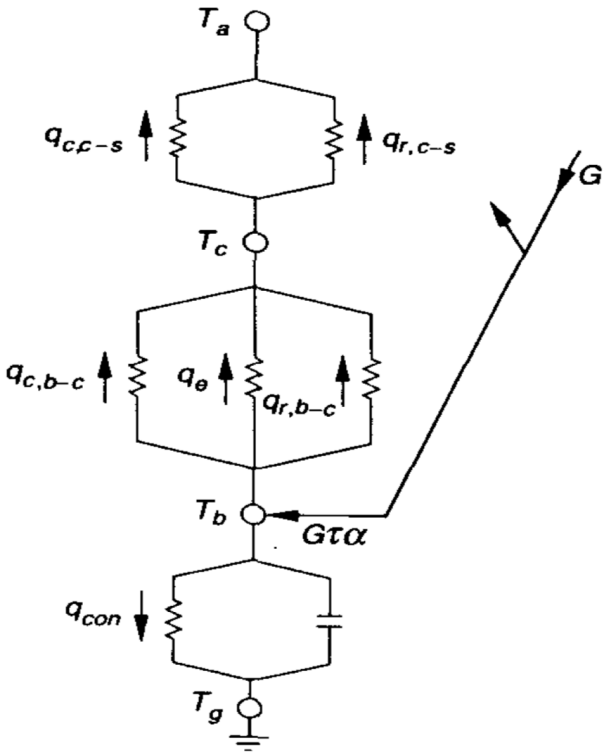

Figure 26: Basic thermal network for basin type still, adopted from [50]

2.3 Mathematical Model:

By operating the measured values of solar radiation incident, ambient temperature and wind speed as input data, the daily productivity along with thermodynamic properties of the solar still can be calculated by utilizing inserting design equations in the model system. The mathematical model is developed according to the relations of heat transfer coefficients, which were acquired by Gwaande [51]. The energy balance equations of the solar still could be written and demonstrated based on the following assumptions:

1. **Solar still (basin with a glass cover):** a signal builder tool in SIMULINK browser is utilized from library browser to insert inputs data such as Solar radiation, ambient temperature, productivity and wind speed. The subject inputs values are taken within time between 9:00 a.m.

and 6:00 p.m. Spring operating conditions are favorable for solar still inputs and it is recommended to work on solar radiations (MJ/m^2).

2. **Photovoltaic Cell:** The absorbed solar radiation energy will be transformed to an electrical energy as a power load of the photovoltaic cell (Q_{load}). Light shining on the solar cell produces both a current and a voltage to generate electric power. The power then will be introduced along with module power to compute the number of modules required for the designed system. Multiple designed parameters such as total system area, cell area and battery storage can be calculated as well.

3. **Feed and Distillate Tanks:** Feed salinity (ppm) is a function of water inlet temperature and density which further affect the rate of water evaporation and the level of brine depth inside the basin. The distillate water productivity is a function of water level inside the distillate which indicates the solar still productivity per m^2. Also, specific heat capacity C_p for feed water and distillate are functions of temperature and salinity.

2.4 Heat analysis in a passive solar still:

Solar energy that is directly received from the sun light and the brackish water in the still is equal to the summation of energy lost by convective heat transfer between water and glass, radiative heat transfer between water and glass, evaporative heat transfer between water and glass and energy gained by the saline water [35]. Figure 27 exhibited solar still energy balances.

The energy balance for the saline water inside the basin can be represented as follow:

$$Q_{c,b-w} + I(t) * \propto_w * \tau_g * A_w = Q_{c,w-g} + Q_{evp,w-g} + Q_{r,w-g} \qquad (1)$$

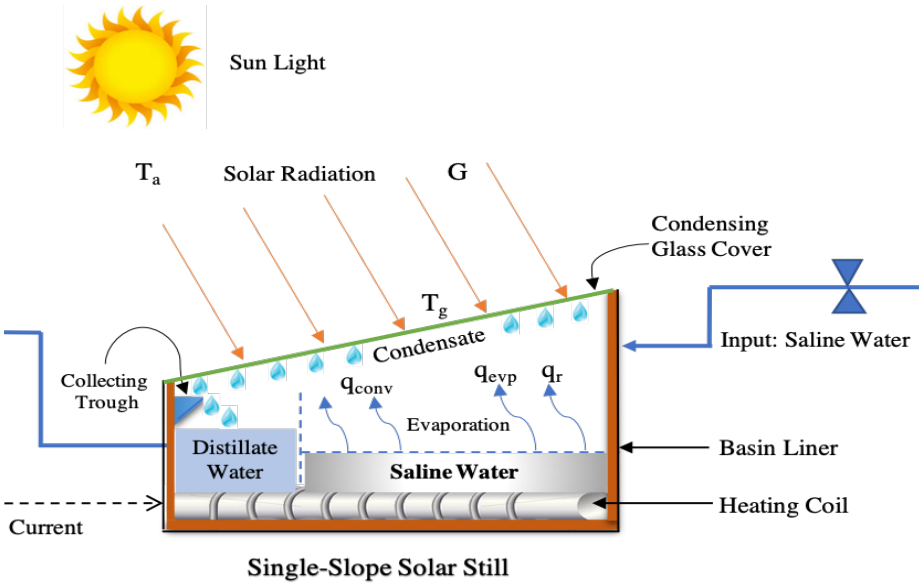

Figure 27: Solar still energy balances

The energy balance equation for the basin:

$$Q_{c,b-w} = \left(A_b * I_b * \propto_w * \tau_g\right) - Q_{c,b-a} \qquad (2)$$

$$Q_{c,b-a} = h_b A_b (T_b - T_{amb}) = Q_{losses} \qquad (3)$$

$$Q_{c,b-w} = I(t) * \propto_b * \tau_g * A_b - h_b A_b (T_b - T_{amb}) \qquad (4)$$

The energy balance equation for the condensing glass cover:

$$Q_{r,g-sky} + Q_{c,g-a} = Q_{c,w-g} + Q_{evp,w-g} + Q_{r,w-g} + \left(I(t) * \propto_g * \tau_g * A_g\right) \qquad (5)$$

$$Q_{r,g-sky} = A_g * \left(\varepsilon * \sigma * \left(\left(T_g + 273\right)^4 - \left(T_{sky} + 273\right)^4\right)\right) \qquad (6)$$

$$T_{sky} = T_{amb} - 10 \quad °C \qquad (7)$$

$$\varepsilon = \left(\frac{1}{\left(\frac{1}{\varepsilon}\right)} + \left(\frac{\left(1 - \varepsilon_g\right)}{\varepsilon_g}\right)\right) \qquad (8)$$

$$\varepsilon = \left(\left(\frac{1}{2}\right) * (1 + \cos(s))\right) \qquad (9)$$

$$Q_{c,g-a} = \left(h_{c,g-a} * A_g * \left(T_g - T_{amb}\right)\right) \qquad (10)$$

$$h_{c,g-a} = a + b(V_a)^n \qquad W/m^2 . K \qquad (11)$$

Heat analysis in active solar still:

- Heat analysis in Photovoltaic Cell:

$$0 = GA - P_{pv} - Q_{tot} \qquad (12)$$

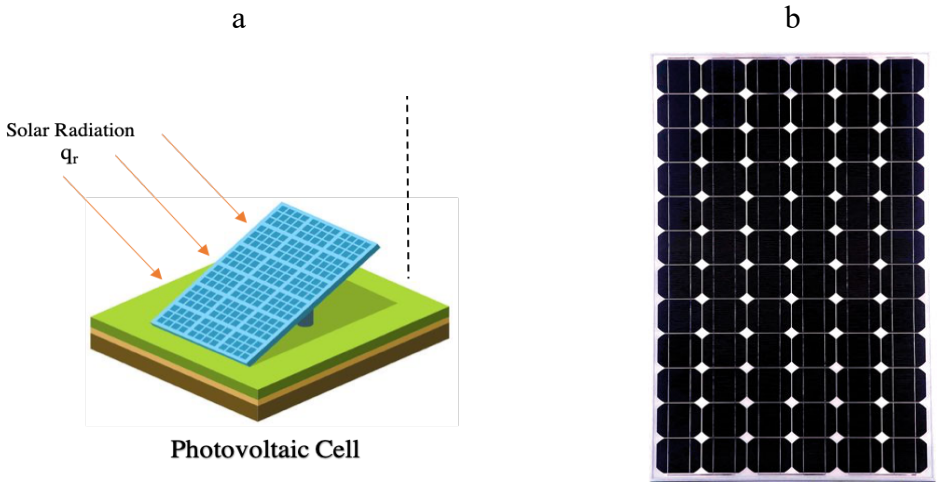

Figure 28: Integrated Heating Element: (a) Photovoltaic Cell, (b) PV Module/Cells

Where,

$$G = G_n . A - G_{rif} . A \qquad (13)$$

$$G_{rif} = \rho . G_n \qquad (14)$$

$$P_{pv} = \eta . G_n . A \qquad (15)$$

$$Q_{tot} = Q_{Conv,f} + Q_{rad,f} + Q_{Conv,b} + Q_{rad,b} \qquad (16)$$

G_n is the specific radiation incident on the module's surface (W/m^2); P_{pv} (W) is the electrical power generation, proportional to the total incident power; η is the photovoltaic conversion efficiency; G_{rif} is the total radiative power reflected from the surface of the PV module that is

proportional to the reflection index ρ [52]. Figure 29 explained the heat exchanges of PV module with storage battery.

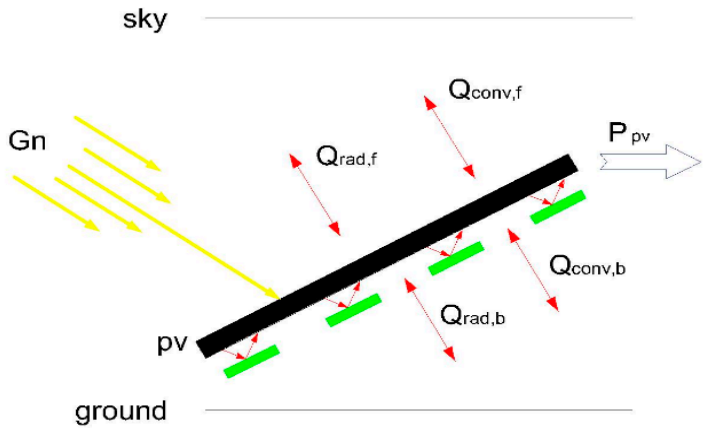

Figure 29: Heat exchanges of PV module with storage battery [52]

Heat loss analysis in PV module can be expressed as follow [53]:

$$\Delta T = \Phi * P_{heat} \qquad (17)$$

Where,

P_{heat} is the heat (power) generated by the PV module.

Φ is the thermal resistance of the emitting surface in °C W^{-1}; and

ΔT is the temperature difference between the two materials in °C.

$$\Phi = \frac{l}{K}\frac{1}{A} \qquad (18)$$

A is the area of the surface conducting heat.

l is the length of the material through which heat must travel; and

k is the thermal conductivity in units of W m^{-1} $°C^{-1}$.

$$P_{heat} = h\,A\,\Delta T \qquad (19)$$

Where:

A is the area of contact between the two materials;

h is the convection heat transfer co-efficient in units of W m^{-2} $°C^{-1}$; and

ΔT is the temperature difference between the two materials in °C.

$$P = \sigma T^4 \quad (20)$$

where:

P is the power generated as heat by the PV module.

σ is the Stefan-Boltzmann constant.

T is the temperature of the solar cell in K.

$$P = \varepsilon \sigma T^4 \quad (21)$$

where:

ε is the emissivity of the surface; and

the remainder of the parameters are as above.

$$P = \varepsilon \sigma (T_{Sc}^4 - T_{amb}^4) \quad (22)$$

T_{sc} is the temperature of the solar cell;

T_{amb} is the temperature of the ambient surrounding the solar cell; and

the remainder of the parameters are as above.

- Heat analysis in basin:

$$Q_{c,b-w} = Q_{c,b-amb} + I(t) * \propto_b * \tau_g * A_b \quad (23)$$

$$Q_{c,b-w} = I(t) * \propto_b * \tau_g * A_b \quad (24)$$

The internal heat transfer coefficient; heat transfer from water to glass cover inside the solar still is attained by three possible modes called evaporation, convection and radiation. Hence, total internal heat transfer coefficient of solar still is the sum of all three modes of heat transfer coefficients.

Where,

$$h_1 = h_{c,w-g} + h_{r,w-g} + h_{evp,w-g} \qquad W/m^2 . K \qquad (25)$$

Overall thermal efficiency of solar still:

Passive solar still:

$$\eta = \frac{\sum_{i=1}^{24} \dot{m}_{ew} L}{(t) A_b} X\ 100 \qquad (26)$$

Active solar still:

The overall thermal efficiency of active solar still is given by:

$$\eta_{active} = \frac{\left(\sum_{i=1}^{24} \dot{m}_{ew} L\right) + \left(\sum_{i=1}^{24} \dot{m}_{hw} C_p (T_{wo} - T_{wi})\right)}{\sum_{i=1}^{24} I * (A_b - A_c)} \qquad (27)$$

Hourly yield

$$\dot{m}_{ew} = \frac{Q_{e,w-g}}{L * A_b} \qquad kg/m^2 . hr \qquad (28)$$

Daily yield

$$M_{ew} = \sum_{i=1}^{24} \dot{m}_{ew} \qquad kg/m^2 . day \qquad (29)$$

2.5 Mathematical Solution

The subject governing equations for energy balances of the entire system and thermodynamic properties will be solved numerically by MATLAB program. Solving the same equations analytically is time consuming, stressful and boring. Not only detailed design equations for the system including solar still, feed and distillate tanks and photovoltaic cell will be presented in appendix B, but also MATLAB code of mathematical model equations will be showed along with detailed flow chart in the appendices. Solving governing equations using MATLAB program can predict solar still productivity and efficiency at different climatic and design parameters presented chapter 3 related to results and figures.

Chapter 3: A New Visual Library for Design and Simulation of a Photovoltaic Assisted Single Slope Solar Still / Methodology and Framework

3.1 Modeling and Design Setup (Methodology):

The proposed topic claims for modeling and simulation of an integrated solar cell heating element (photovoltaic cell) system accompanied with a single slope solar still for performance improvement, process optimization and efficiency enhancement. The main objective of this study is to develop a software using SIMULINK in order to design and simulate solar desalination systems single slope solar still and photovoltaic cell.

The developed software (SIMULINK) is designed for different analysis including different modifications, and comparisons. It has some features in that it has the quality of being logically, very flexible to use and easy to handle. In this work, designing a survey about the significance of utilizing a photovoltaic cell assisted with a single slope solar still for saline water desalination process is made.

Setting up and designing the required software for the proposed model system is performed. Carrying out the validation results is accomplished based on different techniques. As a result, a developed software package (Photovoltaic Cell Assisted with a Single Slope Solar Still) is established to model/design and simulate an active single slope solar still accompanied with a photovoltaic cell. Also, a comparison for other type of a passive solar still (without a photovoltaic cell) is performed for design and cost analysis.

As depicted in figure 30, the design model of the proposed system set up that is simulated using SIMULINK program comprises but not limited to the following components:

- Single Slope Solar Still (basin with a glass cover).
- Feed and Distillate Tanks.

- Photovoltaic Cell (Solar Cell).

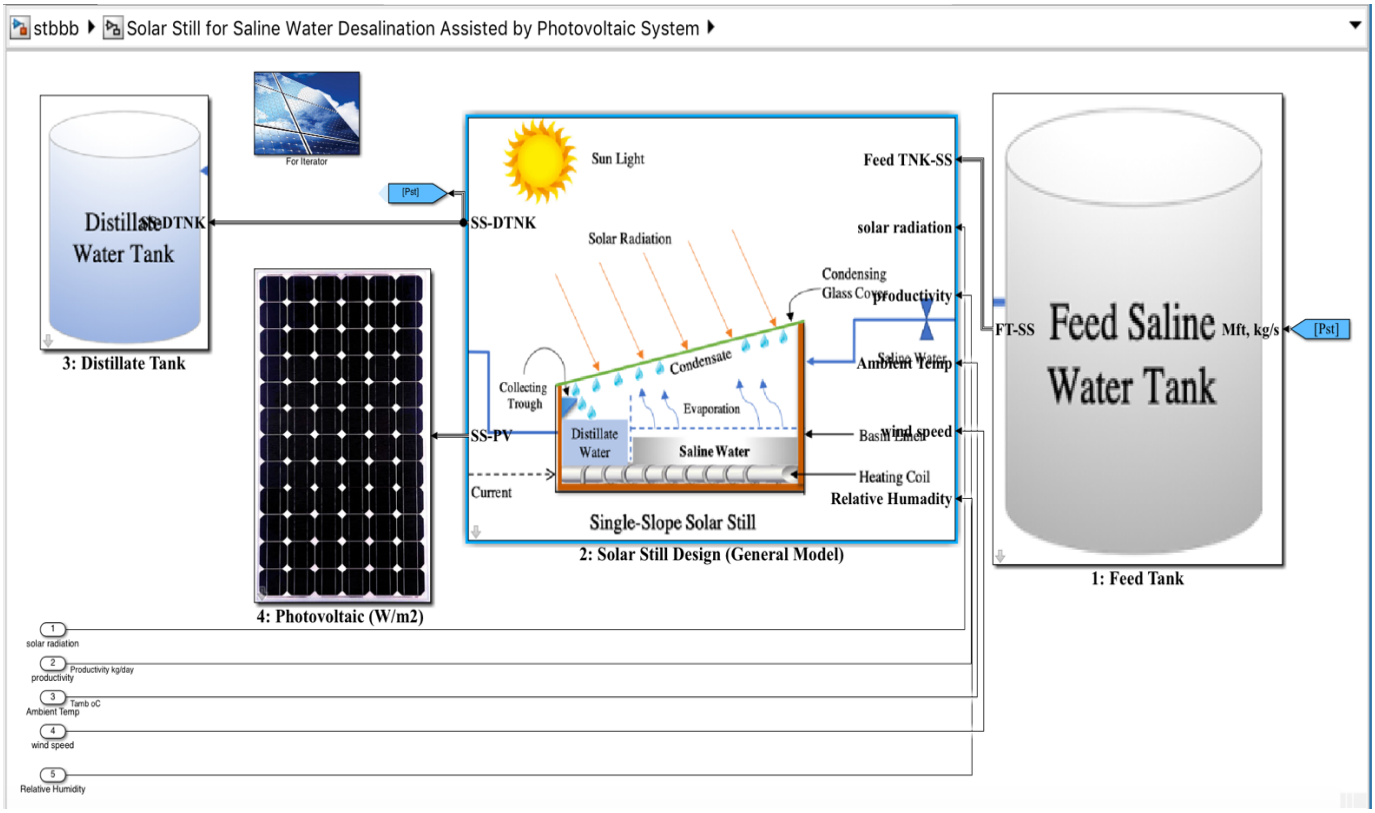

Figure 30: Design model of a proposed system in SIMULINK program

3.2 System and Process Description:

Saline Water from the storage feed tank will introduce the solar still (basin) through a single tube with 2 inches diameter and a valve, to maintain constant water level in the solar still. The purpose of the installed valve is to control the fed water mass flow rate. The amount of water inside the basin will be directly exposed to the sun light which in turn will absorb the solar thermal energy (radiation). Thus, that solar energy will increase water temperature causes it to evaporate. The evaporation process will take place when there is a temperature difference between basin water (high) and glass cover (low). The addition of the black dye inside the still basin was placed and considered as part of the modeling to figure out the effect and behavior of the still productivity [40]. A transparent cover made of glass or plastic will be installed at the top of the basin with an

inclined angle to facilitate condensate transfer to the collection trough. Normally the area of the glass cover is less than the area of the basin base due to the tilted angle required in the model design. The area underneath the basin was filled with a liner made from a saw dust for insulation purpose. In order to facilitate the deflection of the condensate return into the collection trough; a small glass piece obstruction was fixed on the inside surface of the glass cover. The gliding distillate/freshwater from the trough will further be transferred into the distillate tank through a 2-inch piping with an installed valve to control the level of the distillate tanks. A photovoltaic (solar) cell is to be installed and integrated with the single slope solar still in order to take the advantage of absorbing the solar intensity. The solar energy will be converted to electrical energy (as a DC current) which in turn will be utilized to heat up the water inside the basin through a heating coil. The objective of the solar cell is to increase distillate water production during nocturnal period and enhance the system's performance and efficiency [54].

3.3 A New Modeling Technique for PV Modules:

Under the industrial revolution, the renewable sources of energy such as solar, geothermal and winds are appealing great attention as an alternative energy as fossil fuels. The photovoltaic (PV) is one form of the renewable energy sources, which is broadly engaged in many low power applications. It is a renowned system that is largely been employed in electric power generation applications. The PV module is considered as the major power conversion unit for a PV generator system. A professional and efficient simulation model of the PV is badly desired, because while designing a process accompanied with a PV powered system, a simulation must be performed for system analysis and parameter settings.

The simulation of PV and solar still system is primarily based on the performance model through using parameters, for instance, temperature distribution, cell performance, cell physical size etc.,

and by assuming the design and physical parameters. In the current case study, the highlight will be on how to build a simulation model-based design technique of modeling the entire system, since the modeling will create the design parameters associated to performance.

The developed model for PV is built based on design technique aspects of modeling but not performance technique. It is worth to mention that in the design model (current model system), the PV input power is assigned and identified in order to estimate and measure the design limits such as, areas, diameters, current, voltage, module efficiency, required costs, etc. On the other hand, in the performance model, design parameters such as areas, current, voltage, and design limits are assigned to compute and measure the power, efficiency, and system performance [55].

3.4 PV & Solar Still Process Modeling Techniques:

Industrial plants comprise several processes units which are integrated to each other. Normally, processes configurations and designs can be acquired when using such wide range of process units. A flexible and reliable computer programs are essential in order to comprehend the behavior of several process units at different operational conditions. By using these subject programs, a lot of flow sheeting problems can be well organized and analyzed. These types of processes problems can be divided into two categories: (a) design problems (current model system) and (b) performance problems. In the design problems, some design parameters such as areas, dimensions, voltage, current, number of cells, unit cost, etc. and feed variables are left unspecified and become unknown to be determined. Though, in the performance problems, the variables accompanying with the feed streams to a process unit in addition to all design parameters such as PV module area, and PV panel's dimensions are assumed to be identified, but the variables associated with the input and output streams are to be unknowns. The superpower of the PV module is basically the boarder streams of the process unit and usually it is known.

Numerous real data are taken from a real manufacture manual of each module type in order to simulate and predict the characteristics of different types of PV system. It is expected that the design limits are to be calculated through identifying the output power from the system application. The PV system is designed and modeled according to the actual data presented through hundreds of collected data points as inputs from manufacturing manuals or literature paper. MATLAB – SIMULINK (http://www.mathworks.com/index.html) browser is availed in order to model and visualize the PV and solar still system program. The design limits for the PV can be summarized as follow:

1. The open circuit voltage (V) and the short circuit current (A).
2. The maximum voltage (Vm) and current (Im).
3. The module and cell efficiencies (%).
4. The number of cells and modules of the system.
5. The module and PV system weights (kg), dimensions (m^3) and areas (m^2).
6. The battery bank capacity.
7. The total costs of the PV system ($).

Regarding the solar still system, the design limits can be summarized as follow:

1. The system dimensions, areas, and efficiency:
    - Solar still area, A_{st} m^2.
    - Glass cover area, A_g m^2.
    - Cover tilted angle degree, ^{o}.
    - Insulation thickness, cm.
2. Brine depth (d, cm) and productivity, $kg/m^2.day$.
3. basin water temperature and temperature differences between water and glass cover.

4. Thermal load inside the still (Q_{load} on photovoltaic cell), kW.
5. Thermodynamic properties including the following:
    - Evaporation Energy (Q_{ev}), kW.
    - Heat transfer between brine water and glass cover by radiation (Q_{rw-g}), kW.
    - Heat transfer between glass cover and the ambient (Q_{rg-amb}), kW.
    - Convective heat transfer coefficient between water and cover (h_c), W/m^2 ^oC.
    - Evaporative Convective heat transfer coefficient between water and cover (h_{evp}), W/m^2 ^oC.
    - Evaporation exergy and total exergy destruction rate (Exev & I_{total}), kW.

MATLAB toolbox is availed to predict the characteristics correlations based on a non-linear technique. MATLAB toolbox support the user to build a new model library by the assist of the graphical user interface. The built modules can be constructed by using the lookup-table correlation method. Figures 31&32 explained the photograph of the software library that represents the PV and solar still design models and parameters. Another benefit is that user can simply drag and drop the module or the unit from the side library to construct and build the whole system [56].

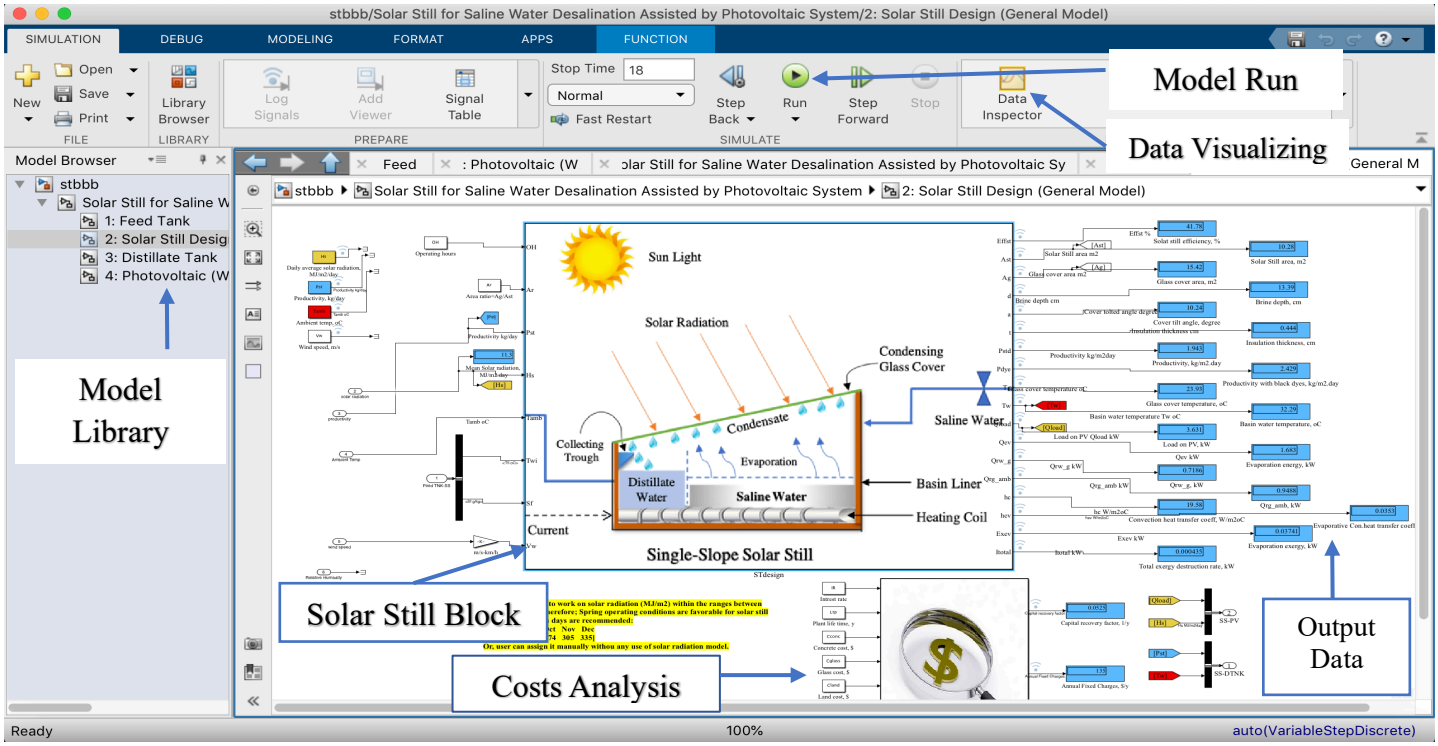

Figure 31: Photograph of the developed design for solar still system

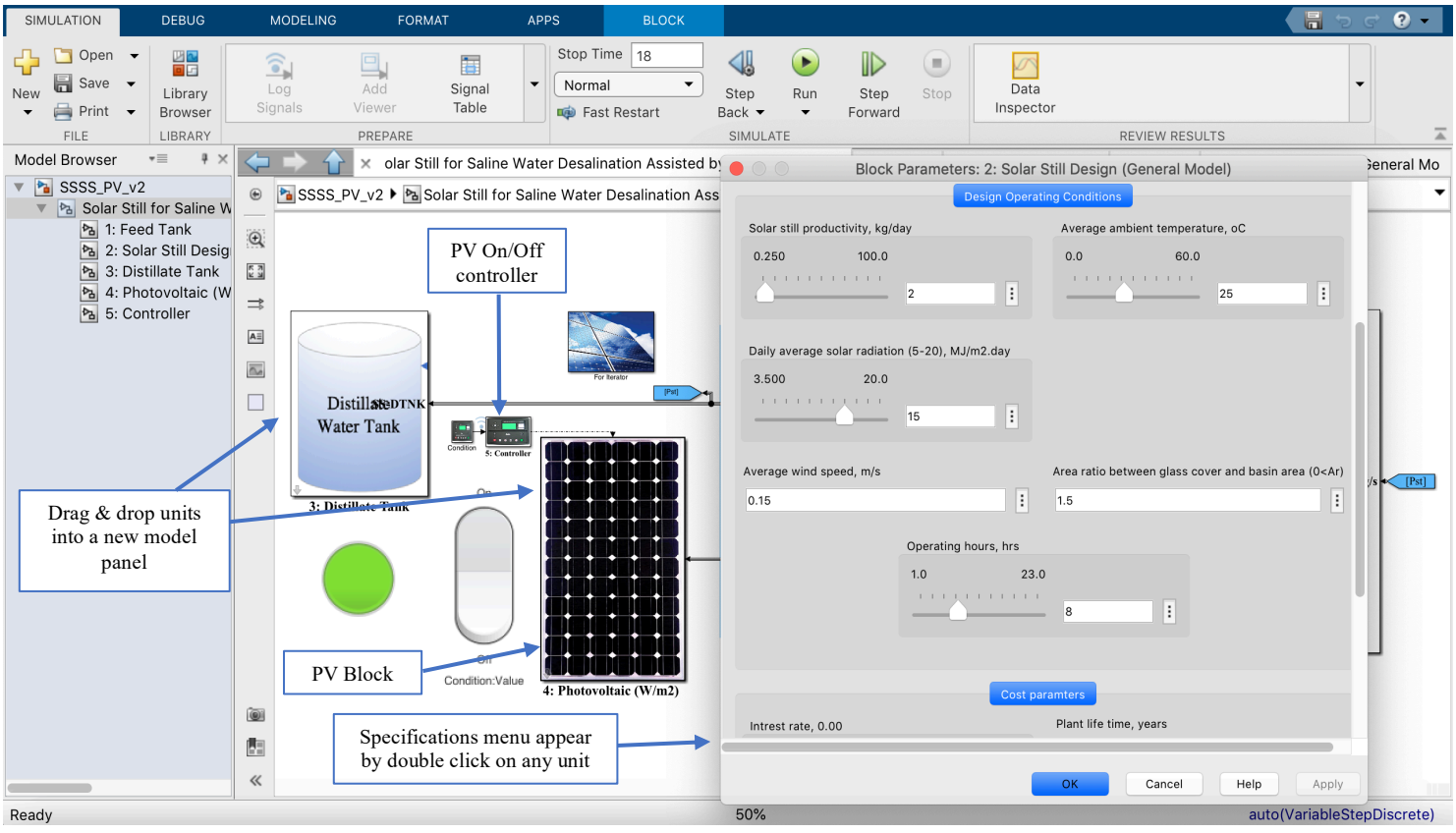

Figure 32: Photograph of the developed design for PV & solar still design parameters

3.5 The New Modeling Techniques for PV and Solar Still:

The PV model that is presented in this work is renowned and totally differ from any other common models in the literature. The main alteration of the model indicated that the actual data collected and presented in the core code of the model is performing the code itself. This technique concluded that data that are fed into the core of the MATLAB code to provide a real sense of the curve fitting. The method that is availed in the model is the use of polynomial lookup tables of Simulink toolbox (polynomial interpolation).

3.5.1 Lookup Table Method for PV:

Figure 33 showed a schematic diagram of the n-D lookup table polynomial method that evaluates a sampled representation of a function in N variables y = F (x1, x2, x3, ..., xn) where the function F can be empirical. The n-D lookup table block plots inputs to an output value by looking up or interpolating a table of values that is defined with block parameters. The n-D block supports flat (constant), linear, and cubic-spline interpolation methods. In breakpoint data sets, in case of matching the values of indices, it outputs the table value at the intersection of the row, column, and higher dimension breakpoints.

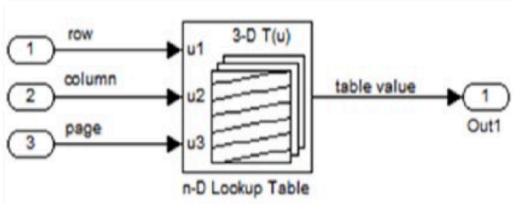

Lookup table block under SIMULINK toolbox can insert the actual data as a matrix. The data can be arranged as a row, column and page. The figure shows the data row versus the breakpoints row.

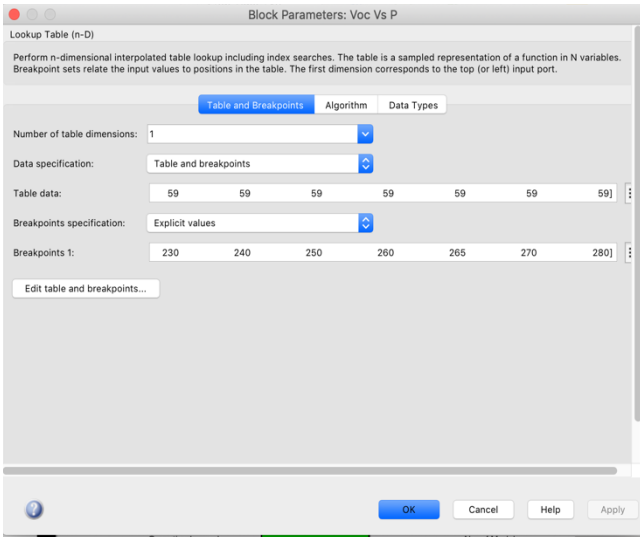

Figure 33: Schematic diagram of the n-D lookup table

The main benefit of such method is that user can easily identify one or two parameters to get many parameters. Only the user has to feed the lookup table with the accurate and required data from the data manual. On the other hand, in case of no matching of the values of indices in breakpoint data sets, but if within range, then interpolates proper table values, by using the interpolation method. In case of nonmatching data that are out of range, then extrapolate the output value, by using the extrapolation method [57]. In this study, the range of the operating module type is from 5 to 280 Watt. Each module watt type can calculate the module specification based on the data inserted in the table. Regarding the module power, the following code can be designed and calculated. The number of PV modules (NOM) could be calculated based on total power and module power as follow:

$$NOM = \frac{THP}{P_m} \qquad (30)$$

And the module area m^2 can be calculated:

$$A_m = \frac{(100 * P_m)}{(Is * EM)} \qquad (31)$$

The total area can be computed as follow:

$$A_t = A_m * NOM \qquad (32)$$

The cell area (cm^2) based on the number of cells (NC) is calculated from the lookup table:

$$BS = \frac{(OH * NOC * THP)}{DOD * Effb} \qquad (33)$$

If a 24-V system is chosen, then the required *AH* of batteries = 16,585/24,700 AH:

$$AH = \frac{BS}{V_m} \qquad (34)$$

The number of batteries can be calculated based on the maximum voltage and the battery voltage as follow:

$$NOB = V_m * \left(\frac{NOM}{V_b}\right) \qquad (35)$$

3.5.2 PV Cost Analysis:

The PV system total costs in (PVCt, $) are then calculated based on the full overboard costs of the modules (FOB price) and the battery costs (Cb):

$$PV_{Ct} = (THP * FOB_c) + (Cb * NOB) \qquad (36)$$

Since the FOB price ($/watt/module) contains the connections, cables, inverter unit, the maintenance costs, and workers' time. The model browser of the PV under the construction of polynomial look up table method is illustrated in figure 34. The obtainable model related to above method has some important characters, by excluding the need for user to deal with complex code or equations, For instance:

1. Flexible model handling: the model system can be easily built by the use of the lookup table block; however, the hardest part is when collecting and arranging the desired data vector.
2. The key specifications can be simply calculated based on one parameter, in that the identification of the module power can drive out nine parameters, but in the other modeling techniques, it is not found that one parameter can result out in nine parameters. It is worth mentioning that such technique of modeling is not investigated before [58].

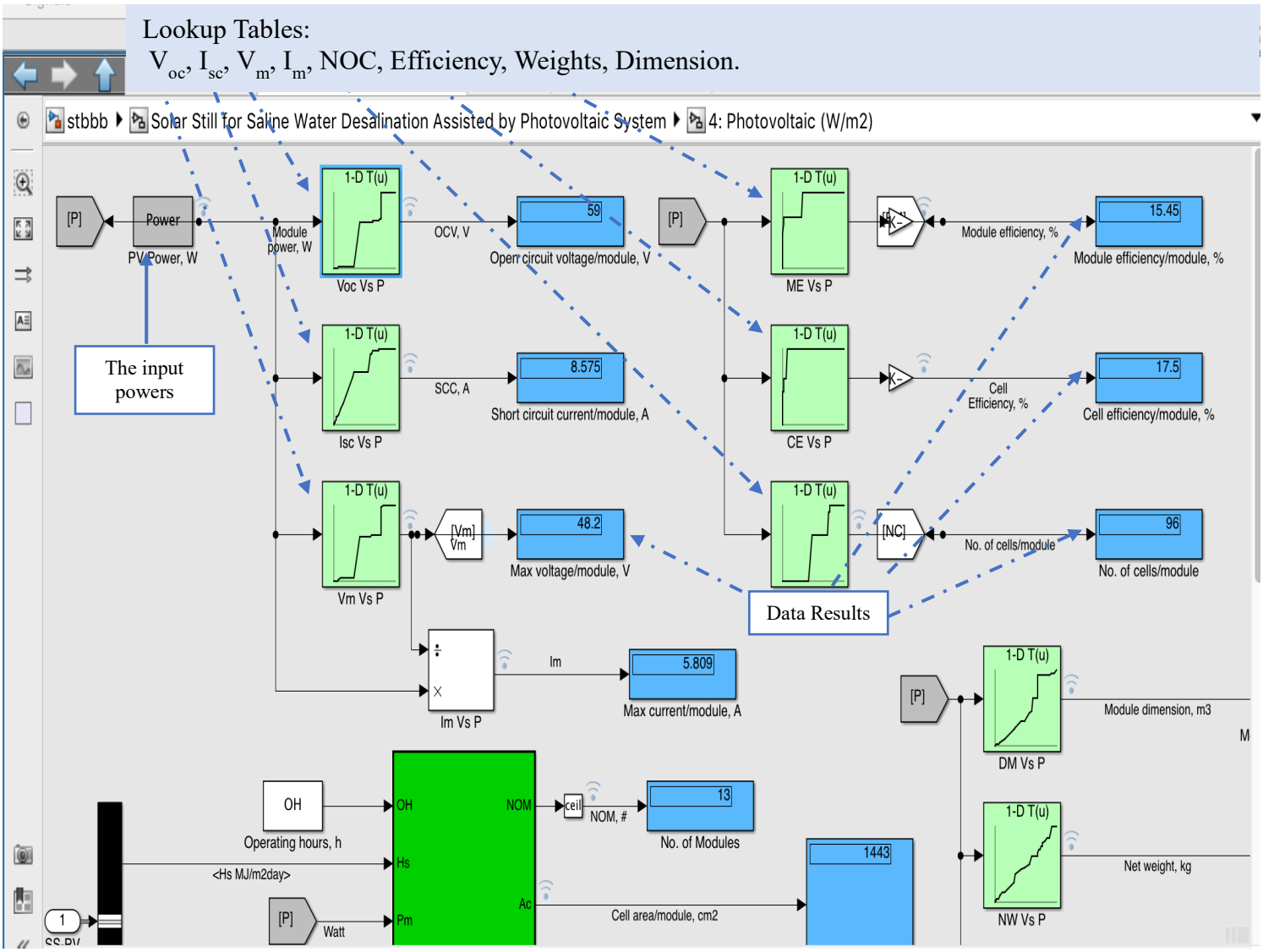

Figure 34: Lookup tables results for PV model browser

3.5.3 Lookup Table Method for Solar Still:

The solar still model system is designed and simulated through the same platform. A visual library is inserted into the Simulink browser by the aid of graphical user interface (GUI) modeling. Figure 30 illustrates the photograph of the solar still library under Simulink browser. The main advantage of using the lookup table method is that the actual data (3200 points) are stored where the model manipulates its real validity based on the real points fitting. The mathematical model could be correlated based on the actual data points stored in the table model. Figure 35 depicts the signal

builder tool which has been utilized from library browser, dragged and dropped into the environment model browser. As explained previously, a hundred data points for each input parameter such as solar radiation, ambient temperature, productivity and wind speed are extracted and fitted by the curve fitting toolbox using the signal builder tool. The subject inputs values are taken within daytime between 9:00 a.m. and 6:00 p.m. Spring operating conditions are favorable for solar still inputs and it is recommended to work on solar radiations (MJ/m^2). The data were obtained and collected from literature in the field of solar stills.

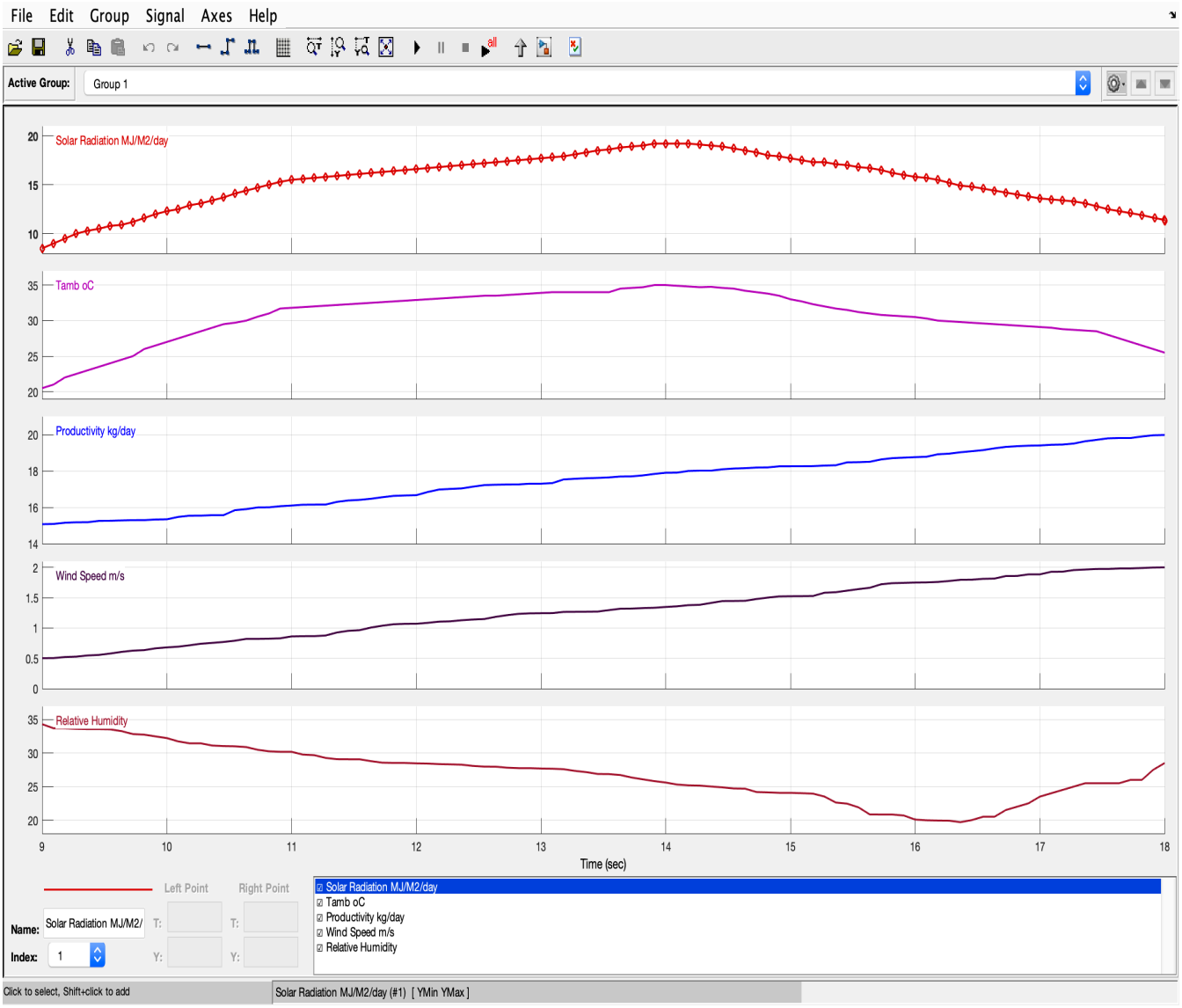

Figure 35: Signal Builder model browser from SIMULINK

The data points are fitted by the curve fitting toolbox. The design code of the solar still falls behind the analysis block of the basin through double clicking the photograph itself. The model is presented and correlated as a function of solar still according to the following design equations:

Solar still productivity based on still area P_{std} kg/m^2.day:

$$P_{std} = (0.244 * H_s) - (0.0294 * T_{amb}) - (0.0073 * V_w) - 0.01222 \qquad (37)$$

Still productivity with black dyes, kg/m^2.day:

$$P_{dye} = 1.2122 * (P_{std})^{1.0467} \qquad (38)$$

Solar still area & glass cover area, m^2:

$$A_{st} = \frac{P_{st}}{P_{std}} \qquad (39)$$

$$A_g = A_{st} * A_r \qquad (40)$$

Solar still brine depth, cm:

$$d = \frac{\left(\log\left(\frac{P_{std}}{4.196}\right)\right)}{-0.0575} \qquad (41)$$

Cover tilt angle degree & insulation thickness, cm:

$$a = 1.763 * exp(0.9057 * P_{std}) \qquad (42)$$

$$t = \left(7.913e^{-5} * exp(2.073 * P_{std})\right) * 100 \qquad (43)$$

Solar Still efficiency & volume:

$$Eff_{st} = \frac{(P_{std} * 2.43 * 100)}{H_s} \qquad (44)$$

$$Vol_{st} = A_{st} * \left(\frac{d}{100}\right) \qquad (45)$$

Thermal load inside the still, kW:

$$Q_{load} = \frac{\left(H_s * 1000 * A_{st} * taw_g * alfa_g\right)}{(OH * 3600 * PC)} \qquad (46)$$

Water temperature difference inside the still, oC:

$$dT_w = \frac{(Q_{load} * 1 * 3600)}{\left(\rho(T_{wi}, S_f) * Vol_{st} * fCp(T_{wi}, S_f)\right)} \qquad (47)$$

Water temperature inside the basin, ^oC:

$$T_w = dT_w + T_{wi} \qquad (48)$$

Evaporation heat transfer, kWatt:

$$Q_{ev} = \left(\frac{P_{std}}{(OH * 3600)}\right) * f\ lh(T_w) * A_{st} \qquad (49)$$

Sky temperature, ^oC:

$$T_{sky} = 0.0552 * ((T_{amb} + 273)^{1.5})$$

Convection heat transfer coefficient between water and cover W/m^2 ^oC:

$$h_C = \frac{(1000 * Q_{ev})}{\left(A_{st} * (T_w - T_g)\right)} \qquad (50)$$

Evaporative convective heat transfer coefficient between water and cover W/m^2 ^oC:

$$h_{ev} = \frac{\left(16.273 * exp(-3) * h_C * (P_w - P_g)\right)}{(T_w - T_g)} \qquad (51)$$

The heat transfer from the water to the cover by radiation, kWatt:

$$Q_{rw-g} = \frac{\left(A_g * 0.9 * (5.67e^{-8}) * \left((T_w + 273)^4 - (T_g + 273)^4\right)\right)}{1000} \qquad (52)$$

The heat transfer from glass cover to the ambient, kW:

$$Q_{rg-amb} = \frac{\left(A_g * 0.9 * (5.67e^{-8}) * \left((T_g + 273)^4 - (T_{sky})^4\right)\right)}{1000} \qquad (53)$$

Evaporation exergy, kW:

$$Ex_{ev} = Q_{ev} * \left(1 - \left(\frac{(T_{amb} + 273)}{(T_w + 273)}\right)\right) \qquad (54)$$

Exergy destruction rate, kW:

$$I_{total} = \left(\frac{P_{st}}{(OH * 3600)}\right) * Cp(T_{wi}, S_f) * (T_w - T_{amb}) * \left(1 - \left(\frac{(T_{amb} + 273)}{(T_w + 273)}\right)\right) \qquad (55)$$

Latent heat of distillate vapor evaporation, kJ/kg:

$$Lh = 2499.5698 - (2.204864 * T) - (2.304 * 10^{-3} * T^2) \qquad (56)$$

Vapor pressure of water, bar:

$$P_{vw} = 0.01677 * exp(0.04133 * T) \qquad (57)$$

Tank cross sectional area, m^2:

$$A_{ft} = \left(\frac{\pi}{4}\right) * {D_{ft}}^2 \qquad (58)$$

Level change in the tank & total head, m:

$$dH = \frac{M_{ft}}{(\rho(T_{ft}, S_f) * A_{ft})} \qquad (59)$$

$$Ht = Hs - dH \qquad (60)$$

Flow velocity out from the tank, m/s:

$$A_{tube} = \left(\frac{\pi}{4}\right) * {D_t}^2 \qquad (61)$$

$$V_f = \frac{\left(\frac{M_{ft}}{(OH * 3600)}\right)}{(\rho(T_{ft}, S_f) * A_{tube})} \qquad (62)$$

Tank pressure, kPa:

$$P_{ft} = \frac{\left((\rho(T_{ft}, S_f) * 9.81) * \left(H_t - \left(\frac{{V_f}^2}{(2 * 9.81)}\right)\right)\right)}{1000} \qquad (63)$$

Feed & distillate tanks volumes, m^3:

$$Vol_{ft} = A_{ft} * dH \qquad (64)$$

$$Vol_{dt} = A_{dt} * dH \qquad (65)$$

Tank cross sectional area, m^2:

$$A_{dt} = \left(\frac{\pi}{4}\right) * {D_{dt}}^2 \qquad (66)$$

Level change in the tank, m:

$$dH = \frac{M_d}{(\rho(T_{dt}, S_d) * A_{dt})} \qquad (67)$$

The number of modules could be calculated based on total power and module power:

$$NOM = \frac{THP}{P_m} \qquad (68)$$

Solar radiation from MJ/m^2.day to W/m^2:

$$Is = \frac{(Hs * 1 * 10^6)}{(OH * 3600)} \qquad (69)$$

3.5.3 Solar Still Cost Analysis:

There are several elements that affect the cost of distillate water produced and acquired by solar desalination unit. The investor that would like to construct or design a photovoltaic cell assisted with a solar desalination system would evaluate the process based on some indicators regardless design limits such as total/ specific solar field area (m^2) , area of desalination unit (m^2), total exergy destruction rate (I_{total}, kW) and water cost per liter ($/L). The key economic profit of solar desalination system is that it can be easily located and simply designed, installed, operated and maintained. Besides, it should not require much infrastructure. Further, unit size, site location, feed water properties and quality are factors that influence both the total (running) and capital cost. The better economic profit on the investment relies on distilled water production cost and its

applicability. As depicted in figure 36, the cost analysis of the solar desalination system is a function of main calculation parameters including but not limited to the capital recovery factor (CRF), Annual fixed charge (AFC), cost per liter (CPL) and total capital cost (TCC).

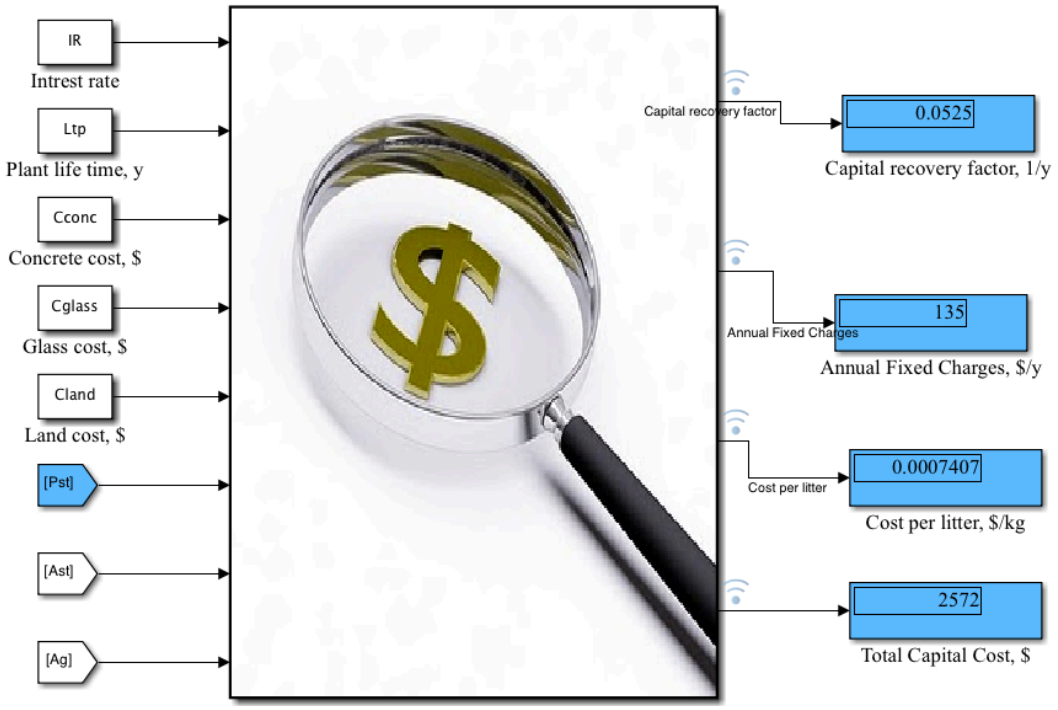

Figure 36: Solar still cost analysis

All aforementioned cost analysis parameters can be expressed in the following equations:

The capital recovery factor can be estimated based on the following relation:

$$CRF = \frac{i * (1+i)^{Ltp}}{(1+i)^{(Ltp-1)}} \qquad (70)$$

Where, i is the interest rate per year set as 5%, Ltp is the plant lifetime and assumed to be 25 years in this model. For the current solar desalination plant, the annual fixed charges in $/year can be estimated as follow:

$$AFC = TCC * CRF \qquad (71)$$

Where, TCC is the total capital cost that should be computed based on solar still area, glass cover area and cost, concrete and land cost:

$$TCC = \left(A_{st} * C_{conc} + A_g + C_{glass} + C_{land} * A_{st}\right) + 0.15 * \left(A_{st} * C_{conc} + A_g * C_{glass} + C_{land} * A_{st}\right) \quad (71)$$

Finally, the CPL (cost of distilled water per liter) can be calculated by dividing the annul fixed charges (cost of the system) to the annual yield of the solar still thorough the plant lifetime.

$$CPL = \frac{AFC}{(P_{st} * Ltp * 365)} \quad (72)$$

3.5.4 Feed Tank Process Modeling Technique:

The feed tank represents the upstream unit in which saline/ brackish water retain before it is introduced to the solar still. The below figure 37 illustrates the design analysis to model the tank with respect to its location and dimensions. The most critical parameter for seawater is its density and specific heat capacity Cp which are functions of feed salinity (ppm) and water temperature (ºC).

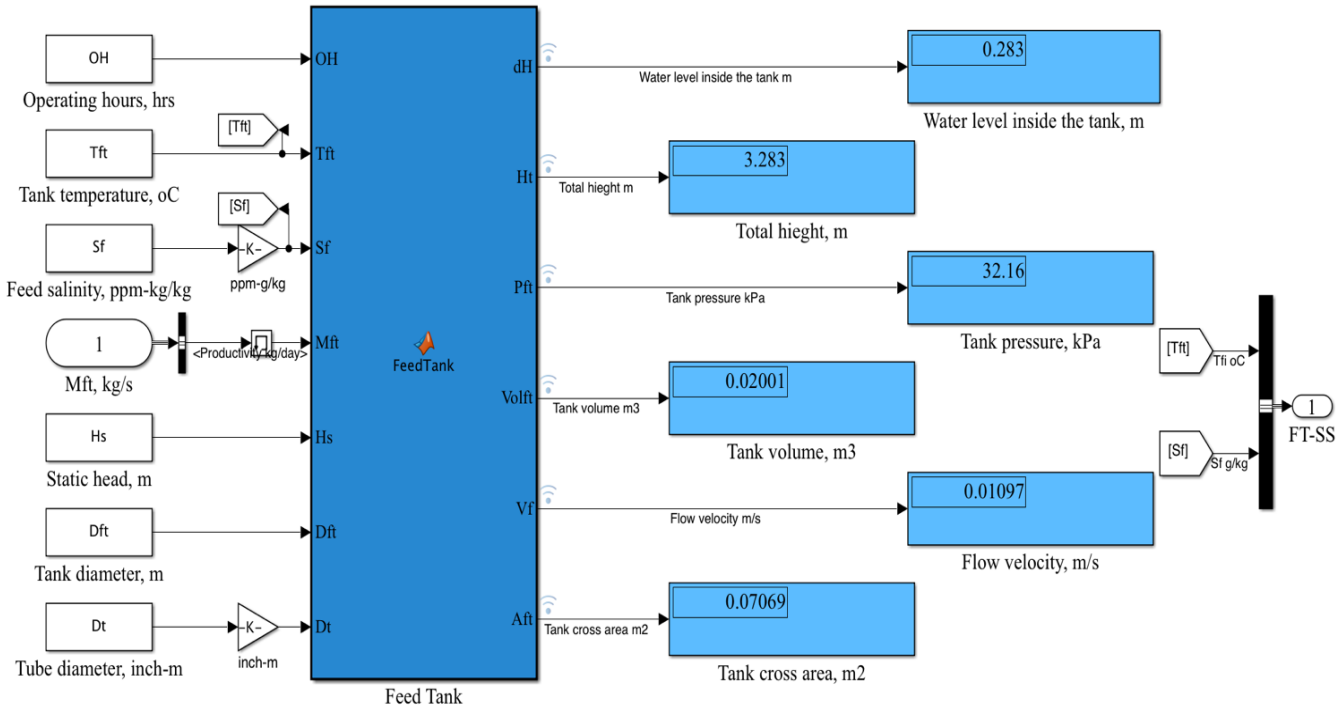

Figure 37: Feed tank model browser

The following design equations are considered in modeling the feed tank:

Feed tank cross sectional area, m^2 where D_{ft} is feed tank diameter:

$$A_{ft} = \left(\frac{\pi}{4}\right) * \left({D_{ft}}^2\right) \qquad (73)$$

The water level inside the tank (dH, m) and total height (m) can be expressed as follow where M_{ft} (kg/day) is water production from the still and Hs is the mean solar radiation (MJ/m^2.day):

$$dH = \frac{M_{ft}}{(\rho * A_{ft})} \qquad (74)$$

$$Ht = Hs + dH \qquad (75)$$

The flow velocity (m/s) out from the tank is follow where A_{tube} is the pipe cross sectional area (m^2):

$$A_{tube} = \left(\frac{\pi}{4}\right) * D_t^2 \qquad (76)$$

$$V_f = \frac{(\frac{M_{ft}}{OH * 3600})}{(\rho * A_{tube})} \qquad (77)$$

Feed tank pressure (kPa) and volume (m^3) are as follow:

$$P_{ft} = \frac{\rho * 9.81 * (Ht - \frac{{V_f}^2}{(2 * 9.81)})}{1000} \qquad (78)$$

$$Vol_{ft} = A_{ft} * dH \qquad (79)$$

3.5.5 Distillate Tank Process Modeling Technique:

The distillate tank act for the downstream unit and last component of the system. It receives the freshwater product directly from the solar sill through a pipe. As presented in figure 38 beneath, the distillate tank design parameters comprise but not limited to water level inside the tank and tank dimensions including tank diameter and cross-sectional area. The level change in the tank

depends on distillate water production, density. As explained in feed tank design analysis, the water density and specific heat capacity Cp are functions of water temperature (°C) and salinity (ppm). Therefore, basin water temperature Tw considered as a major parameter that affects the level change inside the distillate tank.

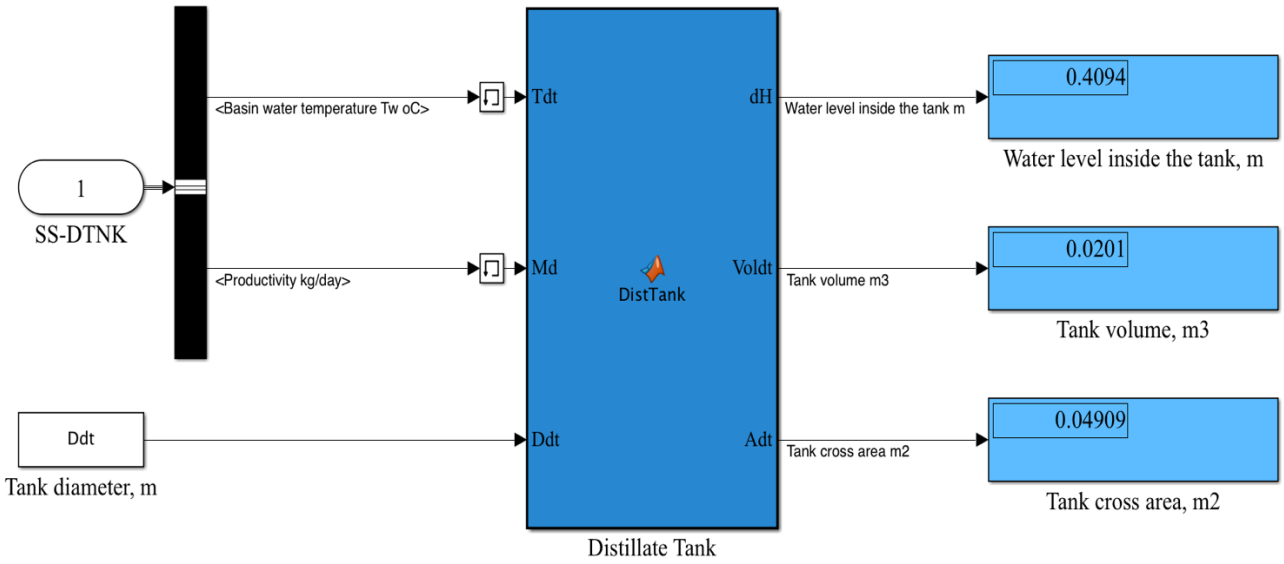

Figure 38: Distillate tank model browser

The following design equations are considered in modeling the distillate tank:

Distillate tank cross sectional area, m^2 where D_{dt} is distillate tank diameter:

$$A_{dt} = \left(\frac{\pi}{4}\right) * \left({D_{dt}}^2\right) \qquad (80)$$

The water level inside the tank (dH, m) and total height (m) can be expressed as follow where M_{dt} (kg/day) is water production from the still:

$$dH = \frac{M_{dt}}{(\rho * A_{dt})} \qquad (81)$$

Distillate tank volume (m^3) is as follow:

$$Vol_{dt} = A_{dt} * dH \qquad (82)$$

Chapter 4: Results and Discussions

4.1 Introduction:

In this work a design model system has been thoroughly carried on a photovoltaic cell assisted with a single slope solar still using a SIMULINK design analysis. As depicted in figure 35, a hundred-point input data such as solar radiation, ambient temperature, productivity and wind speed is collected and fitted into a signal builder browser, that is identified in the main environment model. These input data are essential to generate the design outputs of the entire system by utilizing the established design code and mathematical model. The design output data include but not limited to solar still area and efficiency, productivity per unit area of the still, thermodynamic properties and cost analysis. In addition, it comprises the photovoltaic design analysis such as total system area, required number of modules and load, battery efficiency etc. The designers would become able to put in mind the solar still dimensions before the establishment operations. By clicking run which is located in the simulation tap, the model system is operated continuously for nine hours from 8:00 a.m. to 6:00 p.m. under different fitted climatic conditions (signal builder) to generate output figures. Investigations were targeted to enhance the still output through improving its operating condition by using a flat plate collector FPC of a photovoltaic cell. The brackish water, glass cover, and tanks dimensions are considered as well by integrating the belonging design equations of the feed water temperature and salinity (ppm) with each component of the system. An engineer/ designer has to set a certain productivity (as an input in signal builder) of a such water treatment plant to produce x kg of distillate water per day per unit area of the still. On the other hand, while validating the system performance, the state-of-the-art claims for having the design parameters such as still area and dimensions ready to enhance the system efficiency and improve its performance. Numerical results are presented in tables (C.1-11) refer to Appendix C.

4.2 Design Results for Solar Still Areas:

As shown in in the below 3-D mesh figure 39, the design model correlates the still solar radiation and productivity with the still area, and it is concluded that the still area (m^2) is directly proportional to the system's productivity (kg/day), in that area is increased by rising its productivity, but with lower value of the solar intensity (MJ/m^2.day). As solar radiation increase, the rate of brine water evaporation inside the still increased with respect to the ambient temperature. Thus, lower required area for the still design. On the other hand, the rest of still areas figures corelate the ambient temperature and productivity. The subject figure is generated through utilizing SIMULINK browser and are presented in data inspector.

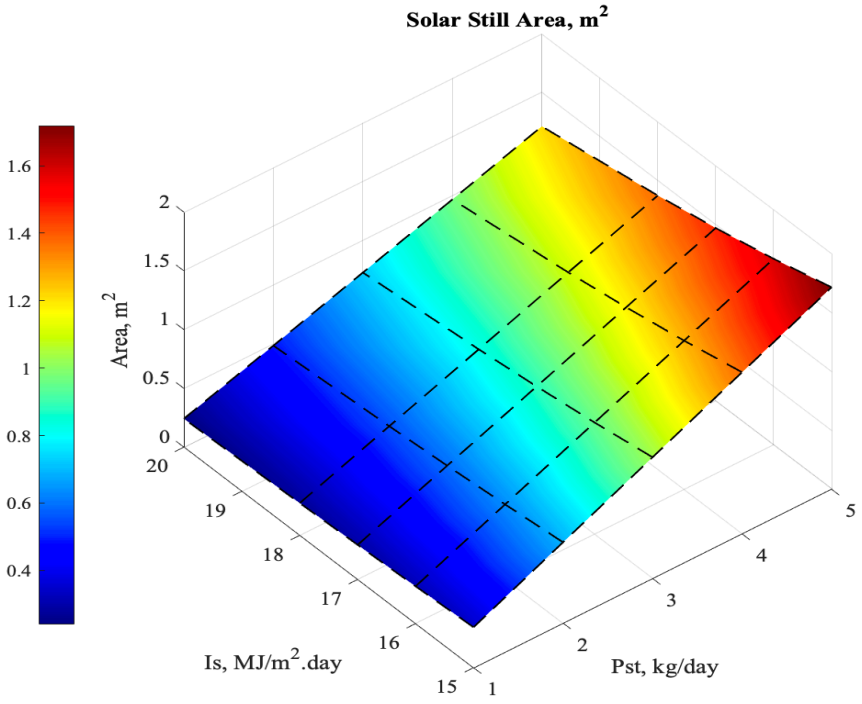

Figure 39: Solar still designed areas, m^2

The next figure 40 has exactly the results but presented in a contour style with numbers to accurately display the exact results of the still area.

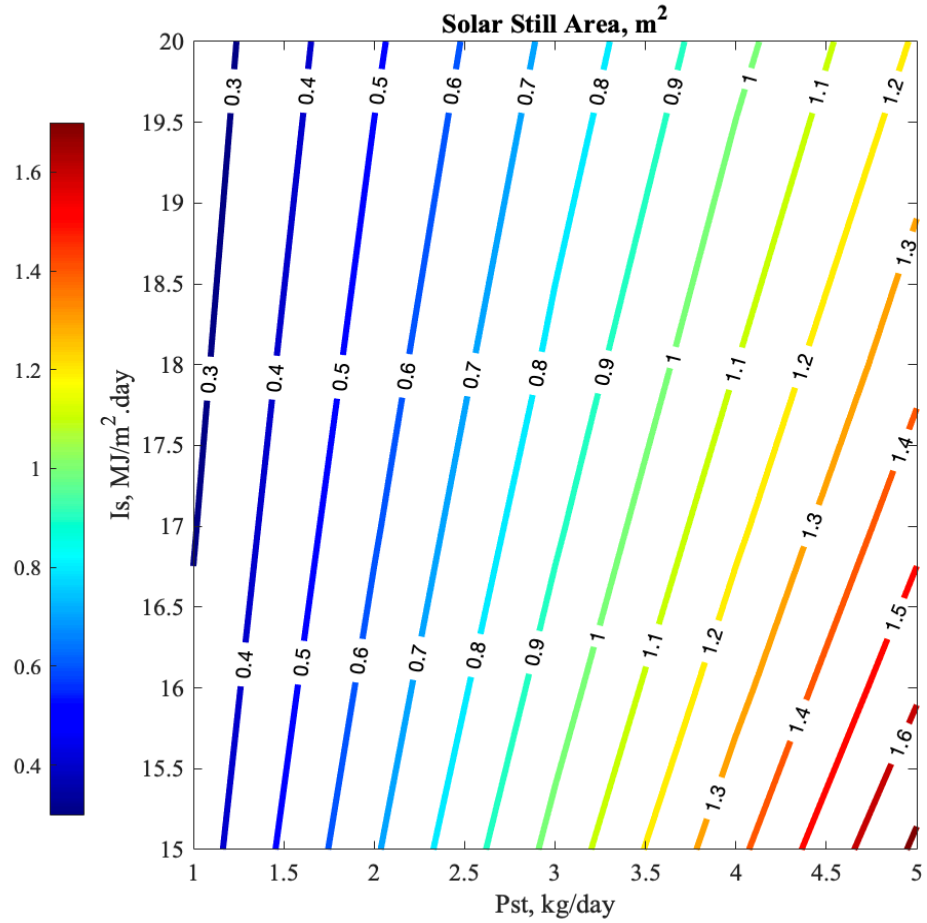

Figure 40: Solar still designed areas, m^2

The other parallel figures 41 represent solar still areas at different solar radiation values (MJ/m^2.day). As illustrated below, when the ambient temperature increased it is required to consider a high still area with respect to the solar radiation which in turn should be low. The temperature gradient (T_W-T_g) between the brine level inside the still and glass cover is a critical thermodynamic property in order to attain the desired and optimal rate of evaporation with respect to solar incident (Is) during the daytime. It is obvious among the all four parallel figures that the highest value of solar radiation is desirable with respect to the ambient temperature, thus will required the lowest still design area and that will save the design and construction costs. It is worth to mention that all results and figures of the still areas are showing the same consistency.

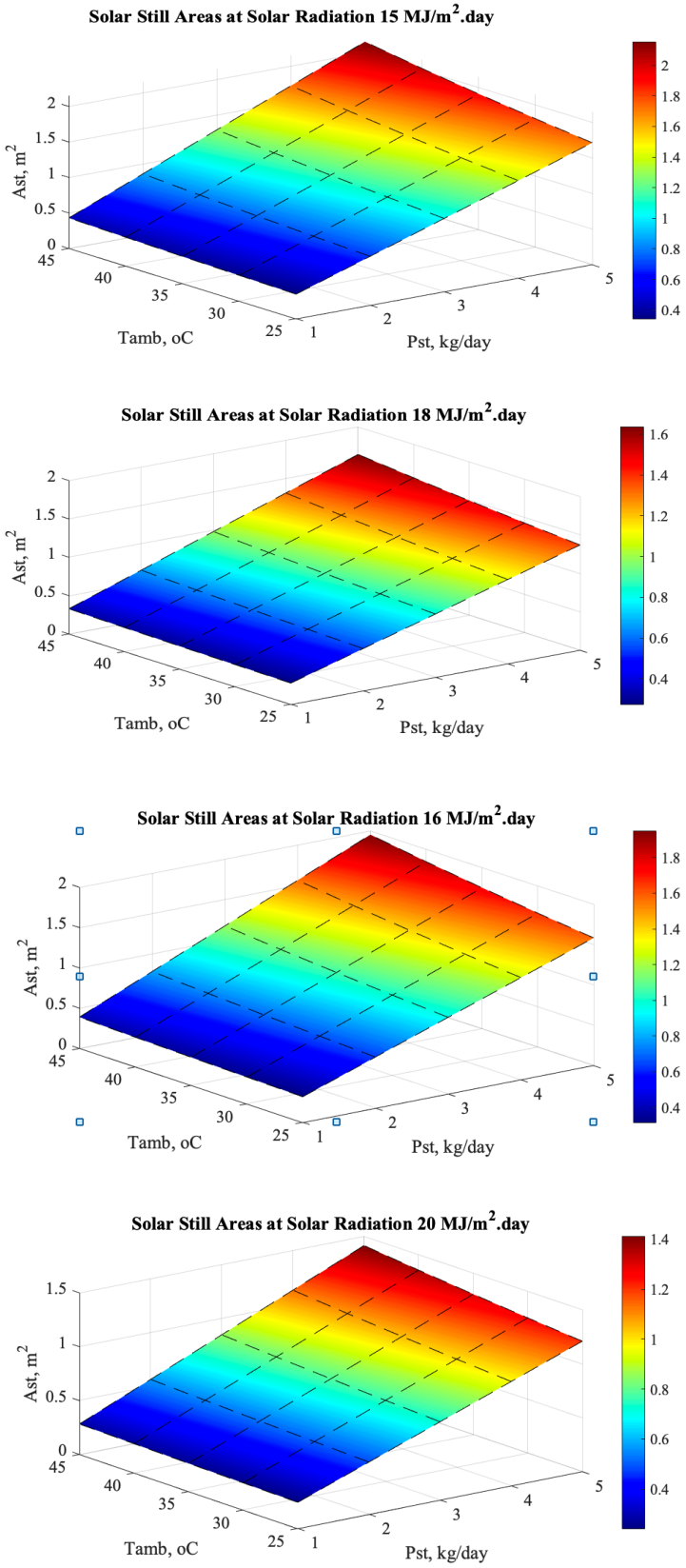

Figure 41: Solar still areas at different solar radiations values, m^2

A 2-D figure 42 can be established as well to clearly demonstrate the solar still design areas at different productivities ranges starting from 5 to 10 kg/day (blue) and from 15 to 20 kg/day (orange). As exhibited in below figure 40, an area required to design a solar still system is almost 11 m^2 when the productivity is between 15-20 kg/day. On the other hand, it requires around 3 m2 still area to design the model system when the productivity is less than 5 kg/day. As depicted, the still area curve is experiencing a downward trend when the solar energy increases as it converges to the afternoon time. It shows almost steady until 4:00 p.m. then it starts to rise again when solar intensity decrease. Thus, low amount of water evaporation inside the still and freshwater production (kg/m^2.day).

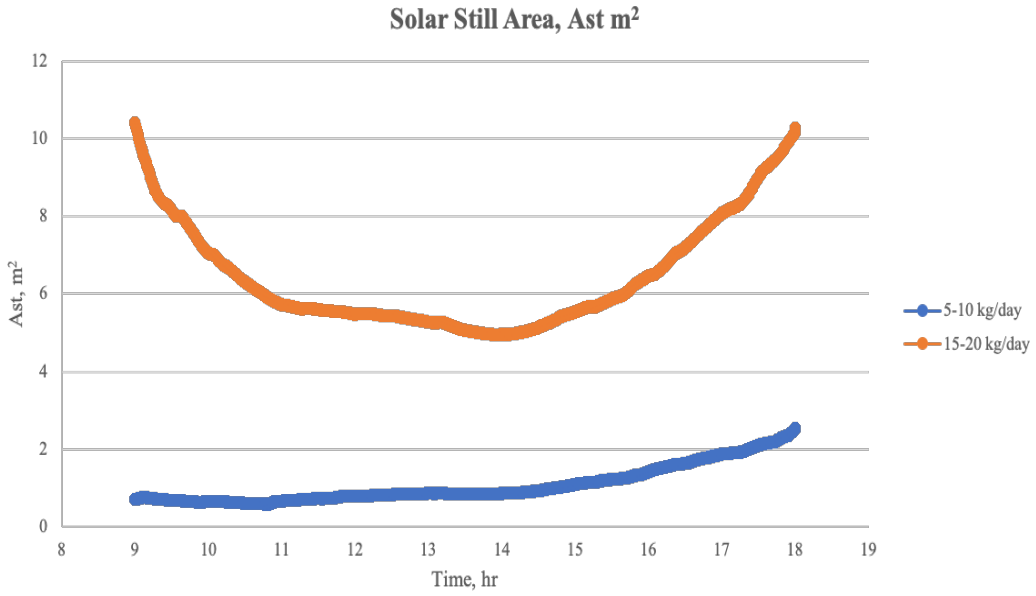

Figure 42: Solar still designed area at different productivities, m^2

Regarding the photovoltaic total system area, it exhibited the same behavior at different still productivities (figure 43). PV total system area includes the constructed modules and cell areas. It is necessary to allocate almost 185 m^2 total area to accommodate the photovoltaic cell and its auxiliaries when considering 15-20 kg/day distillate water production. In contrast, only 50 m^2 is fairly enough to design a PV model with still productivity less than 5 kg/day.

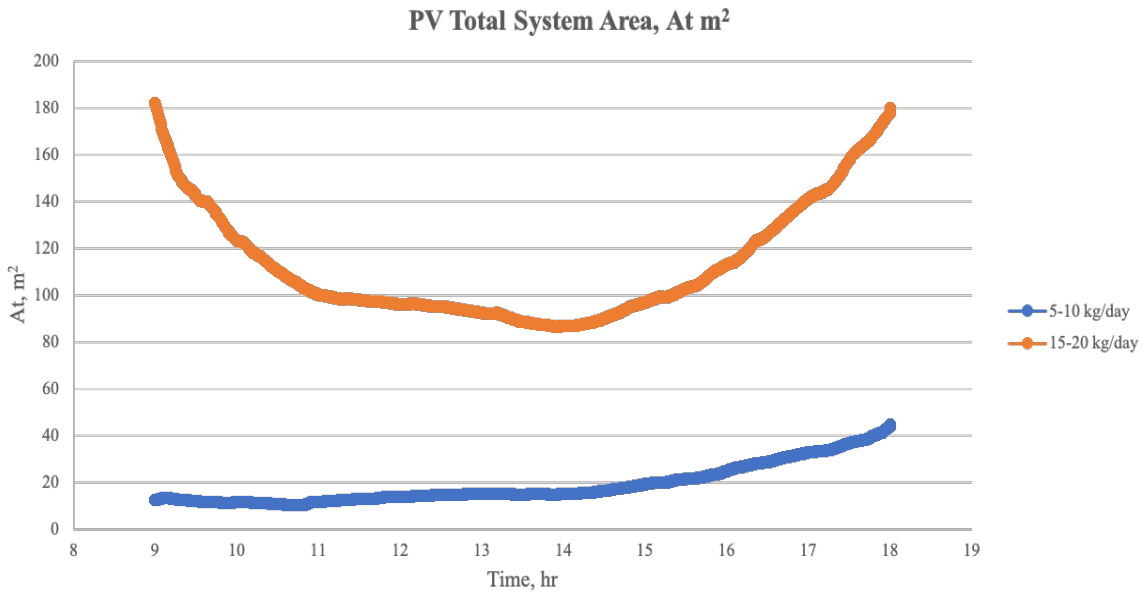

Figure 43: PV total system area, m^2

4.3 Design Results for Solar Still Glass Cover Area:

Another critical output design parameter is the solar still glass cover area (m^2). As shown in the following 3-D mesh figures 44 & 45, while the still productivity (kg/day) increased the glass cover area increase with rising the still ambient temperature and diminishing the solar radiation. As discussed previously, the highest value of solar radiation 20 MJ/m^2.day is desirable with respect to the still ambient temperature ranging between 25 – 45 °C. Consequently, the solar still required the lowest design area and that will save the design and construction costs.

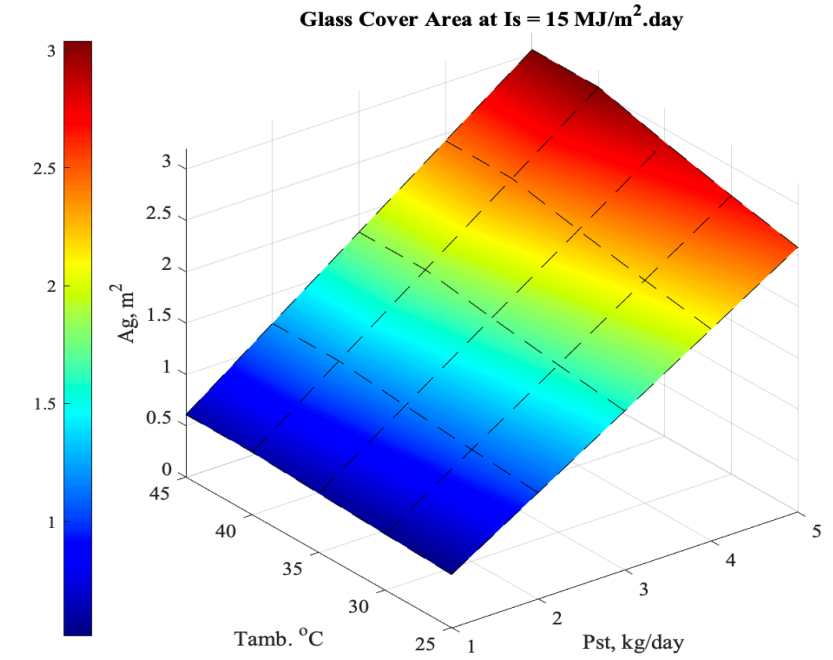

Figure 44: Solar still glass cover area at Is=15 MJ/m^2.day, m^2

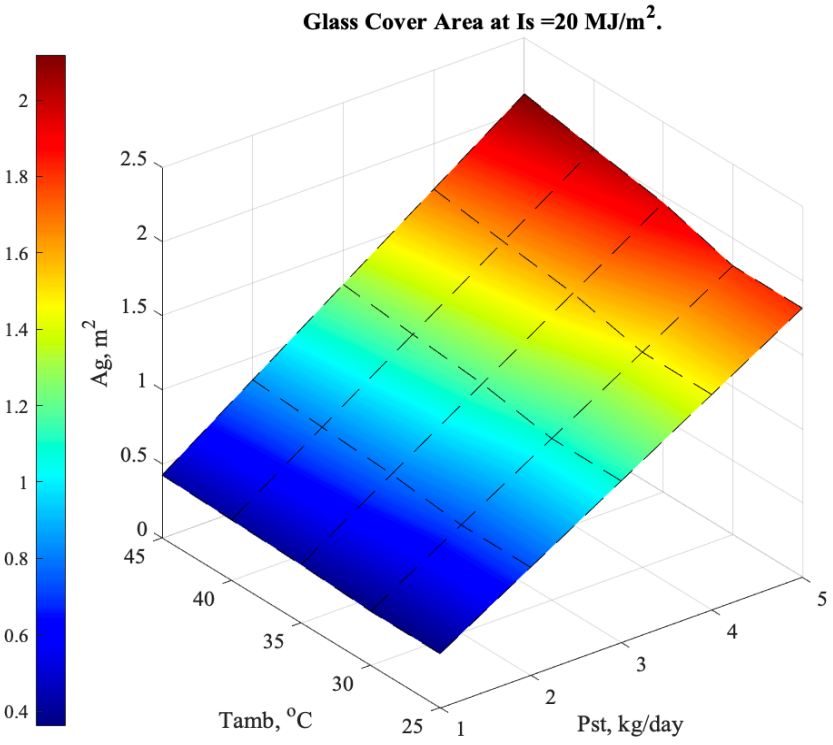

Figure 45: Solar still glass cover area at Is=20 MJ/m^2.day, m^2

The same concept is applicable when designing the still's glass cover area. The below 2-D figure 46 evidently displays the solar still design glass cover area at different productivities ranges initially from 5 to 10 kg/day (blue) then from 15 to 20 kg/day (orange). As shown below, a glass cover area needed to design the model system is almost 16 m^2 when the productivity is between 15-20 kg/day. However, it obliges around 4 m^2 to design the model system when the productivity is between 1- 5 kg/day. As represented in figure 44, the still glass cover area fitted curve showed a significant decline when the solar radiation growths as it meets to the afternoon time. It displays a steady at noon time, then it starts to rise again over the period when solar incident decrease. Therefore, low amount of water evaporation inside the still and freshwater production (kg/m^2.day).

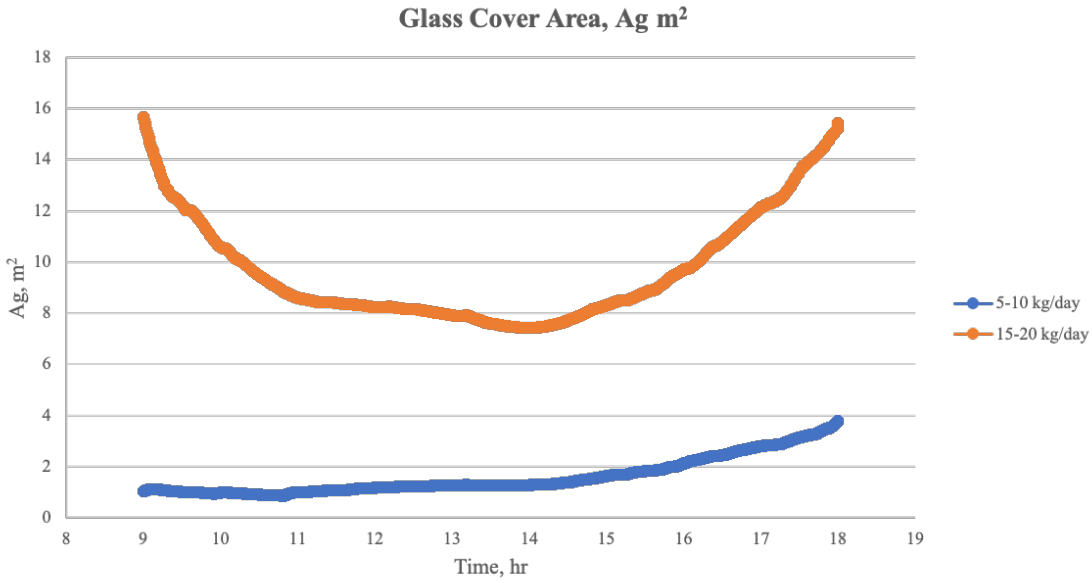

Figure 46: Solar still glass cover area, m^2

4.4 Design Results for Solar Still Productivity:

It is desirable to achieve optimal and high distillate water production from the solar still design system. Therefore, it is important to figure out which climatic condition and design parameters are essential to hit that target. When the model system design parameters have been fitted using a signal builder browser, it is subjected for simulation (run button) and the generated figures of the

still productivity are depicted below in figure 47. The still ambient temperature is adversely proportional to the freshwater production in kg per unit area per day. However, it is directly proportional to the solar radiation Is (MJ/m^2.day). As solar radiation increases the productivity of the still increase with respect to the ambient temperature (^{o}C). It has been explained preciously that for the distillation equipment with a good insulation, lower ambient temperature will assist to cool the glass cover faster, thus increasing the temperature gradient between the brine water layer and glass cover and freshwater productivity. In contrast, when the distillation equipment is not well insulated, low ambient temperature leads to rise heat loss of the still device, thus a reduction in water temperature in the equipment will take place accordingly.

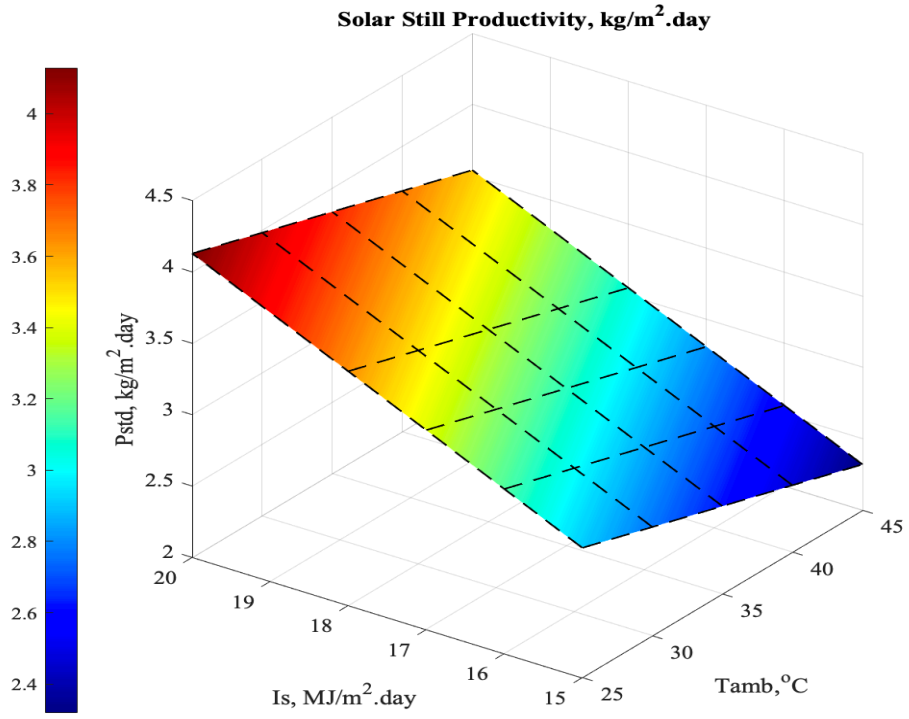

Figure 47: Solar still productivity, Pstd kg/m^2.day

It can be concluded that in case the still is well insulated, the decrease in ambient temperature may leads to a higher production of distilled water, whereas in the case the still is not insulated, the reverse behavior is detected.

The following figure 48 is related to freshwater production with the impact and addition of black dye. It is clearly from the subject figure there is a significant impact of adding dye on still performance. The presence of a black dye in particular inside the still enhances the rate of water distillation because solar radiation is absorbed in a very thin upper layer, hence increasing the surface temperature of the brine, and the rate of water evaporation will be promoted. Consequently, the productivity of the distillate water will definitely rise. The productivity of the still with a black dye produce more than 5 kg/m^2.day, whereas it is lower in production without additives of dye.

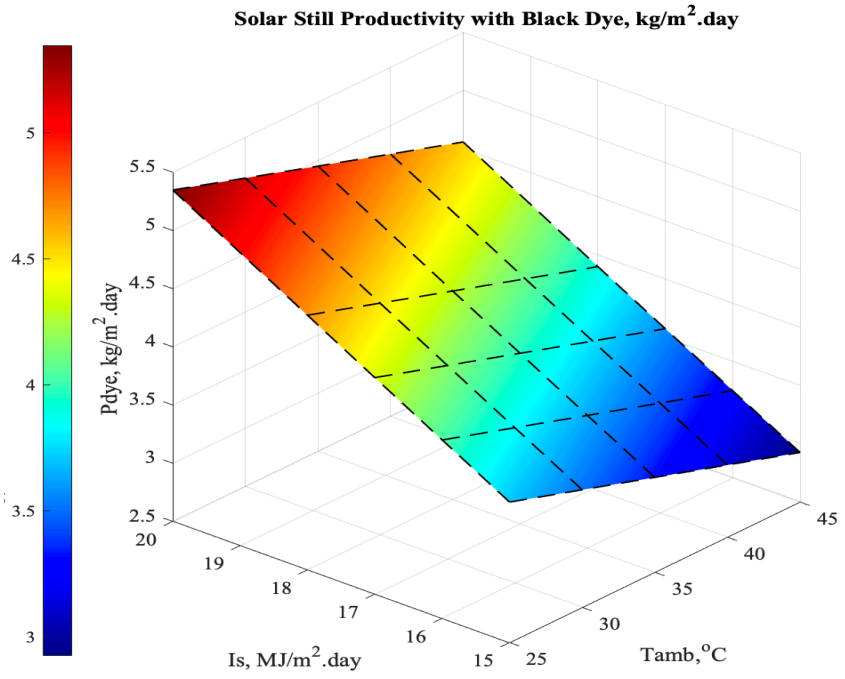

Figure 48: Solar still productivity, Pdye kg/m^2.day

As shown in the following figure 49, the distillate water production significantly rose when the solar radiation energy increased throughout the period. Otherwise, it declined due to the less amount of water evaporation inside the basin. As discussed, black dyes have a major effect on solar still productions. It can produce almost 5 kg/m^2.day of freshwater during the peak period.

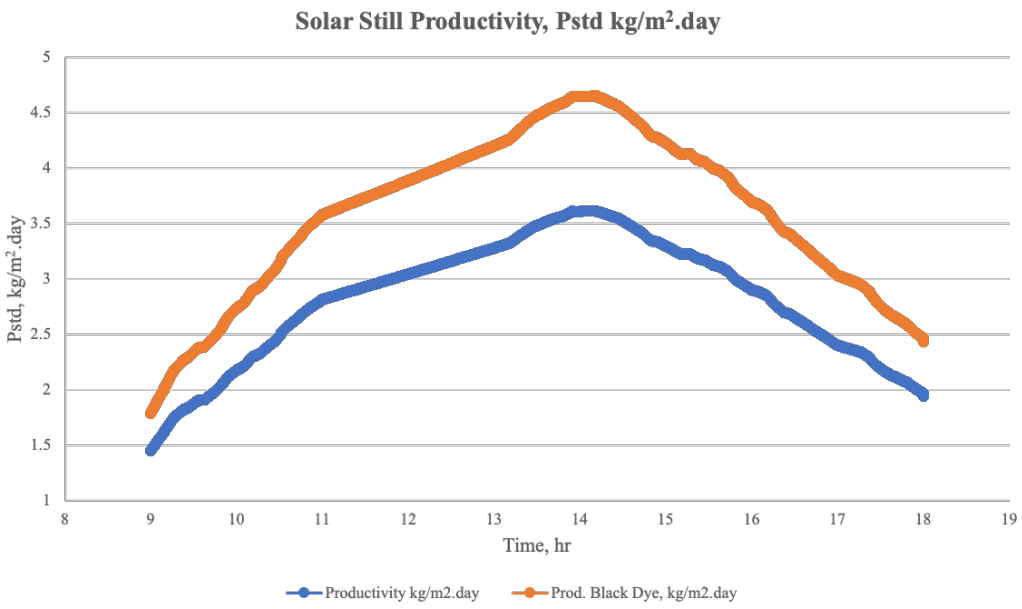

Figure 49: Solar still productivities kg/m2.day

4.5 Design Results for Solar Still Evaporation Energy:

The below 3-D mesh figures 50, 51 are dedicated to demonstrating the energy of evaporation versus solar radiation and ambient temperature. They actually illustrate the effect of solar still evaporation energy on solar radiation and ambient temperature, which is relatively small and can be neglected; however, at high ambient temperature it shows almost a steady curve as solar radiation increase. The evaporation energy is trending up when the design productivity increased up to 5 kg/day. The evaporation heat transfer (kwatt) is function of the solar still productivity subject to the design input, still area and latent heat of distillate water evaporation (kJ/kg) required for water evaporation enhancement and phase change.

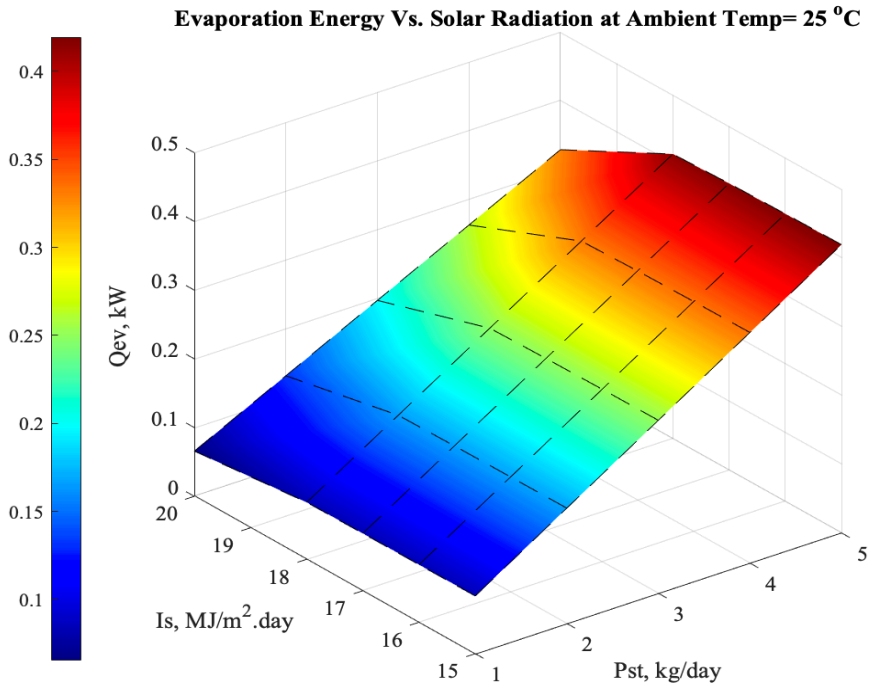

Figure 50: Evaporation heat transfer Vs. solar radiation at diff. temps.

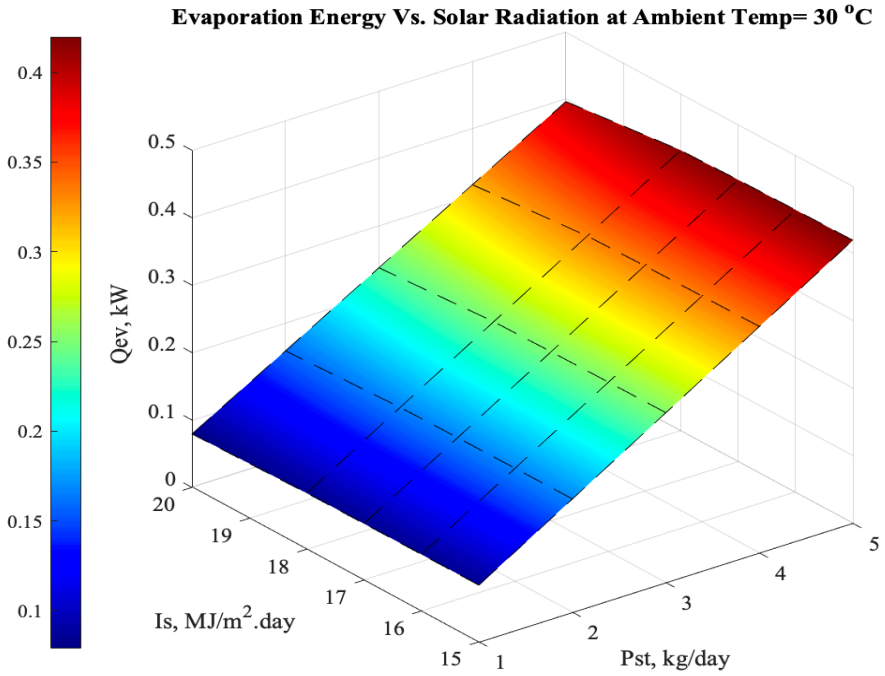

Figure 51: Evaporation heat transfer Vs. solar radiation at diff. temps.

The following 2-D figure 52 depicted the evaporation energy of a designed solar still at diverse water productions (kg/day). It can be concluded that it experienced an upward trend over the period, and it showed higher evaporation energy values when the productivity increased. The evaporation heat transfer is function of the latent heat of distillate water evaporation, solar still area Ast (m^2), operating hours of the still, and distillate water production (Pstd, $kg/m^2.day$).

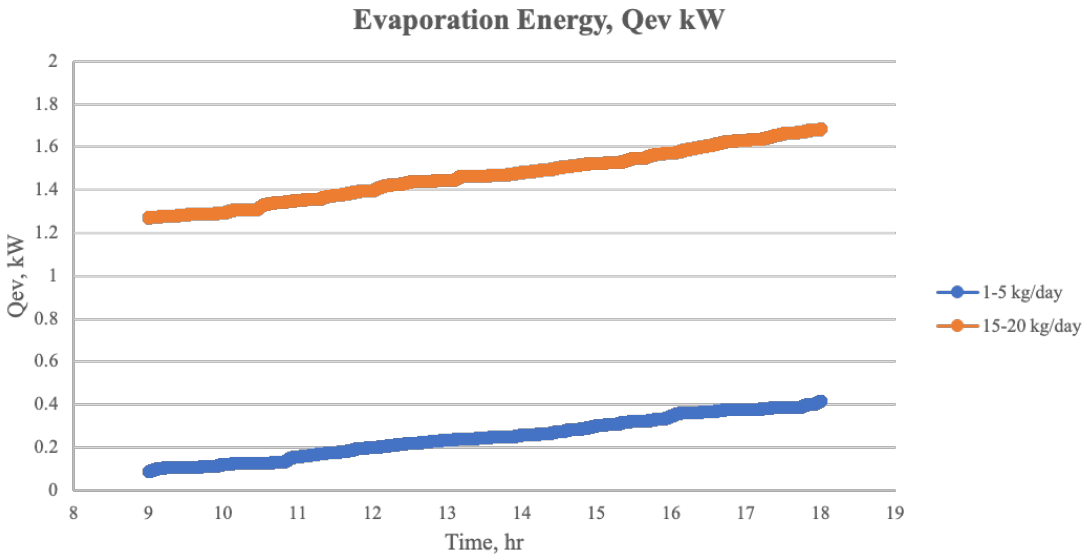

Figure 52: Evaporation heat transfer energy at different productivities.

4.6 Design Results for Thermal Load inside Solar Still:

The thermal load inside the still is mainly function of solar radiation and still area, but not the ambient temperature. The thermal load inside the still is introduced to the photovoltaic cell as a total power along with module power required to calculate the PV number of modules. As depicted in the following 3-D mesh figure 53, at ambient temperature equal to 25 ^oC, the thermal load on PV experienced an upward trend when the still productivity and area increased, while it experienced a downward trend when the solar radiation Is rise.

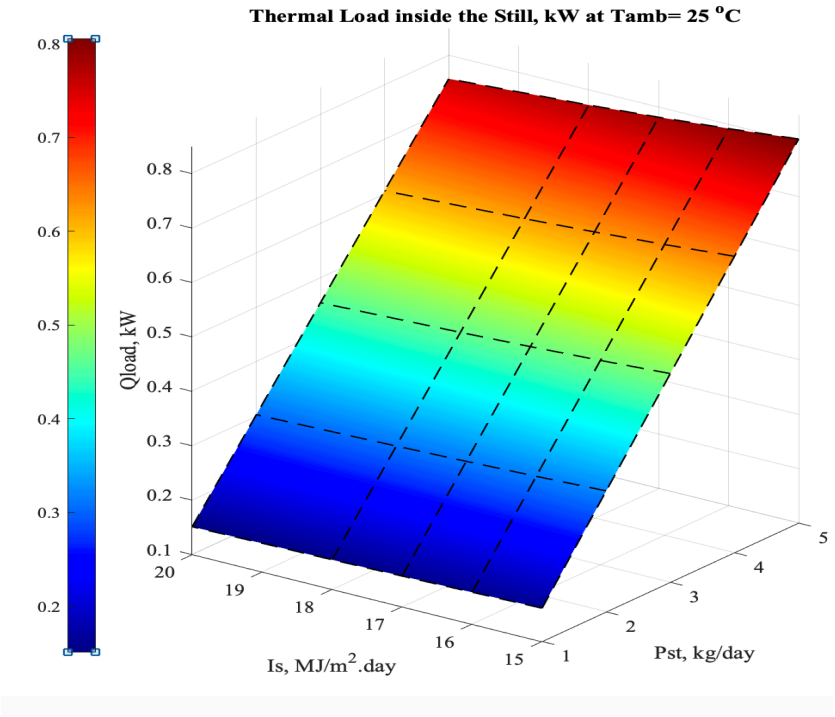

Figure 53: Thermal load inside the solar still at diff. solar radiations & productivities

The next 2-D contour figure 54 is clearly reflecting the same thermal load on PV results with displayed accurate numbers on colorful vertical lines (contours). For example, at 5.00 kg/day water production, the thermal load Q_{load} on PV should equal to 0.8 kW and so on.

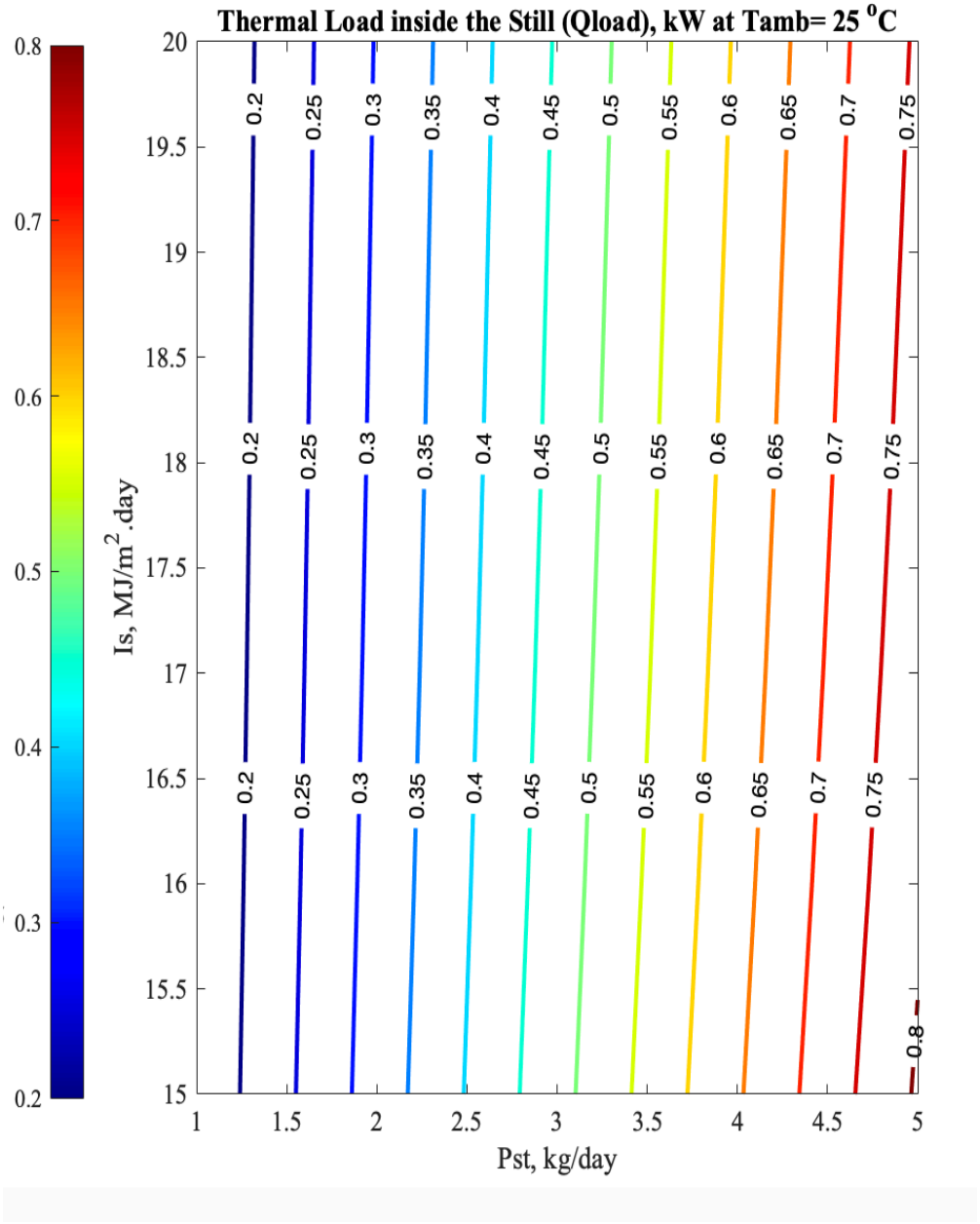

Figure 54: Thermal load inside the solar still at diff. solar radiations & productivities

It is obvious from the following 2-D figure 55 that the thermal load on PV is directly proportional to the amount of water retain inside the still. Logically, the thermal load in kW increased sharply throughout the period at different still productivities (kg/day), knowing that as the design claims for high production rate, the still needs higher thermal load.

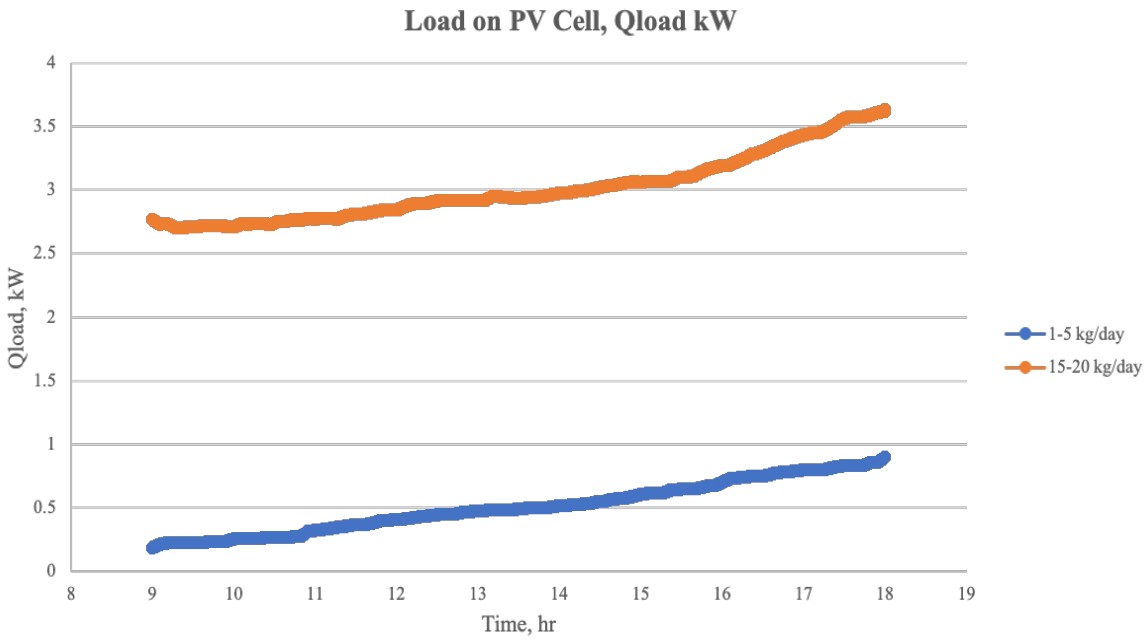

Figure 55: Thermal load inside the solar still at different productivities

4.7 Design Results for Solar Still Heat Transfer Energy:

The following 3-D mesh figures 56 is reflecting the radiative heat transfer energy from water to glass cover inside the solar still at a certain ambient temperature 30 ^{o}C. As shown in the figure, radiative heat transfer is corelated with design still productivity (kg/day) and solar radiation energy (MJ/m^2.day). It is clearly from the figure that the radiative heat transfer from water to glass cover experienced an upward trend when both solar radiation and still productivity increased. It is risen sharply throughout the end of the period. The highest value of the energy in kW is at Pst= 5 kg/day and Is = 20 MJ/m^2.day.

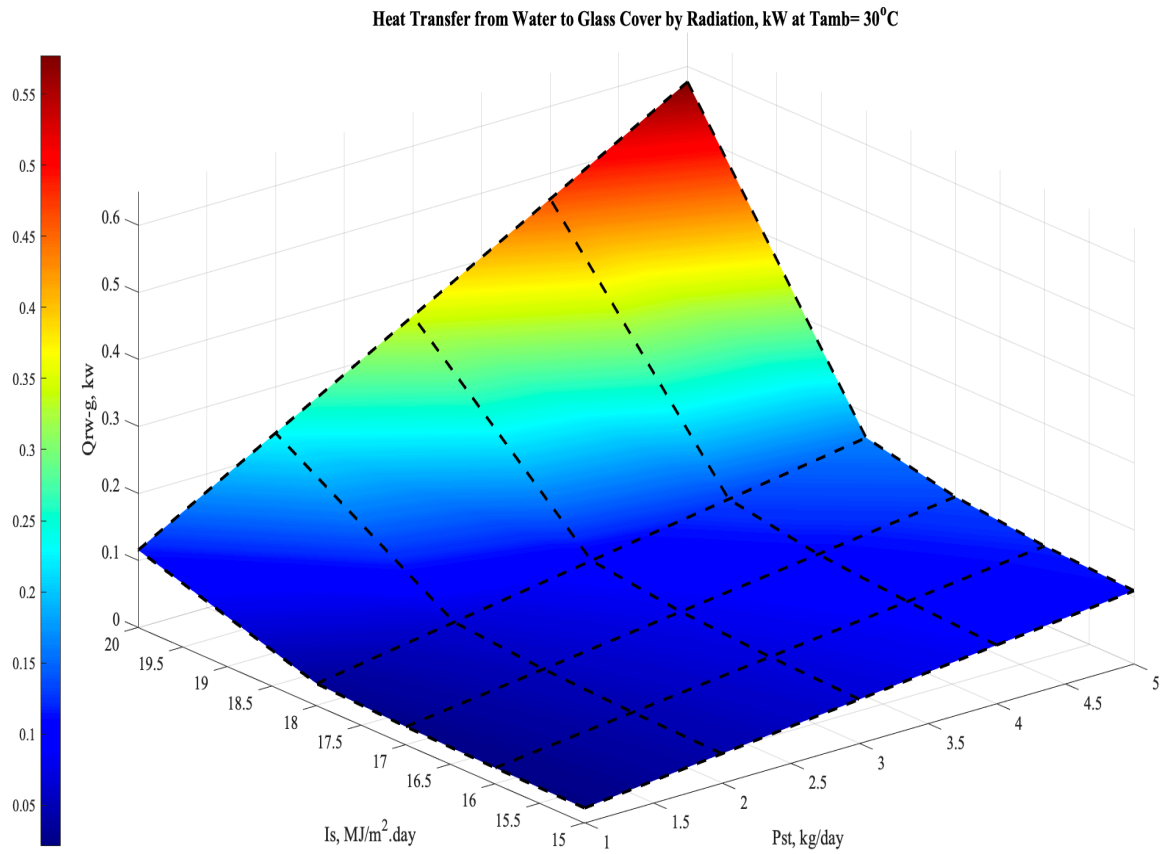

Figure 56: Heat Transfer from Water to Glass Cover by Radiation, kW

Besides, the 2-D figure 57 illustrate Qrw_g with respect to the still's productivities ranges between 1 to 20 kg/day. As shown, the peak value of the heat transfer energy is when the solar radiation energy is at the highest value through the daytime between 1:00 p.m. and 3:00 p.m. otherwise it declined but shows steady in some periods.

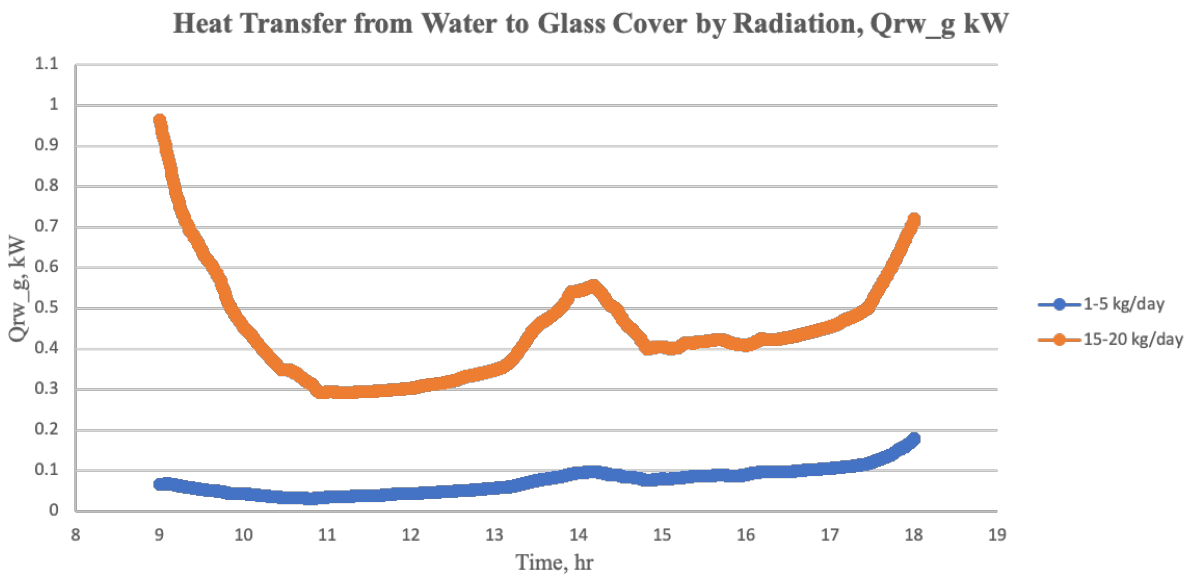

Figure 57: Heat transfer from water to glass cover by radiation at diff. productivities

The second figure 58 is illustrating the heat transfer energy from glass cover to the ambient with respect to solar radiation energy and still productivity. Similarly, when refer to the former figure, the heat transfer energy grew to 0.55 kW when both the still productivity is 5 kg/day and the solar radiation is Pst = 20 MJ/m^2.day are having optimal values. However, it is at the lowest trend when the productivity is 1 kg/day, and solar radiation is Is =15 MJ/m^2.day.

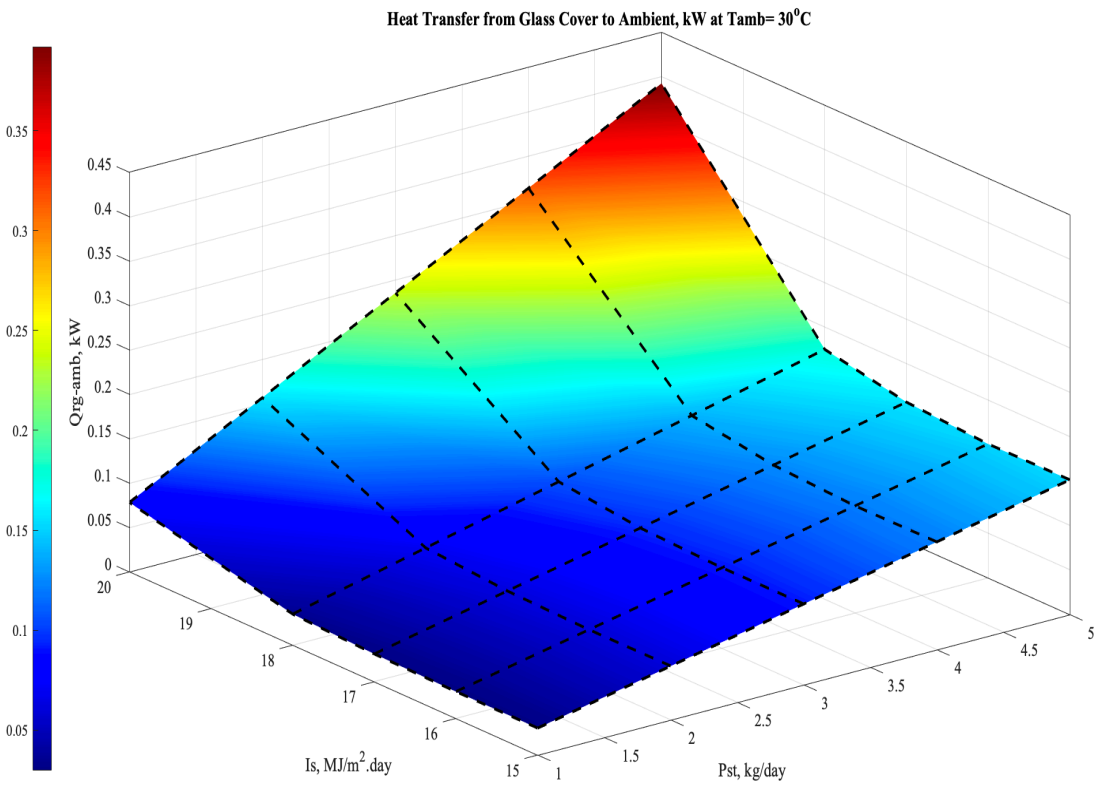

Figure 58: Heat transfer from glass cover to ambient, kw

It can be noticed that the heat transfer energy from glass cover to ambient corresponds to the same behavior when compared with heat transfer Qrw_g from water inside the still to glass cover. As depicted in figure 59, Qrw_amb experienced a decrease in the early morning but showed a steady then started to slightly increase in the afternoon. Similarly, the peak value of the heat transfer energy is when the solar incident is at the highest value through the daytime between 1:00 p.m. and 3:00 p.m. else it showed a downward trend but steady in some periods.

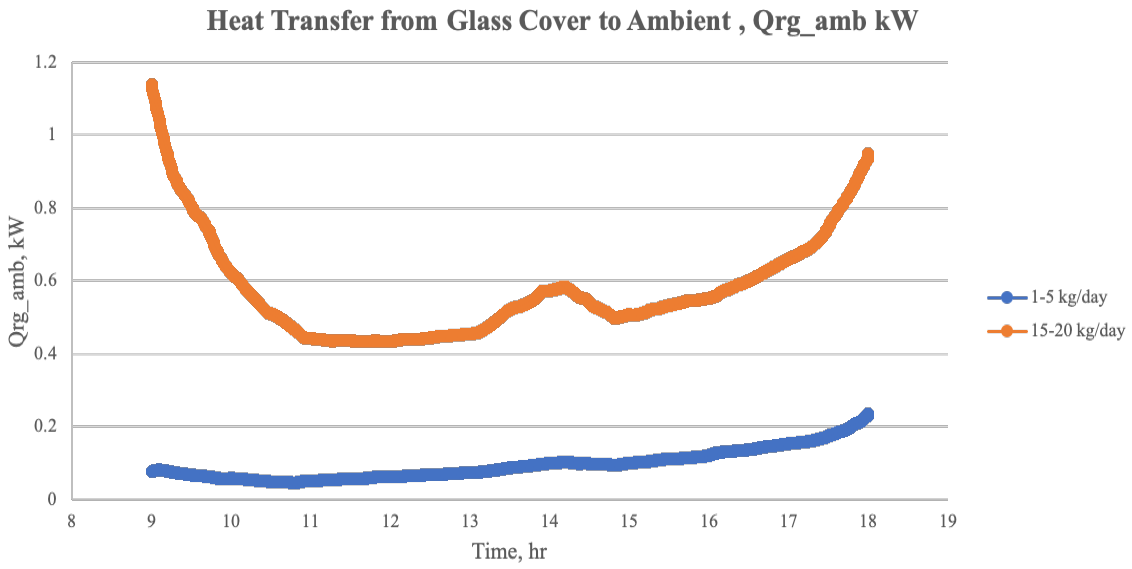

Figure 59: Heat transfer from glass cover to ambient, kw

The following figure 60 is expressing the convective heat transfer coefficient correlation with respect to the solar radiation and ambient temperature. As depicted in the below figure, the convective heat transfer coefficient experienced an upward trend when the solar radiation values are decreasing to the lowest value 15 MJ/m^2.day, while the ambient temperature values are uprising to 35 ºC. However, it remained almost steady when both solar radiation and ambient temperatures are declined. It is worth to mention, the convective heat transfer coefficient is a function of water evaporation energy, solar still area and the temperature difference between water and glass cover.

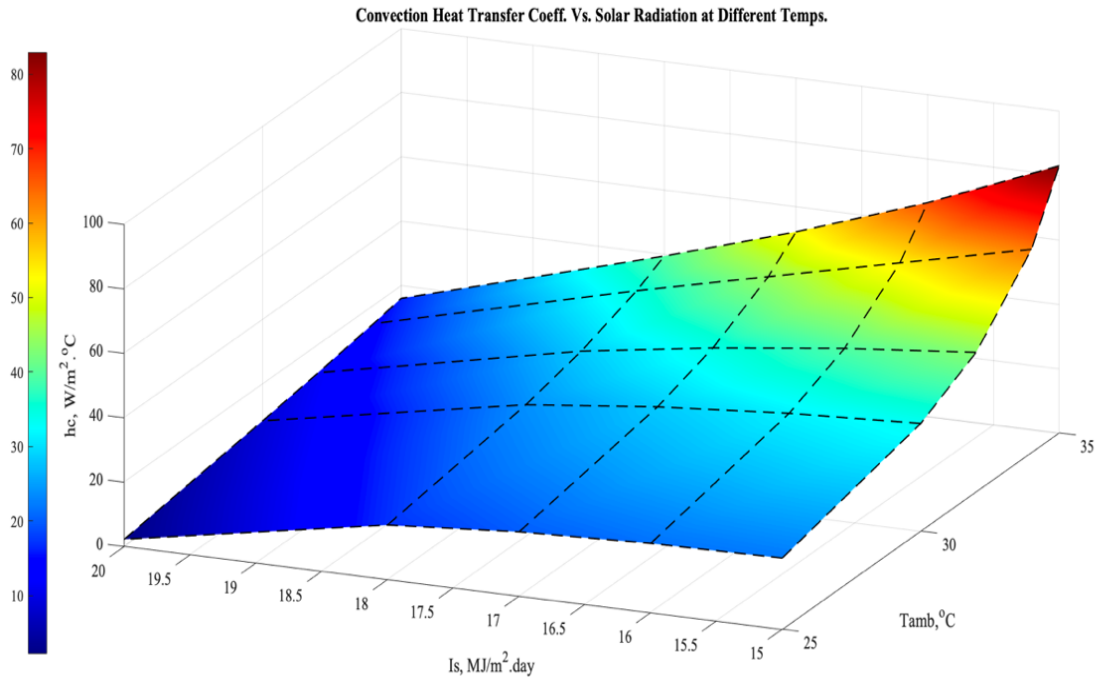

Figure 60: Convection heat transfer coefficient with solar radiation at diff. temps

The line graph in the following 2-D figure 61 illustrates the convective heat transfer coefficient hc throughout the period. It showed a major increase when solar radiation required to absorb thermal energy rises, but it slightly reduces during the afternoon time due to the effect of wind speed. the hc curve is fluctuating throughout the period because the radiative heat transfer coefficient between water and glass decreases with increasing wind velocity.

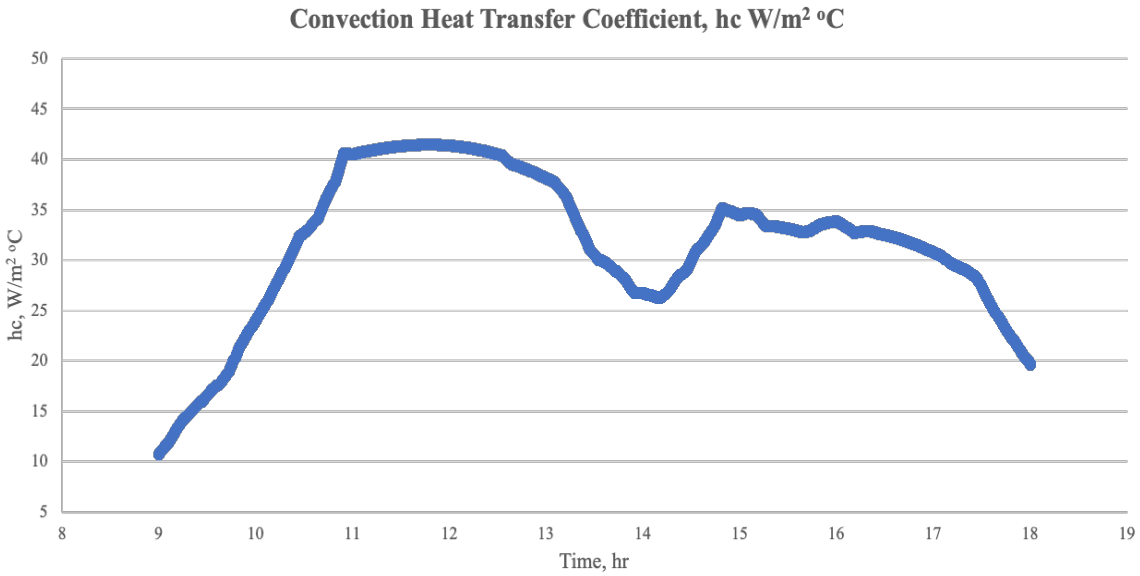

Figure 61: Convection heat transfer coefficient with solar radiation at diff. prods.

It can be noticed from the below figure 62 that evaporative heat transfer coefficient, hev experienced an upward trend in the morning but showed a steady throughout the noon time. It then drastically reduces over the end of the period. The result indicated that for set ambient and water temperature, the wind speed is insignificant relation with (hev) between water and glass cover. Evaporative heat transfer coefficient is a critical parameter when it comes to the still design because it is attributed to water evaporation and condensation rates which should be always be maintained high enough to meet the optimal and maximum distillate water production and still performance.

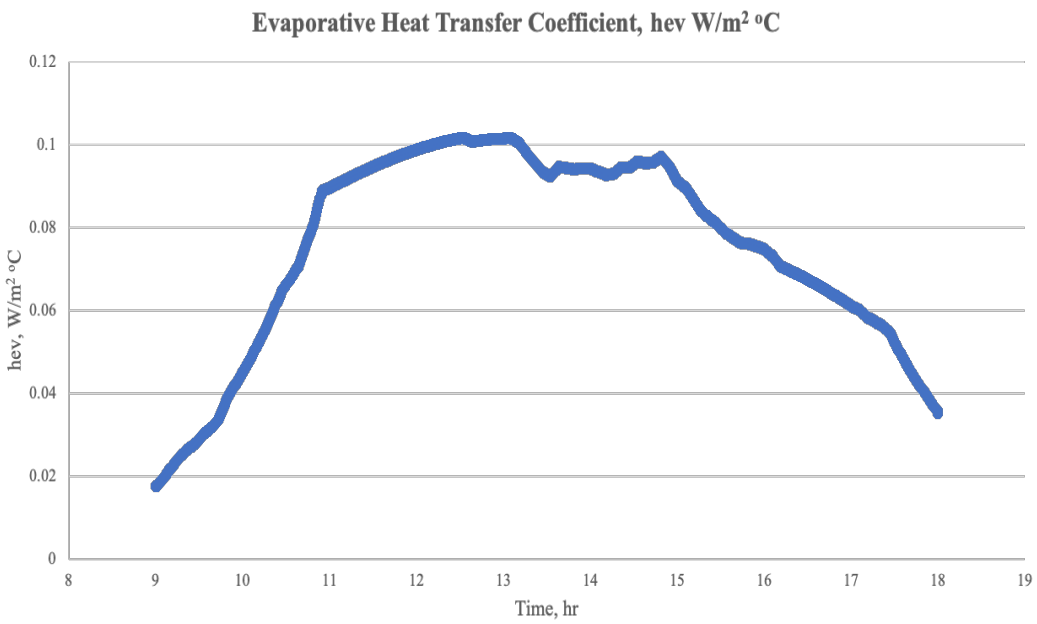

Figure 62: Evaporative heat transfer coefficient with solar radiation at diff. temps.

As depicted in the below figure 63, the change in water and glass cover temperature have been noticed throughout the daytime. Results showed that basin water temperature is always greater than glass cover temperature in order to attain the evaporation/ condensation process. It can be explicitly observed that increasing (T_w-T_g) difference will promote the rate of evaporation, boost water production and enhance the system performance.

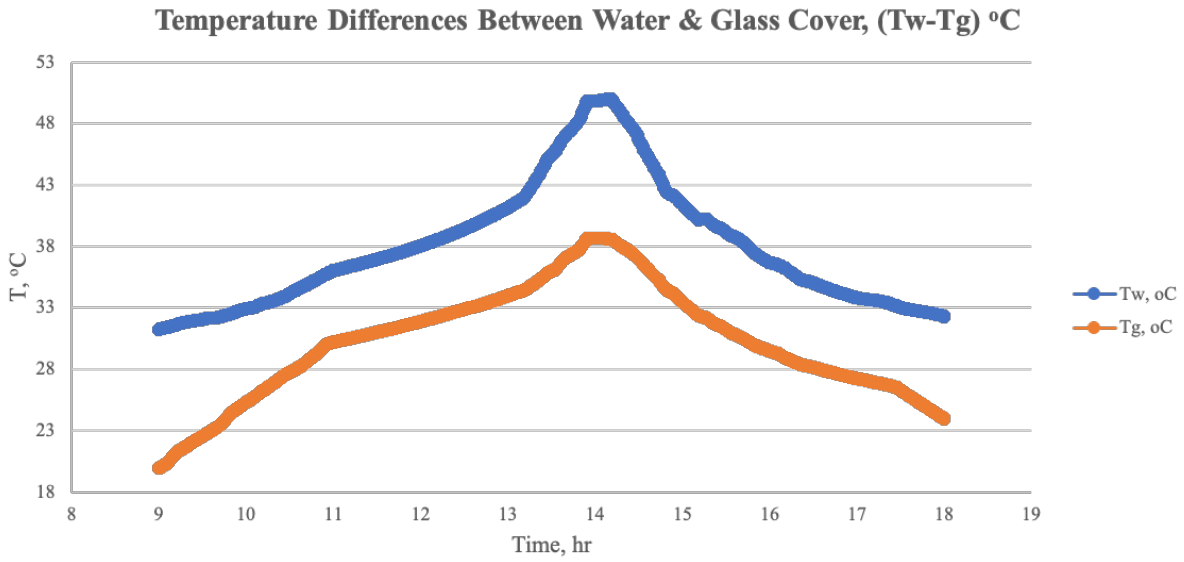

Figure 63: Temperature differences between water and glass cover, (Tw-Tg) °C

4.8 Design Results for Brine Depth & Solar Still Efficiency:

The below 3-D figure 64 shows a critical parameter affecting the still productivity per unit area which is the brine depth inside the solar still. The subject brine depth parameter shows a significant rise over the period when the ambient temperature is augmented up to 45 °C. In contrast, the solar radiation is adversely proportional to brine depth, cm. While solar radiation energy increased the rate of water evaporation increased, thus water depth will be diminished inside the still.

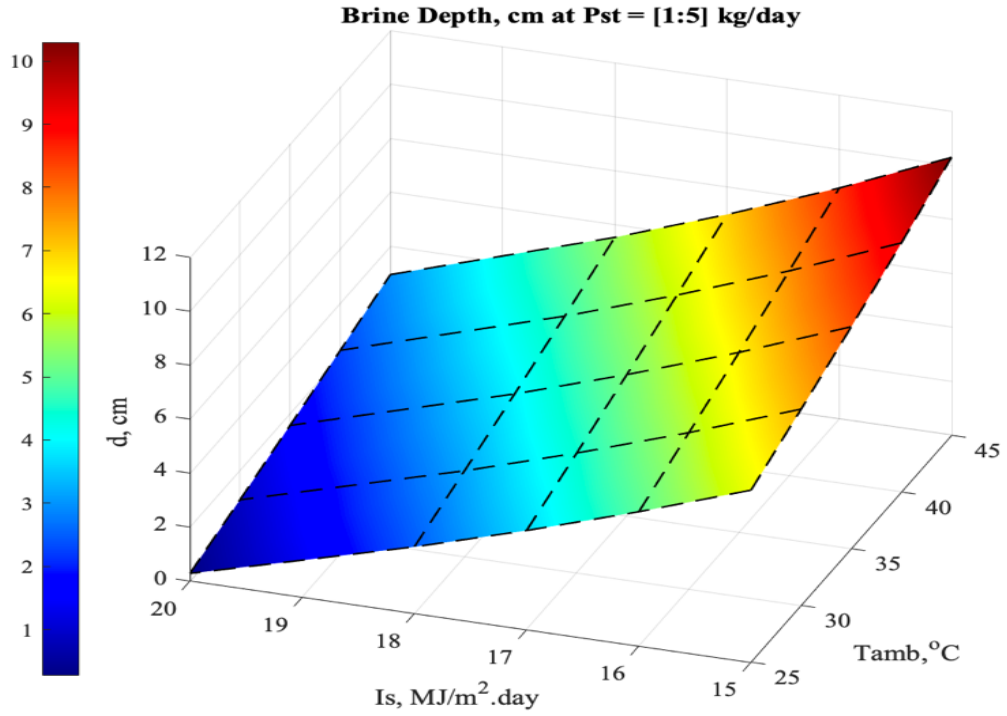

Figure 64: Brine depth inside the solar still, cm

As shown in the following 2-D figure 65, the brine water level inside the still experienced a downward trend but showed a significant rise over the period. The reduction of brine level is an indication of water evaporation development inside the still during the daytime.

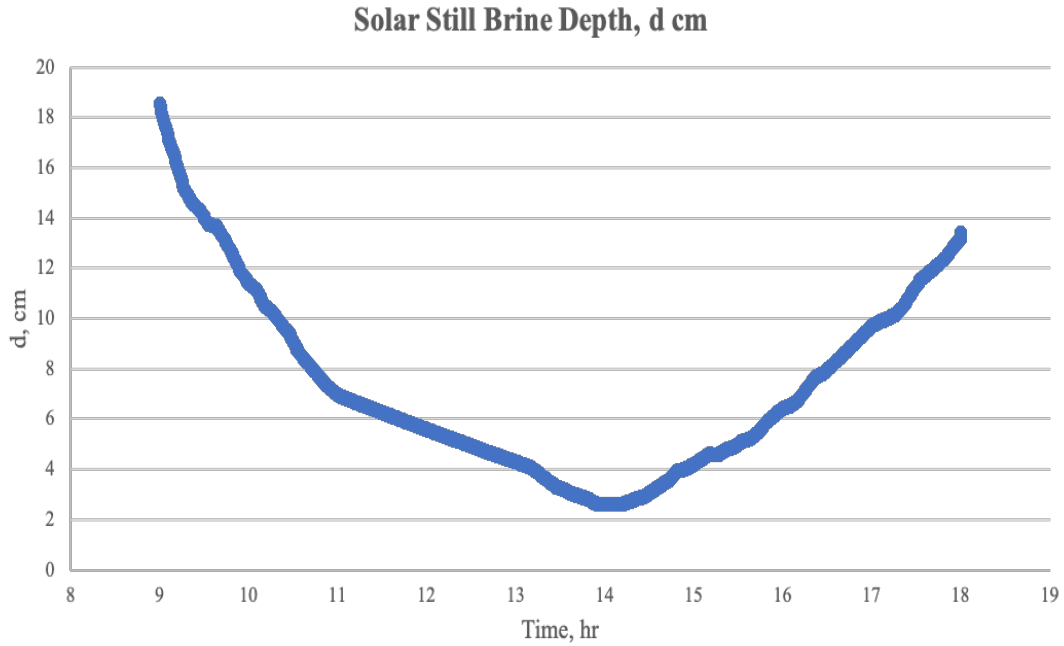

Figure 65: Brine depth inside the solar still during the day, cm

It is depicted in the following contour figure 66 that solar still design productivity does not affect the still efficiency, and all have the same results at different productivities kg/day. On the other hand, the still can reach the optimal efficiency value 50% when the ambient temperature is low at 25 ^{o}C. The high solar still efficiency can be achieved when the ambient temperature ranges between 25 and 34 ^{o}C and solar radiation energy sharply increased to 45 MJ/m^2.day.

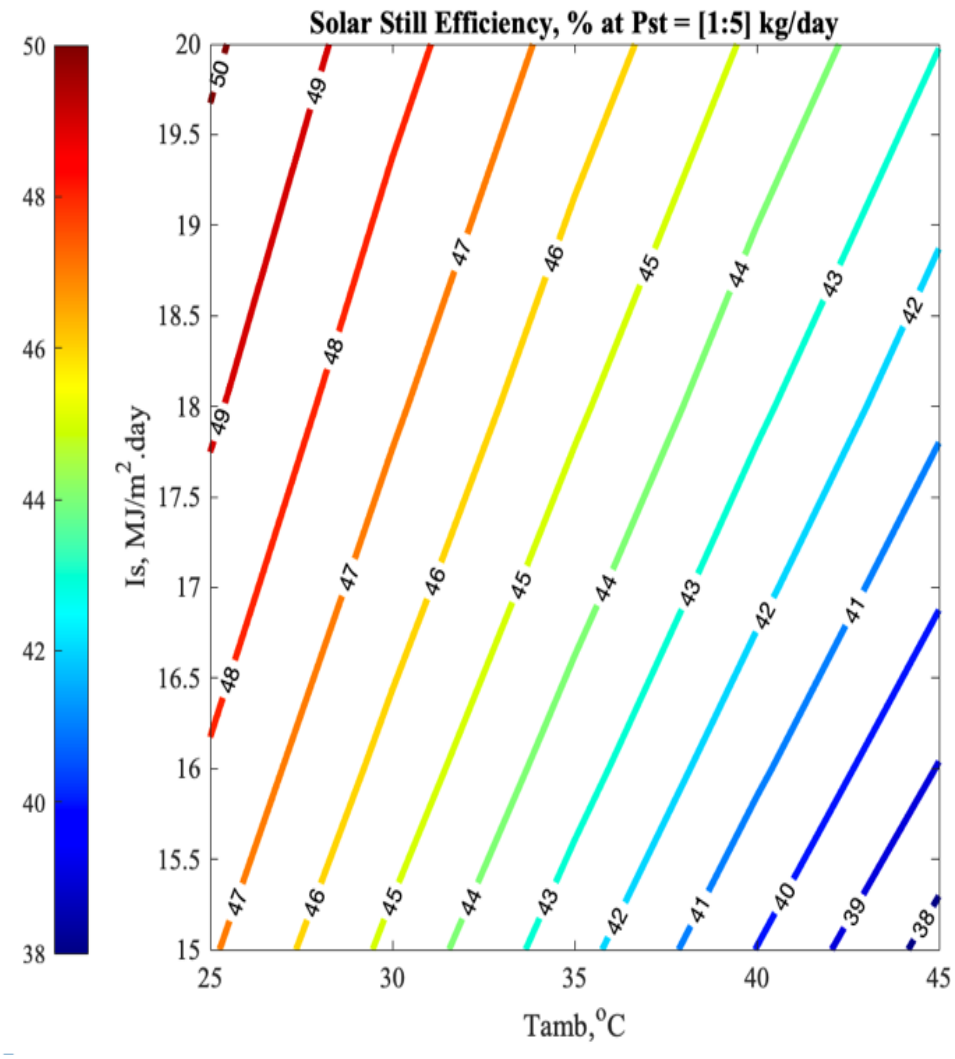

Figure 66: Solar still brine depth, cm & efficiencies, %

Referring to figure 67, it can be concluded from evaluating the results in this design study that integrating a photovoltaic cell with a single slope solar still boost distillate water production, improve the system performance and enhance the entire model system efficiency. As illustrated in the below figure, the still achieved more than 45% corresponding to the still production per unit area (kg/m^2.day), maximum value of (T_w-T_g), evaporative (hev, W/m^2 ^{o}C) and radiative heat transfer coefficient (hc, W/m^2 ^{o}C) between water and glass cover.

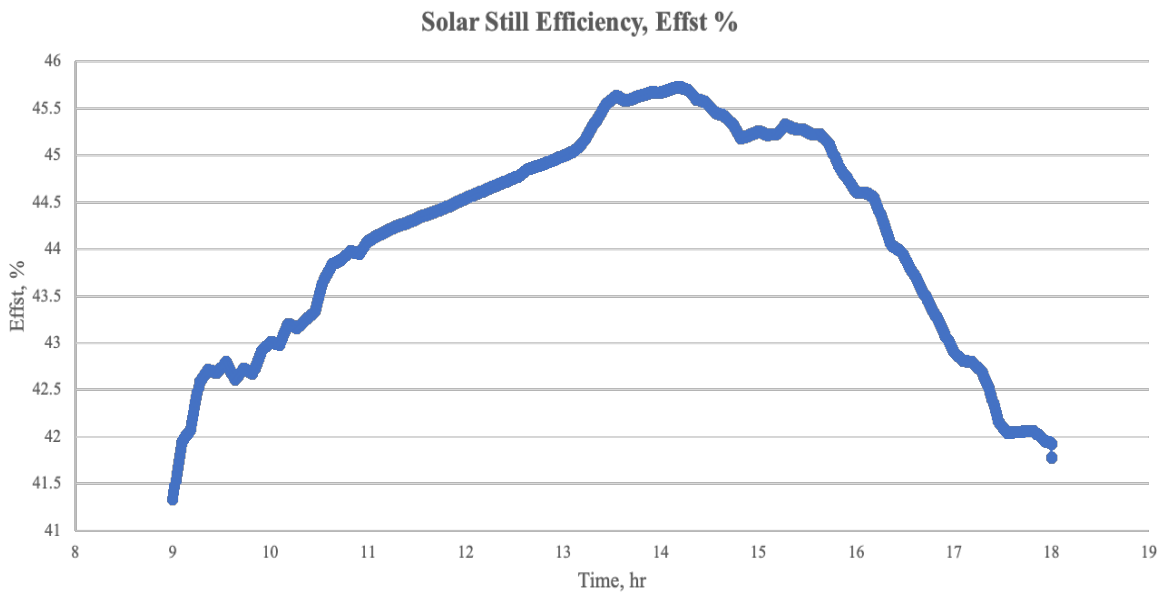

Figure 67: Solar still efficiency, Effst %

4.9 Design Results for Solar Still Cost Analysis:

The following 3-D mesh figure 68 represents the solar still annual fixed charges per year at ambient temperature equal 30 ºC. As shown below figure, while the solar still production increase the annual fixed charges trending upward and reaches the highest point (marked red) with respect to solar radiation energy. Absorbing as much solar energy effectively contributes to rise the rate of water evaporation, hence increase the amount of freshwater production per unit area.

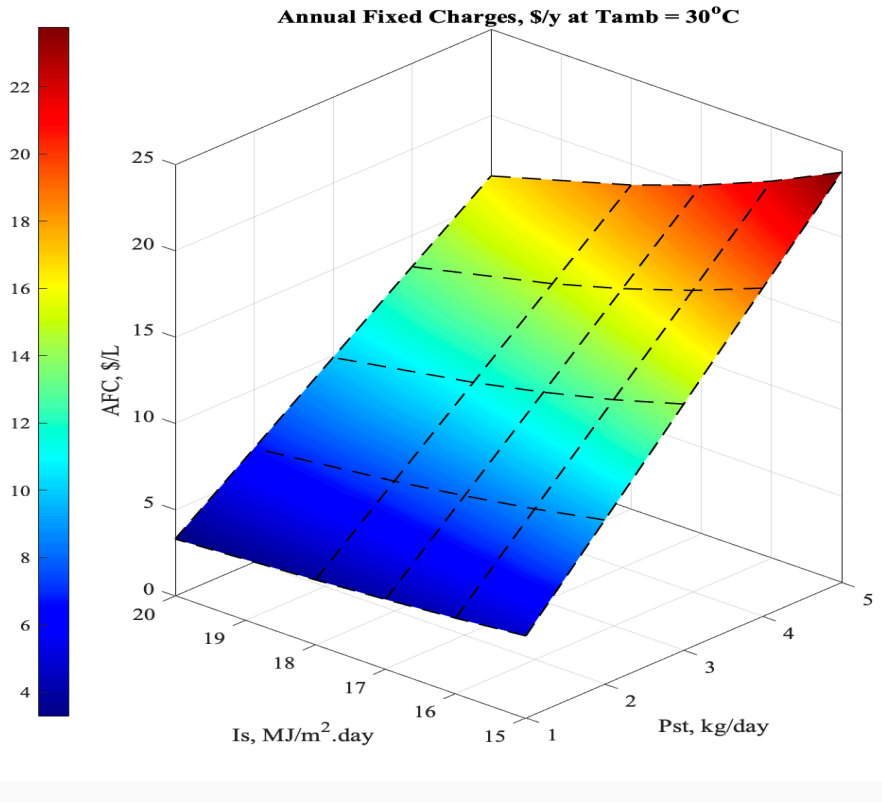

Figure 68: Solar still annual fixed charge, $/y

Another interesting way of expressly displaying the results by numbers of the still annual fixed charges per year is to present it in a 2-D contour graph 69. For instance, at ambient temperature 30 ^{o}C, the value of annual fixed charges becomes almost 25 when the solar radiation is at its minimum value 15 MJ/m^{2}.day.

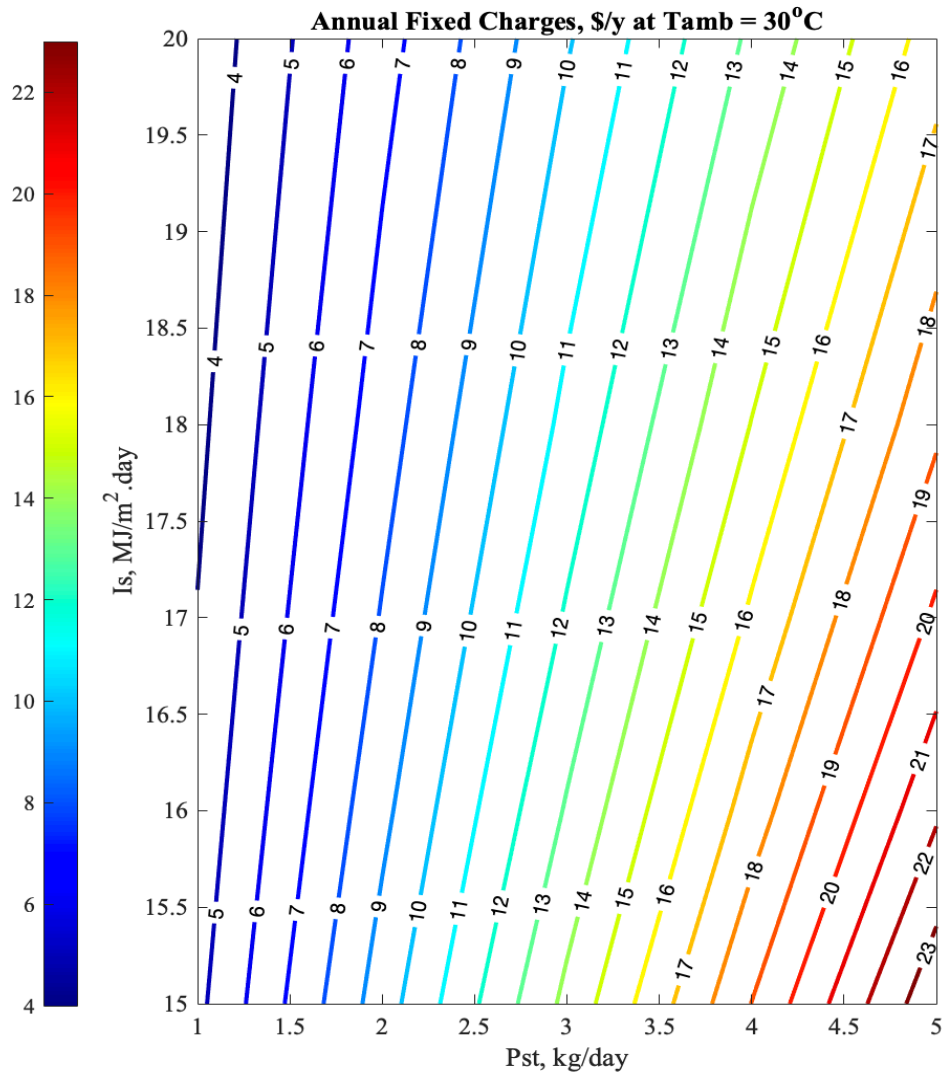

Figure 69: Annual Fixed Charges for a Solar Still, $/yr.

The below 2-D figure 70 is another form of illustrating the relation between the distillate water productions throughout the period. Logically, more water production requires more spent costs and vice versa. The valley value of the curve during the afternoon indicates that the still is at the highest level of production with lowest annual fixed charge.

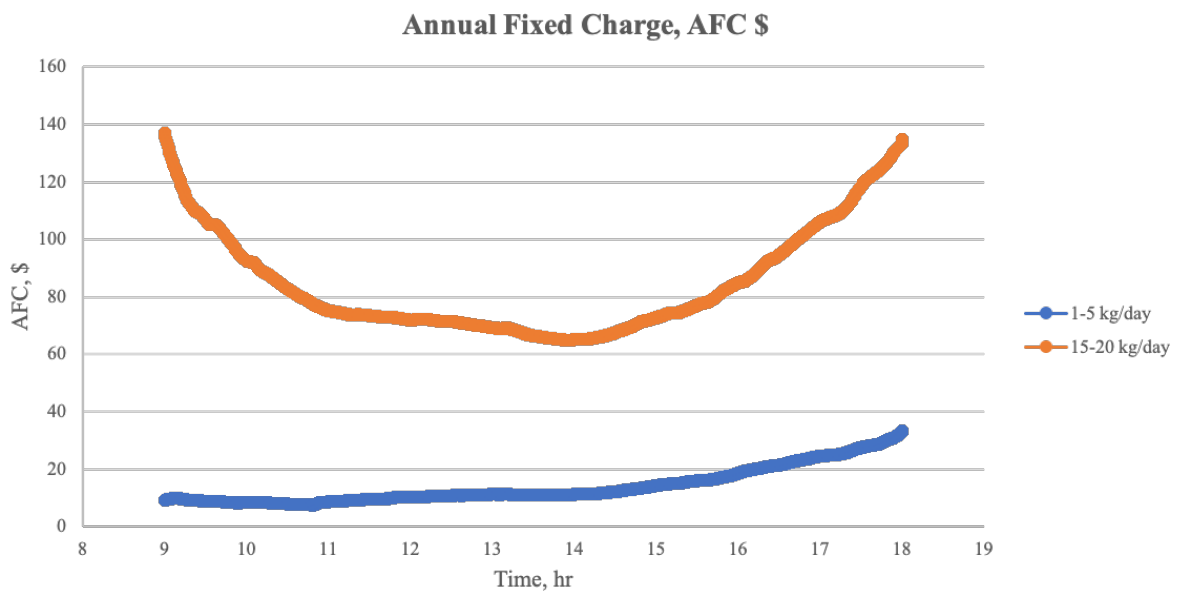

Figure 70: Solar still annual fixed charge, $/y

The total photovoltaic costs are a vital factor that should be taken into consideration in the design model, especially when accompanied with a solar still system. The total system area of a PV is a function of the total power introduced into the cell through load on PV, PV full overboard cost $, number of batteries and battery costs (refer to design cost). It can be seen from the following 3-D mesh figure 71 that the total photovoltaic cost risen sharply throughout the still production (up to 5 kg/day). As explained previously, absorbing as much solar energy effectively contributes to rise the rate of water evaporation, hence increase the amount of freshwater production per unit area. Therefore, the total cost will be reduced while the solar radiation energy keeps trending upward (20 MJ/m^2.day). The minimum PV costs can be pointed out when the solar incident is at the highest value, whereas the mass production per day is relatively low 1 kg/day.

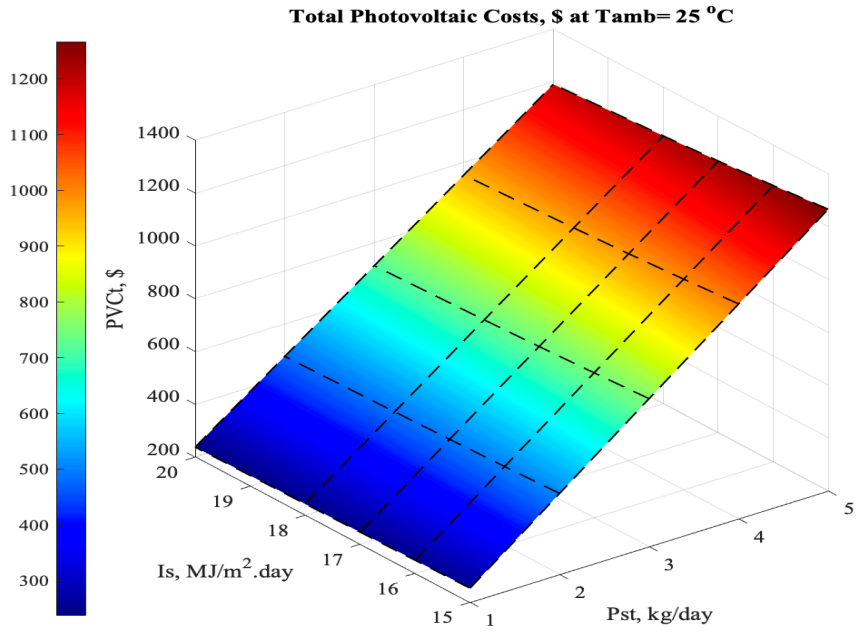

Figure 71: Total photovoltaic cell cost, $ at different ambient temp.

Regarding the impact of ambient temperature, it is obvious from the 3-D graph 72 that PV costs much more (around $1400) when the ambient temperature surrounded the solar still is increased. The reason behind that, when the ambient temperature is low, it will contribute to cool the still glass cover faster, which leads to increase the temperature difference between the brine water layer and glass cover. Thus, increase rate of water evaporation and production with a low cost.

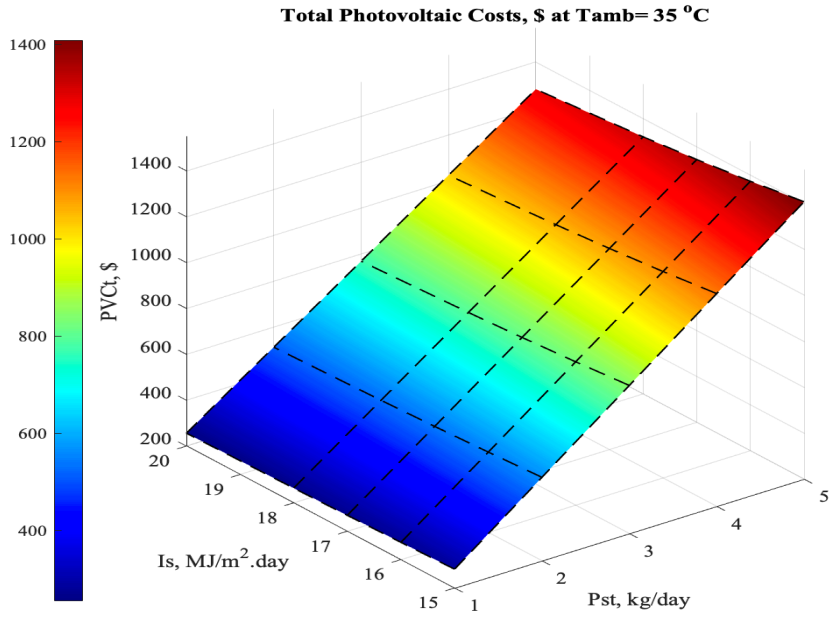

Figure 72: Total photovoltaic cell costs, $ at different ambient temp.

PV costs can be expressed in a 2-D figure 73 with various productivities as well. As depicted, when the investor decides to design a solar still with a certain water production, he has to consider the PV costs along with the total capital costs. It is obvious that higher distillate water demand (kg/day) requires more costs to be spent in designing and constructing the system.

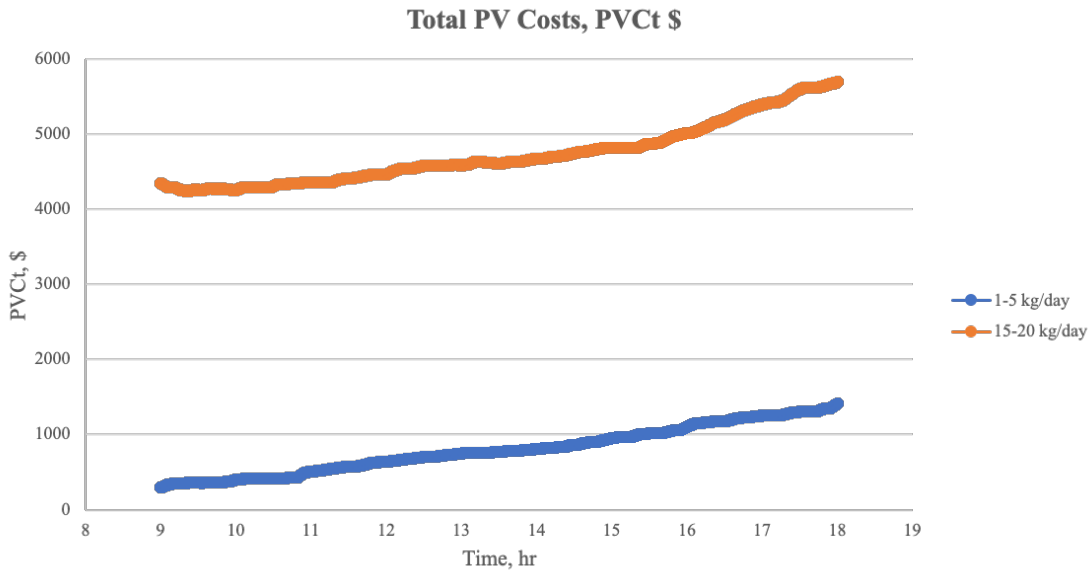

Figure 73: Total photovoltaic cell costs, $

The same concept is applicable when considering the cost per liter ($/L) of the solar still. The below 3-D mesh figure 74 corelates the solar radiation energy and ambient temperature. The cost per liter experienced an upward trend when solar radiation required to be absorbed by the still is reduced to 15 MJ/m^2.day.

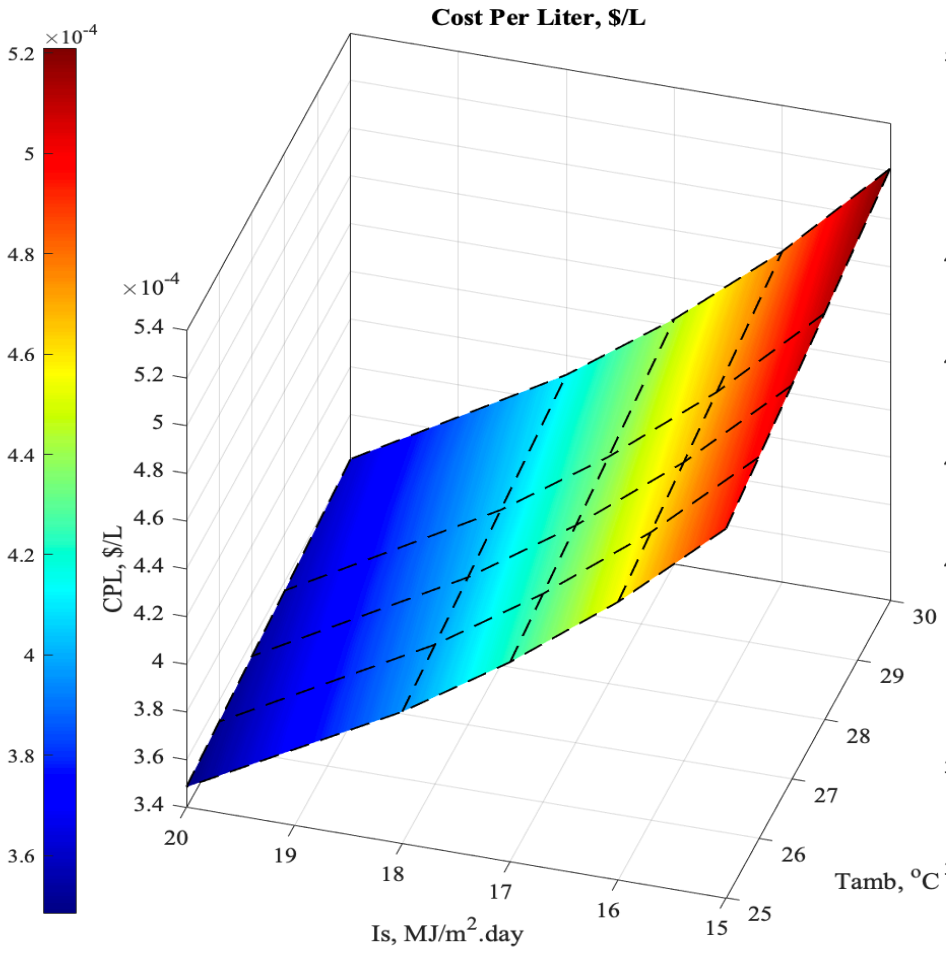

Figure 74: Solar still cost per liter, $

It was clearly discussed the effect of ambient temperature on the still production and costs. The other 2-D contour figure 75 exhibits cost per liter results with accurate numbers, so it will be much easier to analyze the design data results.

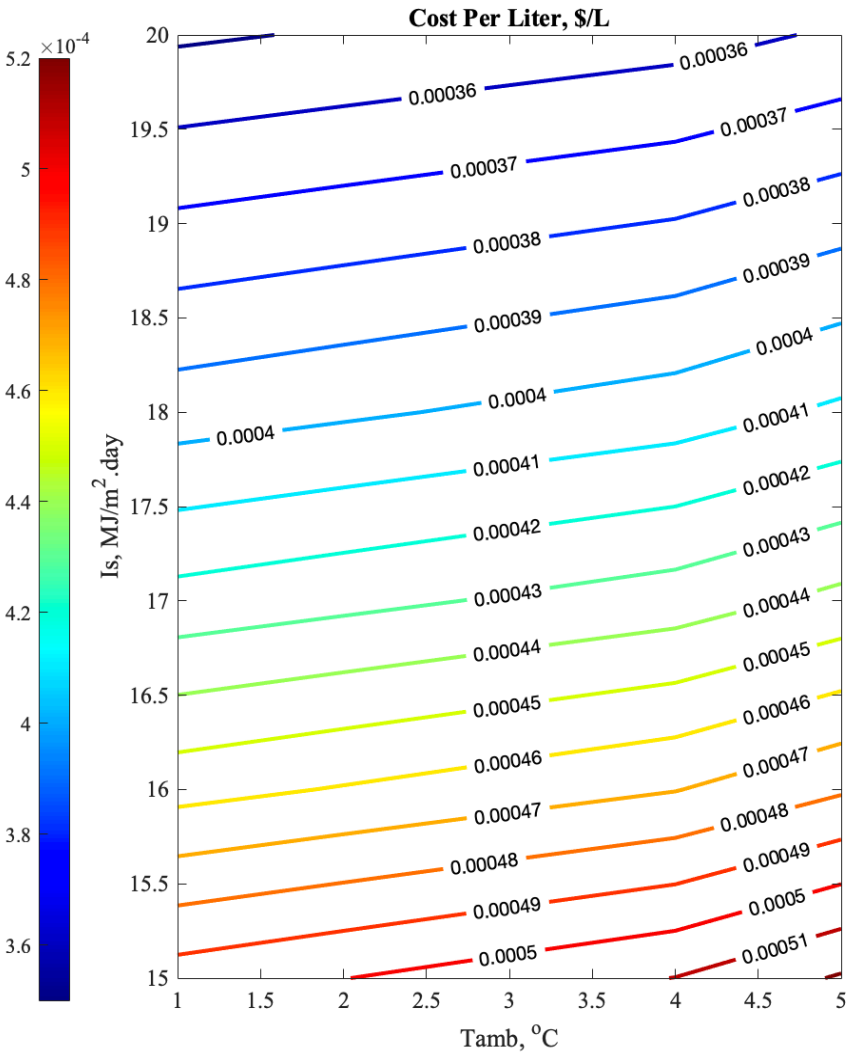

Figure 75: Solar still cost per liter, $/L

The 2-D figure 76 exhibits a significant decrease for the cost per liter over the period, then it gradually rises in the afternoon when the rate of water evaporation reduces due to the low solar energy absorbed by the saline water inside the basin. The minimum cost per liter that still can achieve for any amount of water production is 0.0004 $ when solar intensity is at peak value.

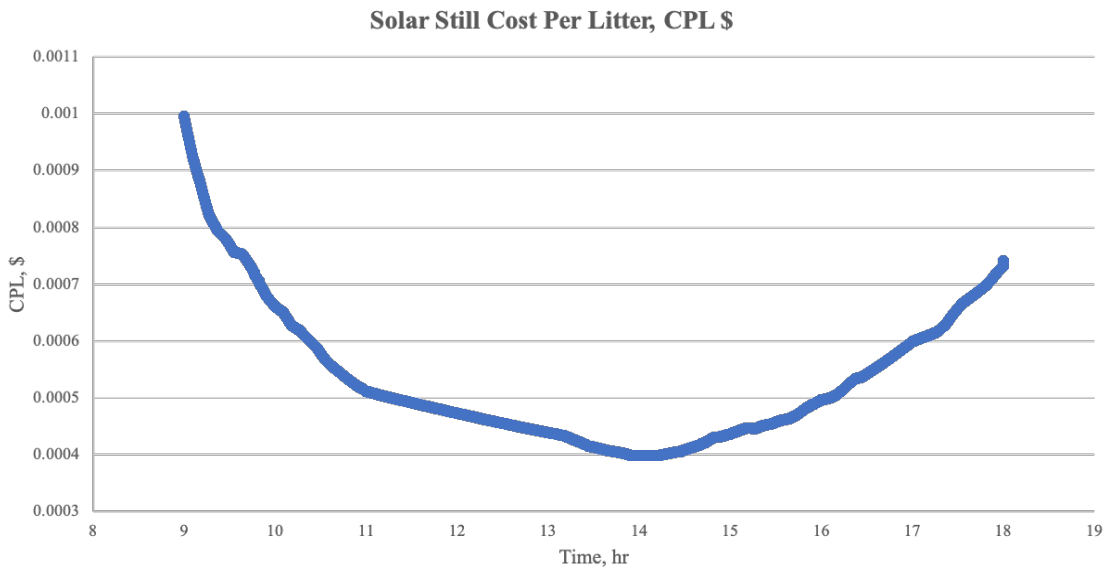

Figure 76: Solar still cost per liter during the day, $/L

The last but not least 3-D mesh figure 77 in solar still cost analysis results is dedicated to the total capital cost required to construct the whole system including each component. At a certain ambient temperature 30 ºC, the total capital cost shows a significant grow when the solar still production per day rise (marked in red), whereas the solar radiation energy has the adverse trend.

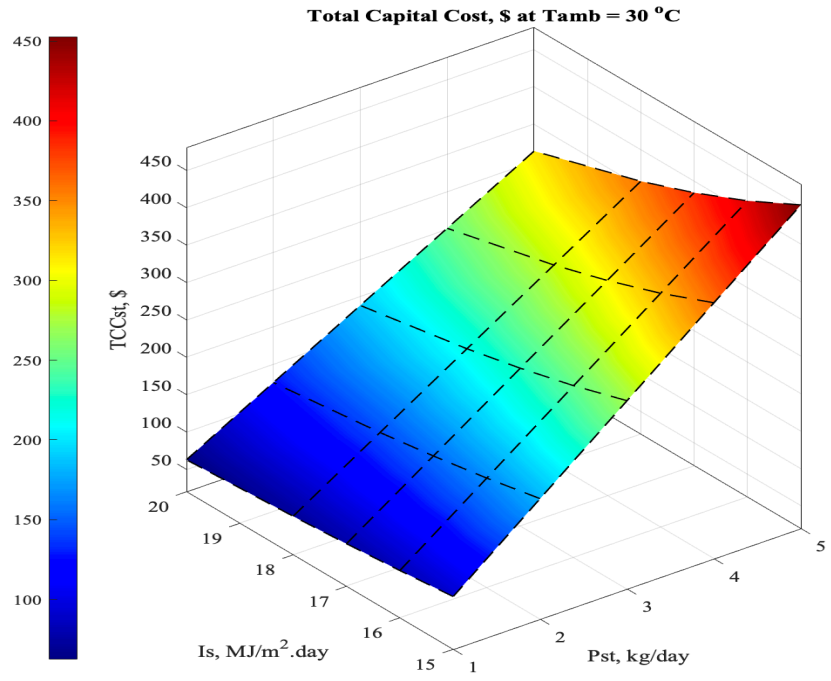

Figure 77: Solar still total capital cost at diff. solar radiation & ambient Temp.

It apparently can be easily figured out when presenting the results in a 2-D contour figure 78. For example, when solar radiation energy is at the optimal and preferred value 20 MJ/m^2.day with respect to 1 kg per day freshwater production, the total capital cost is at its lowest value 70 $.

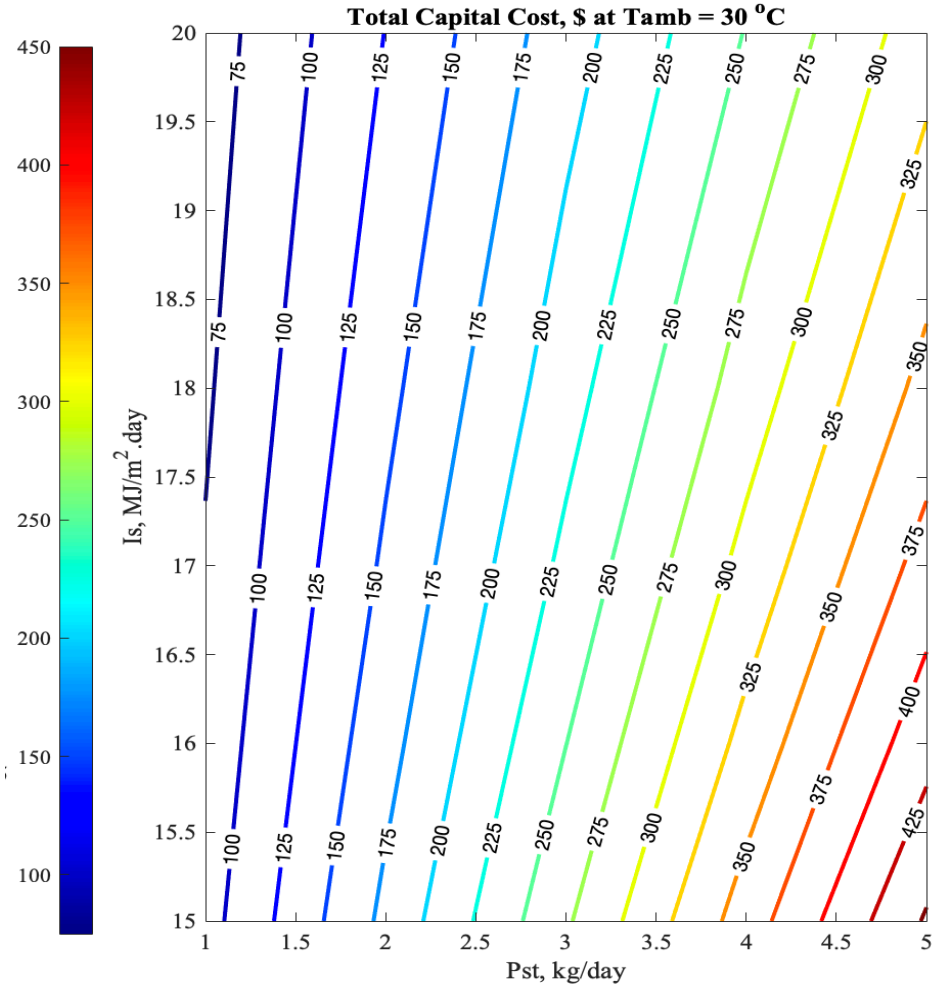

Figure 78: Solar still total capital cost at diff. solar radiation & ambient temp.

It is apparent from the below 2-D figure 79 that the total capital cost for the solar still is much greater when the productivity needed for a design is high than for a limited distillate water output from the still. For a productivity ranging from 15-20 kg/day, the TCC is dramatically declined to below $1500 when solar incident is at the optimal value (2:00 p.m.). However, when decided to

design a still with productivity less than or equal to 5 kg/day, the total capital cost won't exceed $500 except in the end of the period.

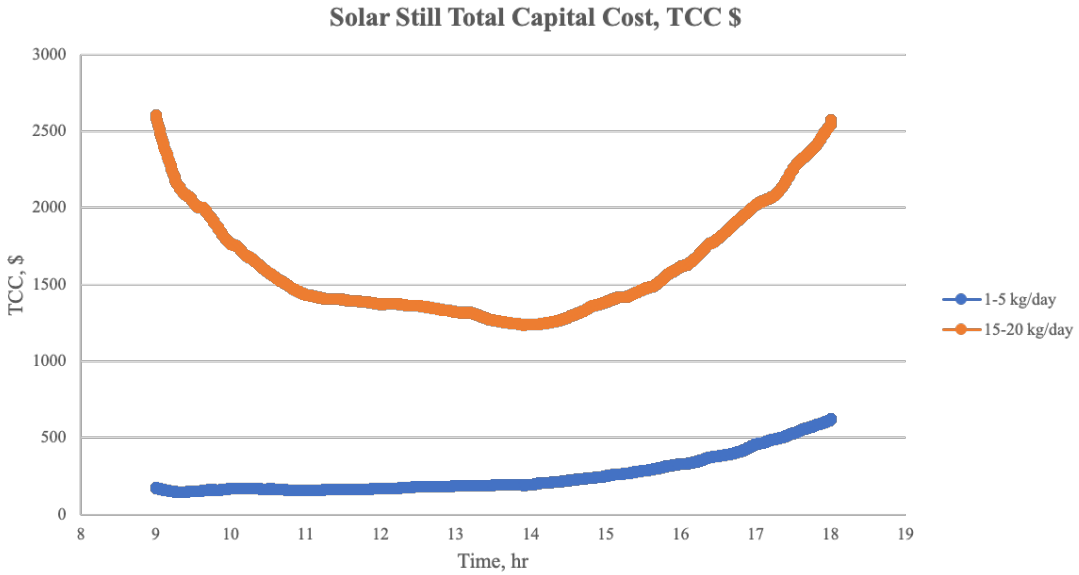

Figure 79: Solar still total capital cost during the day, TCC $

4.10 Comparison Between Design System Areas and Costs Analysis:

The following two figures 80 & 81 depicted a comparison between design areas for each component of the model system. In terms of systems area, it can be noticed that solar still (blue bar) features compact dimensions and can accommodate not more than 3 m^2 at a designed system with water production 5 kg/day. On the other hand, designers/ investors have to consider that the photovoltaic cell (orange bar) standalone system requires greater zone to be constructed including modules, cells and batteries. The gray bar represents the combined system area including solar still and photovoltaic cell, which is definitely demand much more space and costs to be established in an appropriate plant. It can be concluded that the design system reflects on the costs of each component that needs to be integrated when decides to construct any water desalination process. The total cost that should be allocated to design a combined process for a solar still assisted with a photovoltaic cell with a distillate water production of 5 kg/day is around $1700.

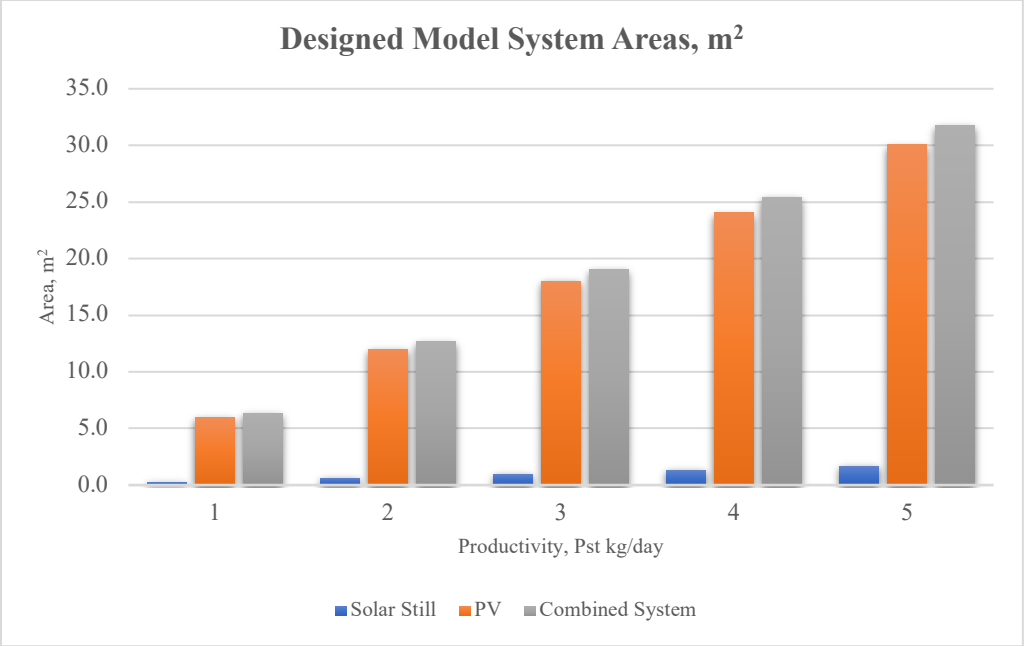

Figure 80: Designed Model System Areas, m^2

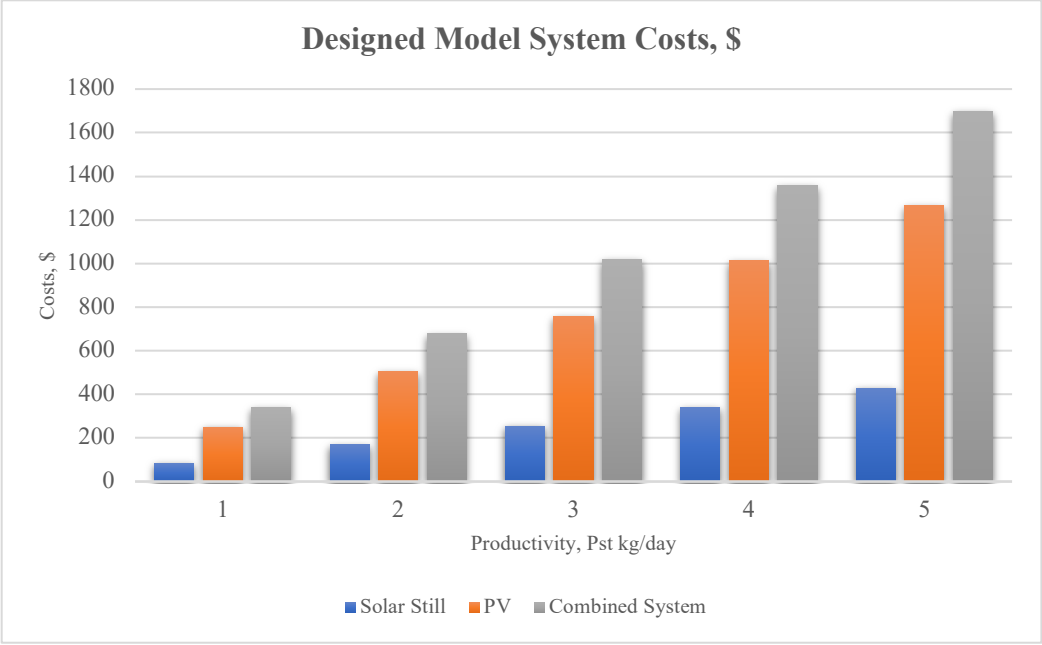

Figure 81: Designed Model System Costs, $

Chapter 5: Conclusion and Future Work

5.1 Conclusion:

According to the proposed model system and a SIMULINK design analysis for a photovoltaic assisted single slope solar still it can be concluded the following:

The solar desalination system demonstrates a considerable economic feature over conventional water desalination processes such as reverse osmosis (RO), multistage flash (MSF) and multi effect (MED) distillation systems due to cost effective and free energy. Moreover, desalination processes associated with solar energy are considered as one of the emerging processes among other different methods that employs renewable source of energy. This technology has multiple advantages comprising simplicity, ease of maintenance, low cost and low environmental impact especially when the need for small plants. The flat plate collector (photovoltaic cell) is effective in the condition with low ambient temperature and low solar incident.

It is quite evident that the productivity of the solar still coupled with the photovoltaic is much higher than the productivity when the still is standalone because of the stored solar energy and converted thermal energy supplied by the heating coil at the very bottom of the basin. Thus, the daily freshwater yields (Pstd, $kg/m^2.day$) becomes more than that of the passive solar still.

It is worth to mention that, while designing the model system, the precise amount of distilled water cannot be compared with the amount produced when the solar still is passive and standalone. However, it can be expressly estimated and compared when establishing a performance model system for the same unit. The design model revealed that there is a substantial effect of adding dye on still performance. The presence of a black dye in particular inside the still enhances the rate of water distillation because solar radiation is absorbed in a very thin upper layer, hence increasing

the surface temperature of the brine, and the rate of water evaporation will be promoted. Consequently, the productivity of the distillate water will definitely rise.

The present solar still design system can also lead to a relatively high distillate water production (> 20 kg/day, upscaling), because the developed software (SIMULINK) is reliable and designed for different analysis including different modifications, and comparisons. The produced fresh water by a solar still with its simplicity would be a plausible an alternative solution to supply isolated communities with no technical facilities.

The theoretical analysis using MATLAB/SIMULINK browser can predict the productivity and investigate the performance of the solar still into upscaling the design under diverse climatic conditions and locations.

The results reveal that solar desalination technique without a photovoltaic cell is astonishing with lower efficiency and performance, while comparing with solar desalination technique assisted with a photovoltaic cell (heating coil) that enhance the efficiency and improve the performance of the whole system.

5.2 Future Work:

The future work study aims to utilize some data analysis techniques such as artificial neural networks (machine learning model) to accurately predict and optimize daily solar distillate water production and attain high freshwater throughput/performance (efficiency) in many industrial applications. The single slope conventional solar still is assisted with a photovoltaic cell panel, which is exposed to a naturally available solar radiation directly from the sunlight. The solar still performance can then be evaluated theoretically and experimentally supported with data [59].

Proposed major subjects to be discussed in the study:

1- Control Systems:

Introducing a control system for water level in the feeding tank, solar still basin and the distillate water tank. In addition, evaluate the effect of lowering feed/ production rate on the performance and efficiency. The process may be integrated with a recycle system to maintain cost and attain high- distillate water production.

2- Novel Modifications & Manipulated Parameters:

A big set of daily weather and distillate water production data are required to conduct the study and predict the system's performance accurately. The following proposed critical factors/parameters can be considered and manipulated to optimize the solar system efficiency and improve its performance:

- Experiment location (photovoltaic cell and solar still positions).
- Climate Condition: humidity, solar intensity, wind velocity and surrounding temperature.
- Solar still insulations (materials selection & thermal conductivity): polystyrene, polyurethane, blackened wall, black rubber pad, basin color, aluminum foil and plexiglass sheet.
- Feed and distillate water temperatures and flowrates (ml/day).
- The effect of calculated convective evaporative heat transfer coefficient (hev) value and solar still's efficiency on the system's performance.
- Glass Type Cover: thickness, water-glass temperature.
- Solar still insolation (radiation) rate, inclination angle.
- Heating coil metallurgy, thermal conductivity and its resistance to corrosion.
- Single slope solar still (SSSS) with nanoparticles in brine.
- Internal solar still reflectors with top glass cover cooling.
- Basin pad/ absorber surface area and water level.

- Solar still with heat storage achieved by:
    - Sensible heat energy storage.
    - Latent heat energy storage (Phase Change Material, PCM), materials releasing heat during nocturnal (night) hours. Optimize the weight percentage of different nanoparticles to impregnate in phase change material (PCM).
- Photovoltaic cell Type (Solar Panel): Monocrystalline silicon cell could be selected and preferred for converting solar energy into electricity, thus useful heat generation. This kind of cells has semiconducting properties, which is considered to be the first commercially available solar cells and made from monocrystalline silicon (an extremely pure form of silicon).

3- Literature data Analysis & Machine Learning Models Predictions Framework:

- Obtained/collected literature input and output data from experiments of 2017 or 2019 year in modeling and designing of a Novel Lab-scale Passive Solar Still paper (Maddah H A. paper or from any paper relevant to the topic).
- Perform one-year literature data training for future10 year data generation after having the desired experimental data from various available data sources.
- Perform data training for the 10 years generated data to further obtain trained models.
- The trained models can be utilized for 10 years future data through machine learning predictions (data analysis & machine learning algorithms) models to further predict certain parameters.
- The proposed predicted parameters comprise but not limited to upscaling, location and photovoltaic integration, which will further generate output data and performance trial.

References:

[1] A. H. Almasoud and H. M. Gandayh, "Future of solar energy in Saudi Arabia," *J. King Saud Univ. - Eng. Sci.*, 2015, doi: 10.1016/j.jksues.2014.03.007.

[2] A. M. El-Nashar, "The economic feasibility of small MED seawater desalination plants for remote arid areas," *Desalination*, 2001, doi: 10.1016/S0011-9164(01)00124-2.

[3] "Where is Earth's water?," 2013. https://web.archive.org/web/20131214091601/http://ga.water.usgs.gov/edu/earthwherewater.html.

[4] "1 in 3 people globally do not have access to safe drinking water – UNICEF, WHO," 2019. https://www.who.int/news-room/detail/18-06-2019-1-in-3-people-globally-do-not-have-access-to-safe-drinking-water-unicef-who.

[5] C. Gasson, "Water management: Don't waste a drop," *Mining magazine*, pp. 41–43, 2011.

[6] A. O. Al-Jasser, "Saudi wastewater reuse standards for agricultural irrigation: Riyadh treatment plants effluent compliance," *J. King Saud Univ. - Eng. Sci.*, 2011, doi: 10.1016/j.jksues.2009.06.001.

[7] O. K. M. Ouda, "Treated wastewater use in Saudi Arabia: challenges and initiatives," *Int. J. Water Resour. Dev.*, 2016, doi: 10.1080/07900627.2015.1116435.

[8] S. Chowdhury and M. Al-Zahrani, "Characterizing water resources and trends of sector wise water consumptions in Saudi Arabia," *J. King Saud Univ. - Eng. Sci.*, 2015, doi: 10.1016/j.jksues.2013.02.002.

[9] G. W. Intelligence, "Global Water Intelligence," *Mark. Anal. Int. Water Ind.*, 2011.

[10] A. Alkhudhiri, N. Bin Darwish, and N. Hilal, "Analytical and forecasting study for wastewater treatment and water resources in Saudi Arabia," *J. Water Process Eng.*, 2019,

doi: 10.1016/j.jwpe.2019.100915.

[11] "Ministry of Environment, Water and Agriculture, Water Consumption for Municipal Purposes," 2017. .

[12] "Ministry of Economy and Planning." https://www.mep.gov.sa/en.

[13] S. Wogan, D., Pradhan, S., & Albardi, "GCC energy system overview–2017," Riyadh, Saudi Arabia, 2017.

[14] M. Abdul-Kareem Al-Sofi, "Seawater desalination - SWCC experience and vision," *Desalination*, 2001, doi: 10.1016/S0011-9164(01)00145-X.

[15] "Saline Water Conversion Corporation (SWCC) Annual Report," 2016. https://www.swcc.gov.sa/English/pages/home.aspx.

[16] D. Wogan, S. Pradhan, and S. Albardi, "GCC Energy System Overview - 2017," *GCC Energy Syst. Overv.*, 2017.

[17] "Saline Water Conversion Corporation." https://www.swcc.gov.sa/English/pages/home.aspx.

[18] A. Maurel, "Seawater/brackish water desalination and other non-conventional processes for water supply," no. France: Lavoisier, 2006.

[19] H. T. El-Dessouky and H. M. Ettouney, "Multi-Stage Flash Desalination," in *Fundamentals of Salt Water Desalination*, 2002.

[20] N. Ghaffour, V. K. Reddy, and M. Abu-Arabi, "Technology development and application of solar energy in desalination: MEDRC contribution," *Renewable and Sustainable Energy Reviews*. 2011, doi: 10.1016/j.rser.2011.06.017.

[21] H. Mahmoudi *et al.*, "Assessment of wind energy to power solar brackish water greenhouse desalination units: A case study from Algeria," *Renewable and Sustainable*

Energy Reviews. 2009, doi: 10.1016/j.rser.2009.03.001.

[22] H. Mahmoudi, O. Abdellah, and N. Ghaffour, "Capacity building strategies and policy for desalination using renewable energies in Algeria," *Renewable and Sustainable Energy Reviews*. 2009, doi: 10.1016/j.rser.2008.02.001.

[23] IRENA, "Water Desalination Using Renewable Energy - Technology Brief," *IRENA - IEA - Etsap*, 2012.

[24] "Solar resource maps of Saudi Arabia," 2019. https://solargis.com/maps-and-gis-data/download/saudi-arabia.

[25] K. Paulsen and F. Hensel, "Introduction of a new Energy Recovery System - Optimized for the combination with renewable energy," *Desalination*, 2005, doi: 10.1016/j.desal.2005.03.060.

[26] J. A. Duffie, W. A. Beckman, and J. McGowan, "Solar Engineering of Thermal Processes," *Am. J. Phys.*, 1985, doi: 10.1119/1.14178.

[27] S. P. P. Sukhatme, J. K. Nayak, and J. K. Naik, *Solar Energy Principles of Thermal Collection and Storage*. 2014.

[28] . A. S., . G. N. T., and . M. S. S., "Energy Conservation Potential of Inner Thermal Curtain in an Even Span Greenhouse," *Trends Appl. Sci. Res.*, 2006, doi: 10.3923/tasr.2006.542.552.

[29] A. Kaushal, "Solar stills: a review," *Renew. Sustain. energy Rev.*, vol. 14(1), pp. 446–453, 2010.

[30] A. J. N. Khalifa and A. M. Hamood, "Effect of insulation thickness on the productivity of basin type solar stills: An experimental verification under local climate," *Energy Convers. Manag.*, 2009, doi: 10.1016/j.enconman.2009.06.007.

[31] T. Tanaka, H., Nosoko, T., & Nagata, “Experimental study of basin-type, multiple-effect, diffusion-coupled solar still,” *Desalination*, vol. 150(2), pp. 131–144, 2002.

[32] H. Tanaka and Y. Nakatake, “Factors influencing the productivity of a multiple-effect diffusion-type solar still coupled with a flat plate reflector,” *Desalination*, 2005, doi: 10.1016/j.desal.2005.07.005.

[33] J. Gräter, F., Dürrbeck, M., & Rheinländer, “Multi-effect still for hybrid solar/fossil desalination of sea-and brackish water,” *Desalination*, vol. 138(1–3), pp. 111–119, 2001.

[34] B. Bouchekima, B. Gros, R. Ouahes, and M. Diboun, “Performance study of the capillary film solar distiller,” *Desalination*, 1998, doi: 10.1016/S0011-9164(98)00194-5.

[35] J. A. S. Moustafa M. Elsayed, Ibrahim S. Taha, “Design of solar thermal systems,” *Sci. Publ. Cent. King Abdulaziz Univ.*, vol. 57–61, no. Jeddah, p. 1994.

[36] D. M. Moustafa, S. M., Brusewitz, G. H., & Farmer, “Direct use of solar energy for water desalination,” *Sol. Energy*, vol. 22(2), pp. 141–148, 1979.

[37] T. Arunkumar *et al.*, “An experimental study on a hemispherical solar still,” *Desalination*, 2012, doi: 10.1016/j.desal.2011.11.047.

[38] A. E. Kabeel, “Performance of solar still with a concave wick evaporation surface,” *Energy*, 2009, doi: 10.1016/j.energy.2009.06.050.

[39] G. N. Lawrence, S. A., Gupta, S. P., & Tiwari, “Experimental validation of thermal analysis of solar still with dye,” *Int. J. Sol. energy*, vol. 6(5), pp. 291–305, 1988.

[40] A. K. Rajvanshi, “Effect of various dyes on solar distillation,” *Sol. Energy*, 1981, doi: 10.1016/0038-092X(81)90020-7.

[41] A. A. Badran, A. A. Al-Hallaq, I. A. Eyal Salman, and M. Z. Odat, “A solar still augmented with a flat-plate collector,” *Desalination*, 2005, doi:

10.1016/j.desal.2004.06.203.

[42] B. T. Nguyen, “SOLSTILL— A simulation program for solar distillation systems,” *Proc. EUROSUN*, pp. 96–105, 2004.

[43] P. I. Cooper, “The absorption of radiation in solar stills,” *Sol. Energy*, 1969, doi: 10.1016/0038-092X(69)90047-4.

[44] H. P. Garg and H. S. Mann, “Effect of climatic, operational and design parameters on the year round performance of single-sloped and double-sloped solar still under Indian arid zone conditions,” *Sol. Energy*, 1976, doi: 10.1016/0038-092X(76)90052-9.

[45] B. T. Nguyen, “Factors Affecting the Yield of Solar Distillation Systems and Measures to Improve Productivities,” in *Desalination and Water Treatment*, 2018.

[46] A. S. Nafey, “Simulation of solar heating systems - An overview,” *Renewable and Sustainable Energy Reviews*. 2005, doi: 10.1016/j.rser.2004.06.001.

[47] A. Gambler and E. Badreddin, “Dynamic modelling of MSF plants for automatic control and simulation purposes: A survey,” *Desalination*, 2004, doi: 10.1016/j.desal.2004.06.073.

[48] J. William, “Palm. SIMULINK, Introduction to MATLAB7 for Engineers.” 2005.

[49] H. A. Maddah, “Modeling and designing of a novel lab-scale passive solar still,” *J. Eng. Technol. Sci.*, 2019, doi: 10.5614/j.eng.technol.sci.2019.51.3.1.

[50] A. Madhlopa, “Development of an advanced passive solar still with separate condenser,” 2009.

[51] J. S. Gawande and L. B. Bhuyar, “Effect of Shape of the Absorber Surface on the Performance of Stepped Type Solar Still,” *Energy Power Eng.*, 2013, doi: 10.4236/epe.2013.58053.

[52] M. Hammami, S. Torretti, F. Grimaccia, and G. Grandi, “Thermal and performance analysis of a photovoltaic module with an integrated energy storage system,” *Appl. Sci.*, 2017, doi: 10.3390/app7111107.

[53] M. S. S. Abujazar, S. Fatihah, A. R. Rakmi, and M. Z. Shahrom, “The effects of design parameters on productivity performance of a solar still for seawater desalination: A review,” *Desalination*. 2016, doi: 10.1016/j.desal.2016.02.025.

[54] V. Velmurugan, M. Gopalakrishnan, R. Raghu, and K. Srithar, “Single basin solar still with fin for enhancing productivity,” *Energy Convers. Manag.*, 2008, doi: 10.1016/j.enconman.2008.05.010.

[55] G. E. Ahmad and J. Schmid, “Feasibility study of brackish water desalination in the Egyptian deserts and rural regions using PV systems,” *Energy Convers. Manag.*, 2002, doi: 10.1016/S0196-8904(01)00189-3.

[56] M. S. Eldean, “Design and simulation of solar desalination systems,” no. Faculty of Petroleum & Mining Engineering, p. 479, 2011.

[57] Z. A. Firatoglu and B. Yesilata, “New approaches on the optimization of directly coupled PV pumping systems,” *Sol. Energy*, 2004, doi: 10.1016/j.solener.2004.02.006.

[58] M. Ben Ammar, M. Chaabene, and Z. Chtourou, “Artificial Neural Network based control for PV/T panel to track optimum thermal and electrical power,” *Energy Convers. Manag.*, 2013, doi: 10.1016/j.enconman.2012.08.003.

[59] H. A. Maddah, M. Bassyouni, M. H. Abdel-Aziz, M. S. Zoromba, and A. F. Al-Hossainy, “Performance estimation of a mini-passive solar still via machine learning,” *Renew. Energy*, 2020, doi: 10.1016/j.renene.2020.08.006.

Appendices

Appendix A: Modeling & Simulation Flow Chart

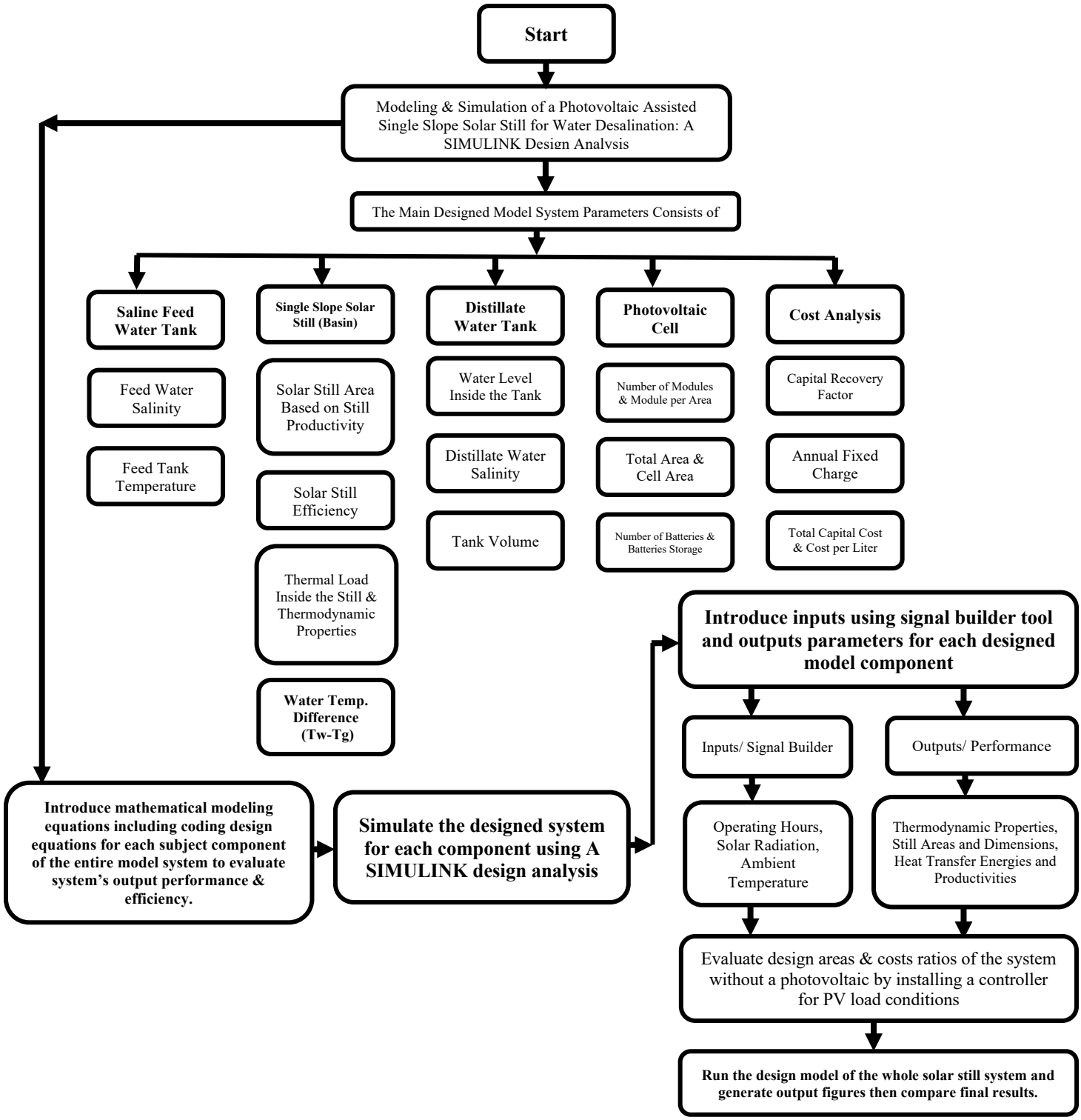

Appendix B: MATLAB Mathematical Codes

The following codes were used to model and design the photovoltaic assisted single slope solar still for saline water desalination using a MATLAB/SIMULINK browser.

Solar Still Design (Main Body Code):

```
function[Effst,Ast,Ag,d,a,t,Pstd,Pdye,Tg,Tw,Qload,Qev,Qrw_g,Qrg_
amb,hc,hev,Exev,Itotal]=STdesign(OH,Ar,Pst,Hs,Tamb,Twi,Sf,Vw)
%#codegen

%Solar still area based on still productivity Pst kg/m2.day,
daily solar
%radiation Hs MJ/m2.day, ambient temperature oC, mean wind
velocity km/h.
% Pstd=((0.244.*Hs)-(0.0294.*Tamb)-(0.0073.*Vw)-0.01222)-
(0.25.*((0.244.*Hs)-(0.0294.*Tamb)-(0.0073.*Vw)-0.01222));
Pstd=(0.244.*Hs)-(0.0294.*Tamb)-(0.0073.*Vw)-0.01222;
% Pstd=0.0393.*(Hs.^1.4)-(0.0294.*Tamb)-(0.00073.*Vw)-0.01222;

%Still productivity with black dyes, kg/m2.day:
Pdye=1.2122.*(Pstd.^1.0467);

%Solar still area, m2:
Ast=Pst./Pstd;

%Glass cover area:
Ag=Ast.*Ar;

%Solar still brine depth, cm:
% d=(log(Pstd./3.884))./-0.0458;
d=(log(Pstd./4.196))./-0.0575;
% d=19.54.*exp(-0.6495.*Pstd);

%Cover tilt angle degree:
a=1.763.*exp(0.9057.*Pstd);

%Insulation thickness, cm:
t=(7.913e-5.*exp(2.073.*Pstd)).*100;

%Solar Still efficiency:
Effst=(Pstd.*2.43.*100)./Hs;

%Solar still volume:
Volst=Ast.*(d./100);
```

```
%Thermal load inside the still, kW:
tawg=0.9;
alfag=0.85;
PC=0.85;
Qload=(Hs.*1000.*Ast.*tawg.*alfag)./(OH.*3600.*PC);

%Water temperature difference inside the still, oC:
dTw=(Qload.*1.*3600)./(fraw(Twi,Sf).*Volst.*fCp(Twi,Sf));

%Water temperature inside the basin, oC:
Tw=dTw+Twi;

%Evaporation heat transfer, kWatt:
Qev=(Pstd./(OH.*3600)).*flh(Tw).*Ast;

%Glass cover temperature calculations:
%Sky temperture, oC:
Tsky=0.0552.*((Tamb+273).^1.5);
hw=2991.684-19.84.*(Tw+273)+0.033.*((Tw+273).^2);
Tg=((((Tw+273).*(2991.684-
19.84.*(Tw+273)+0.033.*((Tw+273).^2)))+(Ar.*hw.*(Tamb+273))+(Ar.
*Tsky.*(0.141.*(Tamb+273)-36.026))).//((2991.684-
19.84.*(Tw+273)+0.033.*((Tw+273).^2))+(Ar.*hw)+(Ar.*(0.141.*(Tam
b+273)-36.026))))-273;

%Convection heat transfer coeff between water and cover W/m2oC:
%vapor pressures for water and glass cover, Pa:
%Pw=fPv(Tw).*1e5;
%Pg=fPv(Tg).*1e5;
% hc=(1000.*Qev)./(Ast.*16.28.*(Pw-Pg));
hc=(1000.*Qev)./(Ast.*(Tw-Tg));
% Evaporative convective heat transfer coeff between water and
cover W/m2oC:
Pw=fPv(Tw);
Pg=fPv(Tg);
hev=(16.273.*exp(-3).*hc.*(Pw-Pg))./(Tw-Tg);

%The heat transfer from the water to the cover by radiation,
kWatt:
Qrw_g=(Ag.*0.9.*(5.67e-8).*(((Tw+273).^4)-((Tg+273).^4)))./1000;

%The heat transfer from glass cover to the ambient, kW:
Qrg_amb=(Ag.*0.9.*5.67e-8.*(((Tg+273).^4)-Tsky.^4))./1000;

%Evaporation exergy, kW:
Exev=Qev.*(1-((Tamb+273)./(Tw+273)));

%dew point temp, oC:
```

```
%Tdp=(273.3.*((log(Hum))+((17.27.*(Tamb+273.3))./(Tamb+273.3))))
./(17.27-(log(Hum))+((17.27.*(Tamb+273.3))./(Tamb+273.3)));

%Exergy destruction rate, kW:
Itotal=(Pst./(OH.*3600)).*fCp(Tw,Sf).*(Tw-Tamb).*(1-
((Tamb+273)./(Tw+273)));

%%%%%%%%%%%%%%%%%%%%%%%%%%%%%%%%%%%%%%%%%%%%%%%%%%%%%%%%%%Function
s%%%%%%%%%%%
%Latent heat of distillate vapor evaporation, kJ/kg:
function Lh=flh(T)
Lh=2499.5698-(2.204864.*T)-(2.304*(10^-3)*(T.^2));

%Vapor pressure of water, bar:
function Pvw=fPv(T)
% Pvw=10.^((8.07131-1730.63)./(233.426+T));
% Pvw=10.^(8.07131-(1730.63./(233.426+T)));
Pvw=0.01677.*exp(0.04133.*T);

% %Specific heat capacity at const pressure, kJ/kgoC:
% function Cp=fCp(T)
% Cp=0.6047.*exp(-0.007588.*T)+3.606.*exp(0.0008706.*T);

%Specific heat capacity of seawater kJ/kgoC (T=oC, S=g/kg)
function Cp=fCp(T,S)
%%the specific heat of water at constant pressure is:
a=4206.8-(6.6197.*S)+(1.2288*(10^-2)*(S).^2);
b=-1.1262+(5.4178*(10^-2).*S)-(2.2719*(10^-4)*(S).^2);
c=1.2026*(10^-2)-(5.3566*(10^-4).*S)+(1.8906*(10^-6)*(S).^2);
d=6.8774*(10^-7)+(1.517*(10^-6).*S)-(4.4268*(10^-9)*(S).^2);
Cp=(a+(b.*T)+(c.*(T.^2))+(d.*(T.^3)))./1000;

%Saline water density based on Temp, oC and salinity, kg/kg:
function RAW=fraw(T,S)
Yc=((2*(mean(T)))-200)/160;
segma=((2000.*S./1000)-150)./150;
ar0=2.01611+0.115313.*segma+0.000326.*((2*(segma.^2))-1);
ar1=-0.0541+0.001571.*segma+0.000423.*((2*(segma.^2))-1);
ar2=-0.006124+0.00174.*segma+0.000009.*((2*(segma.^2))-1);
ar3=0.000346+0.000087.*segma+0.000053.*((2*(segma.^2))-1);
RAW=(0.5*ar0+ar1.*Yc+ar2.*(2*(Yc.^2)-1)+ar3.*(4.*(Yc.^3)-
3*Yc)).*1000;
```

Photovoltaic Module Calculations:

```
function[NOM,Ac,Am,At,BS,AH,NOB,PVCt]=PVcalc(OH,Hs,Pm,THP,EM,NC,
NOC,DOD,Vm,Vb,Effb,FOBc,Cb)
```

```
%#codegen

%The number of modules could be calculated based on total power
and module
%power:
NOM=THP./Pm;

%Solar radiation from MJ/m2.day to W/m2:
Is=(Hs.*1e6)./(OH.*3600);

%The Module area m2:
Am=100.*Pm./(Is.*EM);

%The total area m2:
At=Am.*NOM;

%The cell area cm2:
Ac=(Am.*10000)./NC;

%Battery storage Wh:
BS=(OH.*NOC.*THP)./(DOD.*Effb);

%If a 24 V system is chosen, the required amp. hours of
batteries=16 585/24=700 AH.
AH=BS./Vm;

%Number of batteries:
NOB=Vm.*NOM/Vb;

%The total system costs:
PVCt=(THP.*FOBc)+(Cb.*NOB);
```

Feed Tank Design Model:

```
function [dH,Ht,Pft,Volft,Vf,Aft]=
FeedTank(OH,Tft,Sf,Mft,Hs,Dft,Dt)
%#codegen

%Tank cross sectional area, m2:
Aft=(pi./4).*(Dft.^2);

%Level change in the tank, m:
dH=Mft./(fraw(Tft,Sf).*Aft);

%Total head, m:
Ht=Hs+dH;
```

```
%Flow velocity out from the tank, m/s:
Atube=(pi./4).*(Dt.^2);
Vf=(Mft./(OH.*3600))./(fraw(Tft,Sf).*Atube);

%Tank pressure, kPa:
Pft=((fraw(Tft,Sf).*9.81).*(Ht-((Vf.^2)./(2.*9.81))))./1000;

%Tank volume, m3:
Volft=Aft.*dH;

% %Specific heat capacity of seawater kJ/kgoC (T=oC, S=g/kg)
% function Cp=fcp(T,S)
% %%the specific heat of water at constant pressure is:
% a=4206.8-(6.6197.*S)+(1.2288*(10^-2)*(S).^2);
% b=-1.1262+(5.4178*(10^-2).*S)-(2.2719*(10^-4)*(S).^2);
% c=1.2026*(10^-2)-(5.3566*(10^-4).*S)+(1.8906*(10^-6)*(S).^2);
% d=6.8774*(10^-7)+(1.517*(10^-6).*S)-(4.4268*(10^-9)*(S).^2);
% Cp=(a+(b.*T)+(c.*(T.^2))+(d.*(T.^3)))./1000;

%Saline water density based on Temp, oC and salinity, kg/kg:
function RAW=fraw(T,S)
Yc=((2*(mean(T)))-200)/160;
segma=((2000.*S./1000)-150)./150;
ar0=2.01611+0.115313.*segma+0.000326.*((2*(segma.^2))-1);
ar1=-0.0541+0.001571.*segma+0.000423.*((2*(segma.^2))-1);
ar2=-0.006124+0.00174.*segma+0.000009.*((2*(segma.^2))-1);
ar3=0.000346+0.000087.*segma+0.000053.*((2*(segma.^2))-1);
RAW=(0.5*ar0+ar1.*Yc+ar2.*(2*(Yc.^2)-1)+ar3.*(4.*(Yc.^3)-
3*Yc)).*1000;
```

Distillate Tank Design Model:

```
function [dH,Voldt,Adt]= DistTank(Tdt,Md,Ddt)
%#codegen

%Tank cross sectional area, m2:
Adt=(pi./4).*(Ddt.^2);

%Level change in the tank, m:
Sd=0;
dH=Md./(fraw(Tdt,Sd).*Adt);

%Tank volume, m3:
Voldt=Adt.*dH;
```

```
% %Specific heat capacity of seawater kJ/kgoC (T=oC, S=g/kg)
% function Cp=fcp(T,S)
% %%the specific heat of water at constant pressure is:
% a=4206.8-(6.6197.*S)+(1.2288*(10^-2)*(S).^2);
% b=-1.1262+(5.4178*(10^-2).*S)-(2.2719*(10^-4)*(S).^2);
% c=1.2026*(10^-2)-(5.3566*(10^-4).*S)+(1.8906*(10^-6)*(S).^2);
% d=6.8774*(10^-7)+(1.517*(10^-6).*S)-(4.4268*(10^-9)*(S).^2);
% Cp=(a+(b.*T)+(c.*(T.^2))+(d.*(T.^3))./1000;

%Saline water density based on Temp, oC and salinity, kg/kg:
function RAW=fraw(T,S)
Yc=((2*(mean(T)))-200)/160;
segma=((2000.*S./1000)-150)./150;
ar0=2.01611+0.115313.*segma+0.000326.*((2*(segma.^2))-1);
ar1=-0.0541+0.001571.*segma+0.000423.*((2*(segma.^2))-1);
ar2=-0.006124+0.00174.*segma+0.000009.*((2*(segma.^2))-1);
ar3=0.000346+0.000087.*segma+0.000053.*((2*(segma.^2))-1);
RAW=(0.5*ar0+ar1.*Yc+ar2.*(2*(Yc.^2)-1)+ar3.*(4.*(Yc.^3)-
3*Yc)).*1000;
```

Appendix C: Tables including 3-D Results and Figures

Solar still integrated with a photovoltaic SIMULINK/ theoretical results are tabulated herein under tables (C1-11):

C.1: Solar Still Area, Ast m^2, Is: Solar Radiation MJ/m^2.day, Pst: Productivity kg/day.

Table 5: Solar still area, Ast m^2, Is: solar radiation MJ/m^2.day, Pst: Productivity kg/day.

Is/Pst	1	2	3	4	5	Ast, m^2
15	0.343780	0.687560	1.031340	1.375120	1.718899	T_{amb}= 25 °C
16	0.317175	0.634349	0.951524	1.268698	1.585873	
17	0.294391	0.588783	0.883174	1.177566	1.471957	
18	0.274662	0.549324	0.823986	1.098648	1.373310	
20	0.242199	0.484398	0.726597	0.968796	1.210994	

C.2: PV Total System Area, At m^2, at ambient temperature 25 °C:

Table 6: PV total system area, At m2, at ambient temperature 25 °C

Is/Pst	1	2	3	4	5	At, m^2
15	6.00780	12.01561	18.02341	24.03122	30.03902	T_{amb}= 25 °C
16	5.54286	11.08571	16.62857	22.17143	27.71428	

17	5.14470	10.28941	15.43411	20.57882	25.72352	
18	4.79992	9.59984	14.39976	19.19968	23.99960	
20	4.23260	8.46520	12.69781	16.93041	21.16301	

C.3: Solar Still Efficiency, Effst %, at ambient temperature 25 ^{o}C:

Table 7: Solar still efficiency, Effst %, at ambient temperature 25 oC

Is/Pst	1	2	3	4	5	Effst, %
15	47.123176	47.123176	47.123176	47.123176	47.123176	T_{amb}= 25 ^{o}C
16	47.883727	47.883727	47.883727	47.883727	47.883727	
17	48.554802	48.554802	48.554802	48.554802	48.554802	
18	49.151313	49.151313	49.151313	49.151313	49.151313	
20	50.165382	50.165382	50.165382	50.165382	50.165382	

C.4: Solar Still Areas at Different Solar Radiation Energies (Is, MJ/m^2.day):

Table 8: Solar still areas at different solar radiation energies (Is = MJ/m2.day)

T_{amb} /Pst	1	2	3	4	5	Ast, m^2
25	0.343780	0.687560	1.031340	1.375120	1.718899	Is=15
30	0.362078	0.724155	1.086233	1.448311	1.810389	
35	0.382433	0.764866	1.147299	1.529731	1.912164	
40	0.405213	0.810426	1.215639	1.620852	2.026065	
45	0.430879	0.861758	1.292637	1.723515	2.154394	
T_{amb} /Pst	1	2	3	4	5	Ast, m^2
25	0.317175	0.634349	0.951524	1.268698	1.585873	Is=16
30	0.332686	0.665372	0.998058	1.330744	1.663430	
35	0.349792	0.699585	1.049377	1.399170	1.748962	
40	0.368754	0.737507	1.106261	1.475014	1.843768	
45	0.389888	0.779776	1.169665	1.559553	1.949441	
T_{amb} /Pst	1	2	3	4	5	Ast, m^2
25	0.274662	0.549324	0.823986	1.098648	1.373310	Is=18
30	0.286218	0.572436	0.858655	1.144873	1.431091	
35	0.298789	0.597579	0.896368	1.195158	1.493947	
40	0.312516	0.625032	0.937547	1.250063	1.562579	
45	0.327564	0.655128	0.982692	1.310256	1.637820	
T_{amb} /Pst	1	2	3	4	5	Ast, m^2
25	0.242199	0.484398	0.726597	0.968796	1.210994	Is=20
30	0.251140	0.502281	0.753421	1.004561	1.255702	

35	0.260767	0.521534	0.782302	1.043069	1.303836	
40	0.271162	0.542323	0.813485	1.084646	1.355808	
45	0.282419	0.564838	0.847257	1.129676	1.412095	

C.5: Solar Still Glass Cover Areas at Solar Radiation Energies (Is=15,20 MJ/m^2.day) respectively:

Table 9: Solar still glass cover areas at solar radiation energies

T_{amb} /Pst	1	2	3	4	5	Ag, m^2
25	0.515670	1.031340	1.547009	2.062679	2.578349	Is=15
30	0.543117	1.086233	1.629350	2.172466	2.715583	
35	0.573649	1.147299	1.720948	2.294597	2.868247	
40	0.607819	1.215639	1.823458	2.431278	3.039097	
45	0.607819	1.215639	1.823458	2.431278	3.039097	
T_{amb} /Pst	1	2	3	4	5	Ag, m^2
25	0.363298	0.726597	1.089895	1.453193	1.816492	Is=20
30	0.363298	0.726597	1.089895	1.453193	1.816492	
35	0.391151	0.782302	1.173452	1.564603	1.955754	
40	0.406742	0.813485	1.220227	1.626970	2.033712	
45	0.423629	0.847257	1.270886	1.694514	2.118143	

C.6: Solar Still Glass Cover Areas at Solar Radiation Energies (Is=15,20 MJ/m^2.day) respectively:

Table 10: Solar still glass cover areas at different solar radiation energies and productions

Is /T_{amb}	25	30	35	40	45	d, cm
15	6.371791	7.273657	8.224862	9.231117	10.299189	Is=15
16	4.970934	5.801309	6.673329	7.591392	8.560633	
17	3.674551	4.443940	5.248948	6.093035	6.980188	
18	2.468136	3.184884	3.932446	4.713591	5.531479	
20	0.280621	0.911099	1.565296	2.245066	2.952492	
Is /T_{amb}	25	30	35	40	45	Effst, %
15	47.123176	44.741776	42.360376	39.978976	37.597576	Is=20
16	47.883727	45.651165	43.418602	41.186040	38.953477	
17	48.554802	46.453567	44.352331	42.251096	40.149861	
18	49.151313	47.166813	45.182313	43.197813	41.213313	
20	50.165382	48.379332	46.593282	44.807232	43.021182	
Is /T_{amb}	25	30	35	40	45	Pstd, kg/m^2.day
15	2.908838	2.761838	2.614838	2.467838	2.320838	

16	3.152838	3.005838	2.858838	2.711838	2.564838	
17	3.396838	3.249838	3.102838	2.955838	2.808838	
18	3.640838	3.493838	3.346838	3.199838	3.052838	
20	4.128838	3.981838	3.834838	3.687838	3.540838	
Is /T_{amb}	25	30	35	40	45	Pdye, $kg/m^2.day$
15	3.706376	3.510560	3.315231	3.120413	2.926137	
16	4.032416	3.835843	3.639719	3.444066	3.248907	
17	4.359637	4.162363	3.965505	3.769083	3.573116	
18	4.687958	4.490030	4.292491	4.095357	3.898645	
20	5.347629	5.148512	4.949739	4.751321	4.553272	
Is /T_{amb}	25	30	35	40	45	Tg, ^oC
15	25.324532	28.649531	32.293758	36.220148	40.399246	
16	26.442429	29.460169	32.884309	36.650444	40.711175	
17	28.346013	30.773475	33.798813	37.289345	41.155974	
18	31.985533	33.120847	35.343097	38.314024	41.835389	
20	104.000656	52.774601	45.244476	43.985461	45.198440	
Is /T_{amb}	25	30	35	40	45	Tw, ^oC
15	36.380204	35.589118	34.942737	34.403945	33.947236	
16	38.723422	37.474787	36.498039	35.712200	35.065461	
17	42.538613	40.367777	38.777716	37.561712	36.600650	
18	49.765523	45.317353	42.405508	40.349645	38.819341	
20	223.159234	89.493498	64.628885	54.143805	48.358881	

C.7: Total Photovoltaic Cost, PVCt $ at Different Ambient Temperature 25, 30, 35 ^oC respectively:

Table 11: Total photovoltaic cost, PVCt $ at different ambient temperatures

Is/Pst	1	2	3	4	5	PVCt, $
15	253.34583	506.69165	760.03748	1013.38330	1266.72913	T_{amb}=25 ^oC
16	249.32186	498.64372	747.96557	997.28743	1246.60929	
17	245.87599	491.75197	737.62796	983.50394	1229.37993	
18	242.89198	485.78396	728.67595	971.56793	1214.45991	
20	237.98204	475.96408	713.94612	951.92816	1189.91019	
Is/Pst	1	2	3	4	5	PVCt, $
15	266.8303	533.6605	800.4908	1067.3211	1334.1513	T_{amb}=30 ^oC
16	261.5149	523.0298	784.5447	1046.0596	1307.5745	
17	256.9977	513.9954	770.9931	1027.9908	1284.9885	
18	253.1114	506.2229	759.3343	1012.4457	1265.5572	
20	246.7678	493.5355	740.3033	987.0711	1233.8389	

Is/Pst	1	2	3	4	5	PVCt, $
15	281.8308	563.6617	845.4925	1127.3233	1409.1542	T_{amb}=35 °C
16	274.9619	549.9237	824.8856	1099.8475	1374.8093	
17	269.1732	538.3464	807.5197	1076.6929	1345.8661	
18	264.2286	528.4572	792.6858	1056.9144	1321.1431	
20	256.2271	512.4541	768.6812	1024.9083	1281.1353	
Is/Tamb	1	2	3	4	5	Pst, kg/day
15/25	253.3458	506.6917	760.0375	1013.3833	1266.7291	PVCt, $
16/30	261.5149	523.0298	784.5447	1046.0596	1307.5745	4-D Plot
17/35	269.1732	538.3464	807.5197	1076.6929	1345.8661	
18/40	276.3672	552.7345	829.1017	1105.4689	1381.8361	
20/45	277.5019	555.0038	832.5057	1110.0076	1387.5095	

C.8: Convective Heat Transfer Coefficient, hc W/m^2.°C at Different Ambient Temperatures and The Same Productivities (i.e. 1-5 kg/day):

Table 12: Convective heat transfer coefficient, hc w/m^2.°c at different ambient temperatures

Is /T_{amb}	25	30	32	34	35	hc, W/m^2.°C
15	22.074659	33.416511	43.288021	63.086631	82.934925	
16	21.489443	31.432206	39.397596	53.765556	66.365625	
17	19.958258	28.307247	34.407454	44.365196	52.162584	
18	16.951520	23.821317	28.275592	34.857124	39.522937	
20	2.277265	8.599214	11.314537	14.379399	16.124937	

Is /T_{amb}	25	26	27	28	30	hc, W/m^2.°C
15	22.074659	23.581894	25.365697	27.509258	33.416511	
16	21.489443	22.866403	24.472176	26.369762	31.432206	
17	19.958258	21.174811	22.565449	24.174268	28.307247	
18	16.951520	18.033575	19.228282	20.564512	23.821317	
20	2.277265	3.555492	4.808283	6.056231	8.599214	

C.9: Heat transfer energies, Q's kW including evaporation, Thermal load inside the still, Energy between water and glass cover, Energy between glass cover and ambient at different solar radiations and productivities respectively:

Table 13: Heat transfer energies, Q's kW at different solar radiations & water productions

Is/Pst	1	2	3	4	5	Qev, kW
15	0.0838995	0.1677991	0.2516986	0.3355982	0.4194977	T_{amb}= 25 °C

16	0.0837061	0.1674122	0.2511182	0.3348243	0.4185304	
17	0.0833892	0.1667784	0.2501676	0.3335568	0.4169460	
18	0.0827826	0.1655651	0.2483477	0.3311302	0.4139128	
20	0.0657220	0.1314441	0.1971661	0.2628882	0.3286102	
Is/Pst	1	2	3	4	5	Qev, kW
15	0.0839647	0.1679293	0.2518940	0.3358587	0.4198233	T_{amb}= 30 °C
16	0.0838093	0.1676186	0.2514278	0.3352371	0.4190464	
17	0.0835698	0.1671396	0.2507094	0.3342791	0.4178489	
18	0.0831569	0.1663139	0.2494708	0.3326277	0.4157846	
20	0.0792985	0.1585969	0.2378954	0.3171939	0.3964923	
Is/Pst	1	2	3	4	5	Qload
15	0.1611468	0.3222936	0.4834405	0.6445873	0.8057341	T_{amb}= 25 °C
16	0.1585873	0.3171746	0.4757618	0.6343491	0.7929364	
17	0.1563954	0.3127909	0.4691863	0.6255818	0.7819772	
18	0.1544974	0.3089948	0.4634922	0.6179896	0.7724870	
20	0.1513743	0.3027486	0.4541229	0.6054972	0.7568715	
Is/Pst	1	2	3	4	5	Qload
15	0.1697239	0.3394479	0.5091718	0.6788957	0.8486197	T_{amb}= 30 °C
16	0.1663430	0.3326859	0.4990289	0.6653719	0.8317148	
17	0.1634697	0.3269394	0.4904091	0.6538787	0.8173484	
18	0.1609977	0.3219955	0.4829932	0.6439909	0.8049887	
20	0.1569627	0.3139254	0.4708881	0.6278508	0.7848134	
Is/Pst	1	2	3	4	5	Qrw_g
15	0.0326568	0.0653137	0.0979705	0.1306273	0.1632842	T_{amb}= 25 °C
16	0.0340464	0.0680928	0.1021392	0.1361856	0.1702320	
17	0.0375591	0.0751183	0.1126774	0.1502366	0.1877957	
18	0.0462730	0.0925460	0.1388190	0.1850920	0.2313650	
20	0.7489958	1.4979915	2.2469873	2.9959830	3.7449788	
Is/Pst	1	2	3	4	5	Qrw_g
15	0.0218563	0.0437127	0.0655690	0.0874254	0.1092817	T_{amb}= 30 °C
16	0.0235029	0.0470058	0.0705087	0.0940116	0.1175145	
17	0.0265642	0.0531285	0.0796927	0.1062569	0.1328211	
18	0.0325427	0.0650854	0.0976281	0.1301708	0.1627135	
20	0.1153985	0.2307970	0.3461955	0.4615940	0.5769924	

Table 14: Energy transfer between water and glass cover, glass cover and ambient at different solar radiations

Is/Pst	1	2	3	4	5	Qrg_amb
15	0.0373261	0.0746523	0.1119784	0.1493046	0.1866307	T_{amb}= 25 °C

16	0.0373360	0.0746721	0.1120081	0.1493441	0.1866801	
17	0.0393052	0.0786104	0.1179156	0.1572208	0.1965260	
18	0.0451996	0.0903992	0.1355989	0.1807985	0.2259981	
20	0.2539616	0.5079231	0.7618847	1.0158463	1.2698079	
Is/Pst	1	2	3	4	5	Qrg_amb
15	0.030345	0.060689	0.091034	0.121378	0.151723	T_{amb}= 30 °C
16	0.030157	0.060314	0.090471	0.120628	0.150784	
17	0.031339	0.062677	0.094016	0.125355	0.156693	
18	0.034984	0.069967	0.104951	0.139935	0.174918	
20	0.078406	0.156811	0.235217	0.313623	0.392028	

C9: Cost Analysis for the design model system at different solar radiations energy, productivities and ambient temperature:

Table 15: Cost analysis for the design model system at different solar radiations energy

Is/Tamb	25	26	27	28	30	CPL
15	0.0004947	0.0004998	0.0005049	0.0005102	0.0005211	Pst= [1:5] kg/day
16	0.0004564	0.0004607	0.0004651	0.0004696	0.0004788	
17	0.0004237	0.0004274	0.0004311	0.0004349	0.0004428	
18	0.0003953	0.0003985	0.0004017	0.0004051	0.0004119	
20	0.0003485	0.0003510	0.0003536	0.0003562	0.0003614	
Is/Pst	1	2	3	4	5	TCCst, $
15	85.98794	171.97589	257.96383	343.95178	429.93972	T_{amb} = 25 °C
16	79.33329	158.66657	237.99986	317.33315	396.66643	
17	73.63466	147.26931	220.90397	294.53863	368.17328	
18	68.69984	137.39969	206.09953	274.79937	343.49922	
20	60.58000	121.16000	181.74000	242.31999	302.89999	
Is/Pst	1	2	3	4	5	TCCst, $
15	90.56469	181.12938	271.69407	362.25876	452.82345	T_{amb} = 30 °C
16	83.21307	166.42613	249.63920	332.85227	416.06534	
17	76.96537	153.93075	230.89612	307.86150	384.82687	
18	71.59033	143.18065	214.77098	286.36130	357.95163	
20	62.81647	125.63294	188.44940	251.26587	314.08234	

C10: Area ratios for solar still standalone, PV standalone and combined together at different solar radiations energy, productivities respectively:

Is/Pst	1	2	3	4	5	Ast, m^2
15	0.3437799	0.6875598	1.0313397	1.3751195	1.7188994	T_{amb} = 25 °C
16	0.3171746	0.6343491	0.9515237	1.2686982	1.5858728	
17	0.2943914	0.5887829	0.8831743	1.1775657	1.4719572	
18	0.2746620	0.5493241	0.8239861	1.0986482	1.3733102	
20	0.2421989	0.4843978	0.7265967	0.9687956	1.2109945	

Is/Pst	1	2	3	4	5	At, m^2
15	6.007804	12.015608	18.023412	24.031215	30.039019	
16	5.542856	11.085713	16.628569	22.171425	27.714282	
17	5.144705	10.289409	15.434114	20.578818	25.723523	
18	4.799919	9.599838	14.399758	19.199677	23.999596	
20	4.232602	8.465204	12.697806	16.930408	21.163010	

Is/Pst	1	2	3	4	5	SS+PV, m^2
15	6.351584	12.703167	19.054751	25.406335	31.757919	
16	5.860031	11.720062	17.580093	23.440124	29.300155	
17	5.439096	10.878192	16.317288	21.756384	27.195480	
18	5.074581	10.149162	15.223744	20.298325	25.372906	
20	4.474801	8.949602	13.424403	17.899204	22.374005	

C11: Cost ratios for solar still stand alone, PV standalone and combined together at different solar radiations energy, productivities respectively:

Is/Pst	1	2	3	4	5	TCCst, $
15	85.98794	171.97589	257.96383	343.95178	429.93972	T_{amb} = 25 °C
16	79.33329	158.66657	237.99986	317.33315	396.66643	
17	73.63466	147.26931	220.90397	294.53863	368.17328	
18	68.69984	137.39969	206.09953	274.79937	343.49922	
20	60.58000	121.16000	181.74000	242.31999	302.89999	

Is/Pst	1	2	3	4	5	PVCt, $
15	253.3458	506.6917	760.0375	1013.3833	1266.7291	T_{amb} = 25 °C
16	249.3219	498.6437	747.9656	997.2874	1246.6093	
17	245.8760	491.7520	737.6280	983.5039	1229.3799	
18	242.8920	485.7840	728.6759	971.5679	1214.4599	
20	237.9820	475.9641	713.9461	951.9282	1189.9102	

Is/Pst	1	2	3	4	5	SS+PV, $
15	339.3338	678.6675	1018.0013	1357.3351	1696.6688	T_{amb} = 25 °C
16	328.6551	657.3103	985.9654	1314.6206	1643.2757	
17	319.5106	639.0213	958.5319	1278.0426	1597.5532	
18	311.5918	623.1837	934.7755	1246.3673	1557.9591	
20	298.5620	597.1241	895.6861	1194.2481	1492.8102	

Appendix C: List of Supplementary Figures

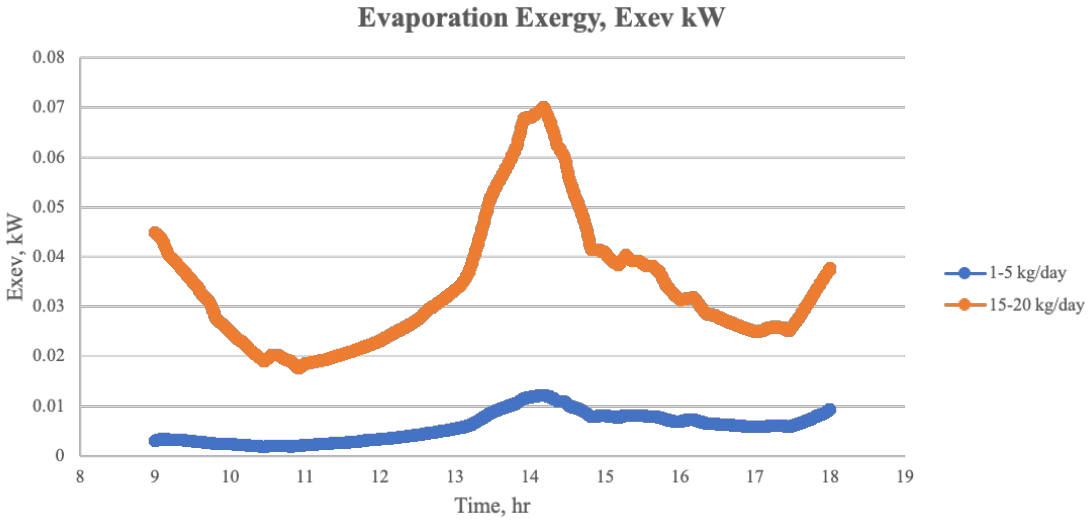

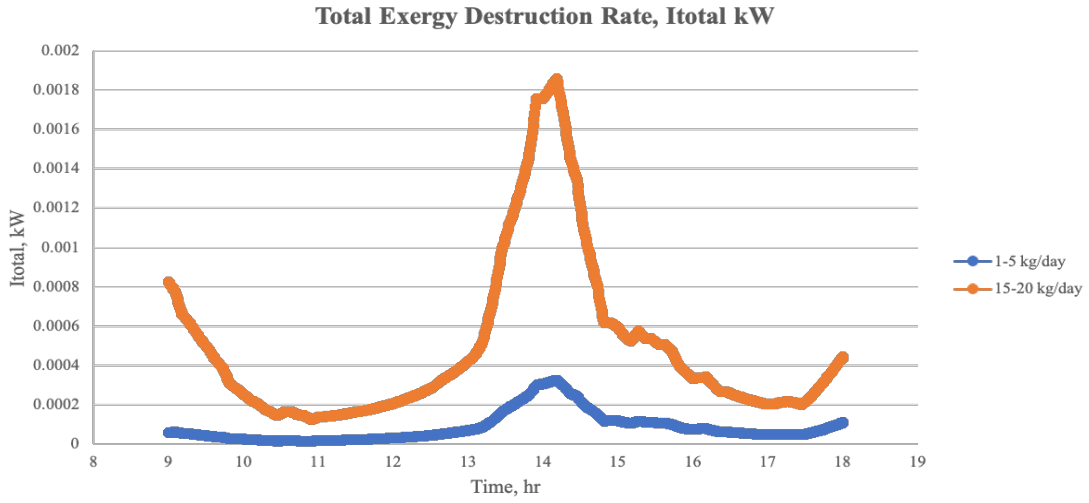

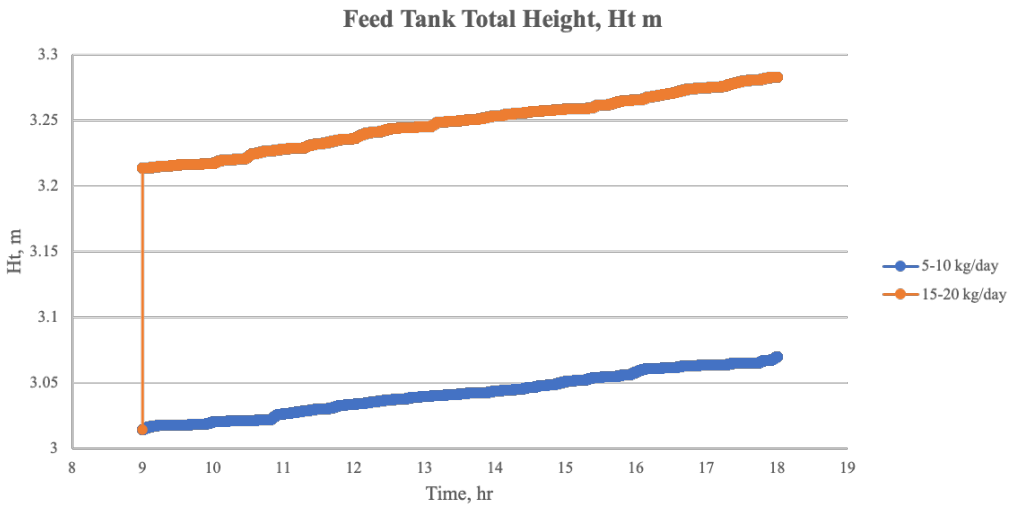
Feed Tank Total Height, Ht m
Ht, m
3.3
3.25
3.2
3.15
3.1
3.05
3
8
9
10
11
12
13
14
15
16
17
18
19
Time, hr
5-10 kg/day
15-20 kg/day

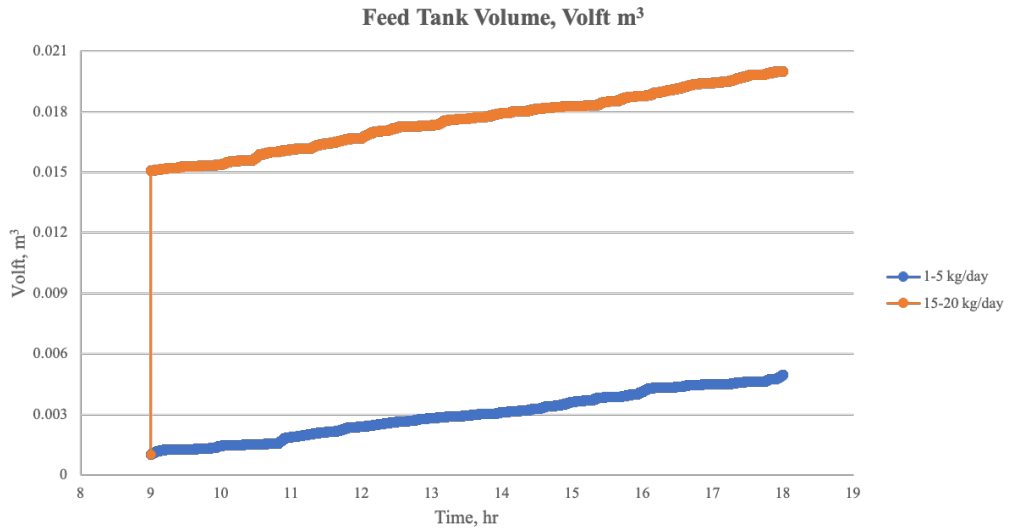
Feed Tank Volume, Volft m3
Volft, m3
0.021
0.018
0.015
0.012
0.009
0.006
0.003
0
8
9
10
11
12
13
14
15
16
17
18
19
Time, hr
1-5 kg/day
15-20 kg/day

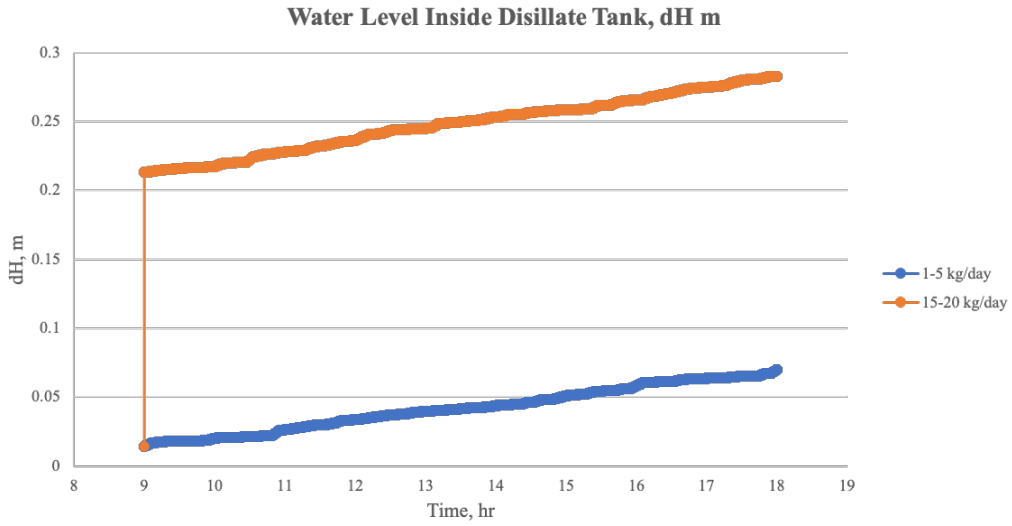
Water Level Inside Disillate Tank, dH m
dH, m
0.3
0.25
0.2
0.15
0.1
0.05
0
8
9
10
11
12
13
14
15
16
17
18
19
Time, hr
1-5 kg/day
15-20 kg/day

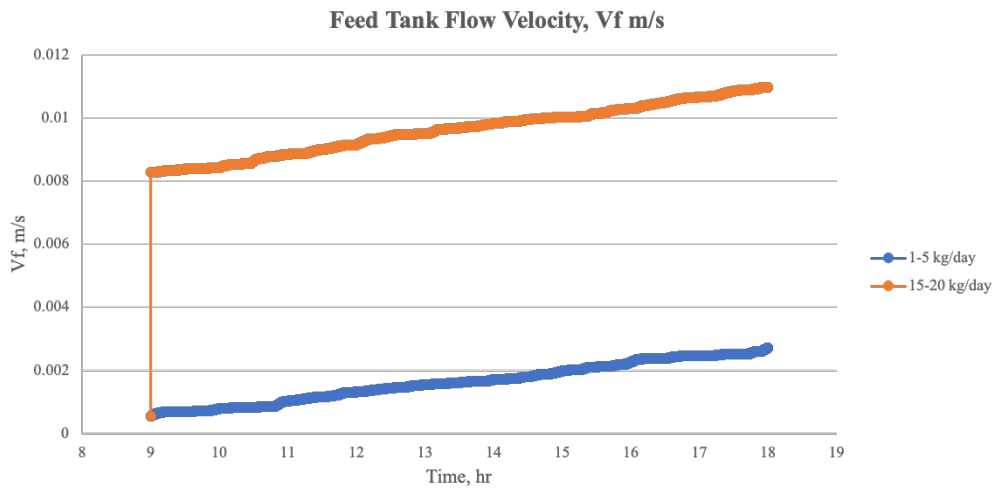
Feed Tank Flow Velocity, Vf m/s
Vf, m/s
0.012
0.01
0.008
0.006
0.004
0.002
0
8 9 10 11 12 13 14 15 16 17 18 19
Time, hr
1-5 kg/day
15-20 kg/day

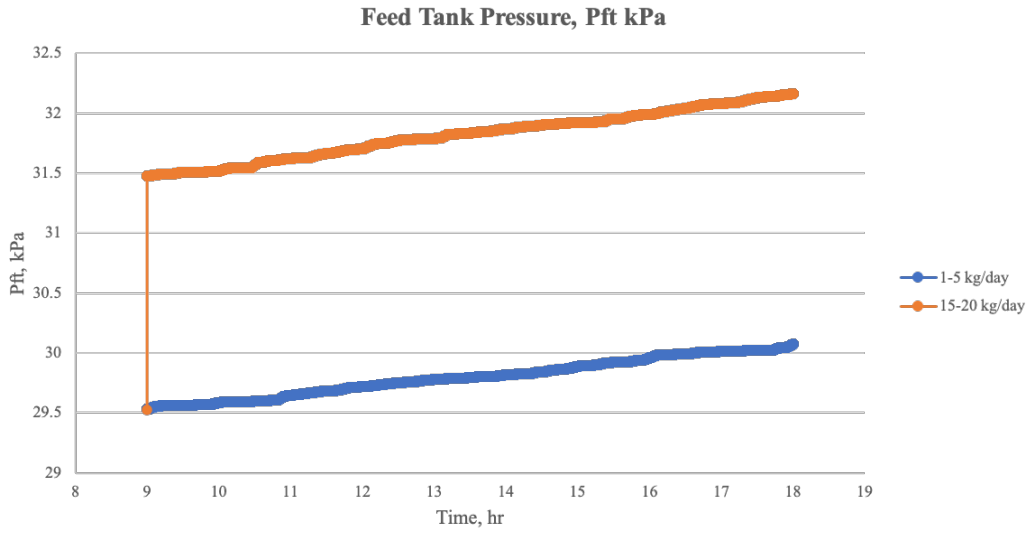
Feed Tank Pressure, Pft kPa
Pft, kPa
32.5
32
31.5
31
30.5
30
29.5
29
8 9 10 11 12 13 14 15 16 17 18 19
Time, hr
1-5 kg/day
15-20 kg/day

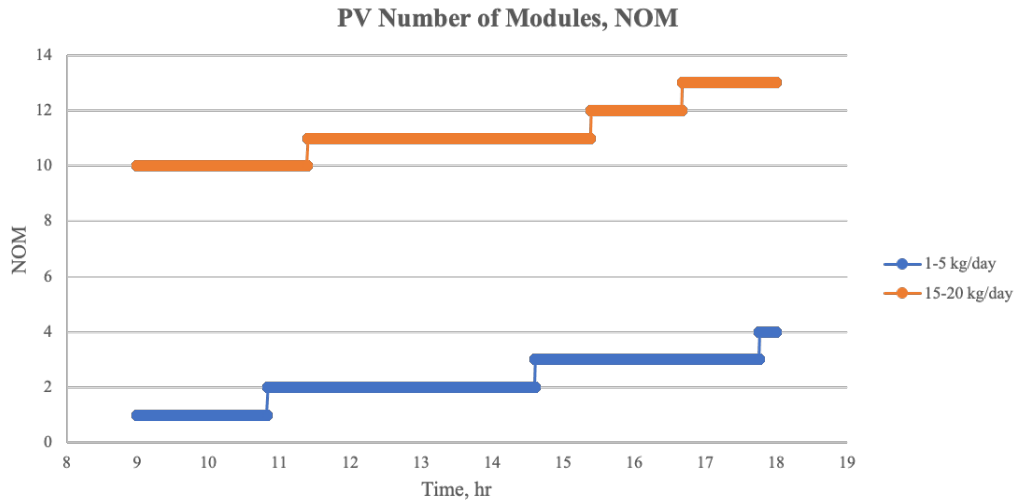
PV Number of Modules, NOM
NOM
14
12
10
8
6
4
2
0
8 9 10 11 12 13 14 15 16 17 18 19
Time, hr
1-5 kg/day
15-20 kg/day

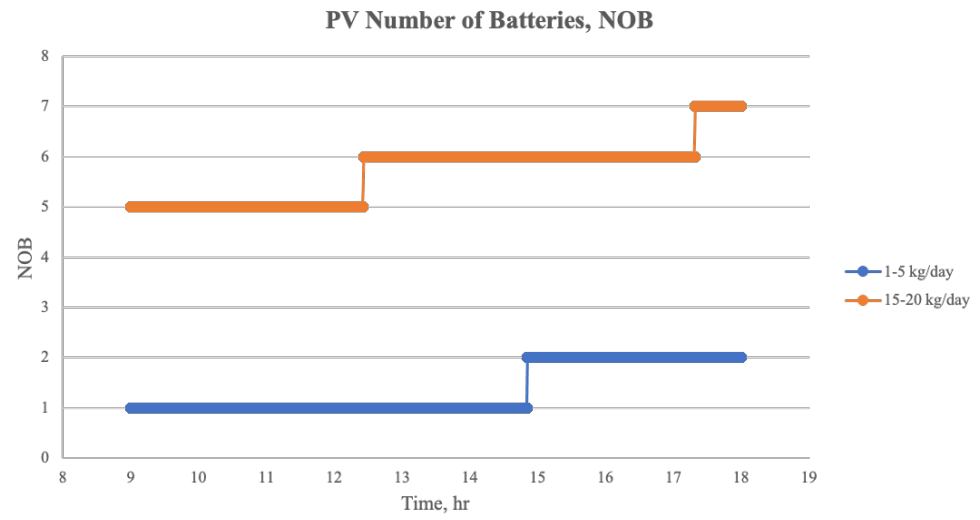
PV Number of Batteries, NOB
NOB
Time, hr
1-5 kg/day
15-20 kg/day

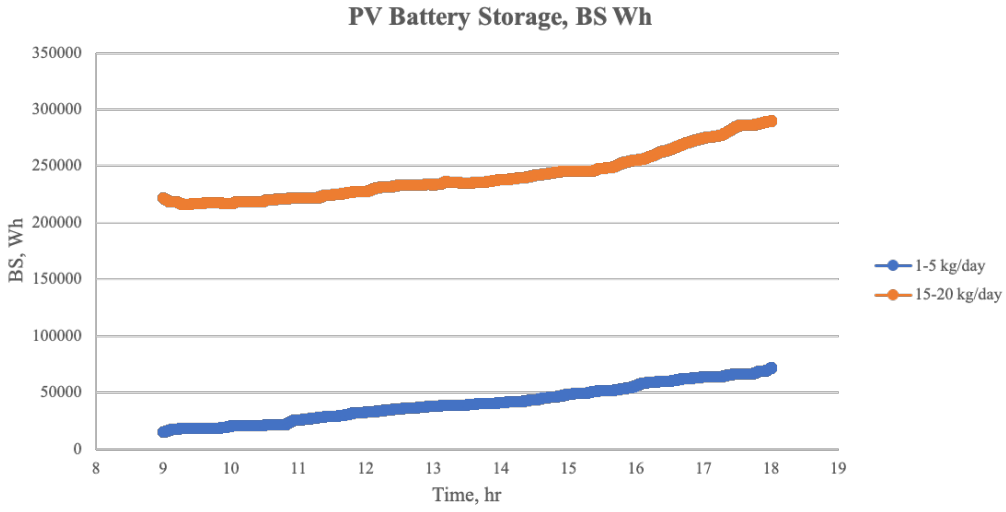
PV Battery Storage, BS Wh
BS, Wh
Time, hr
1-5 kg/day
15-20 kg/day

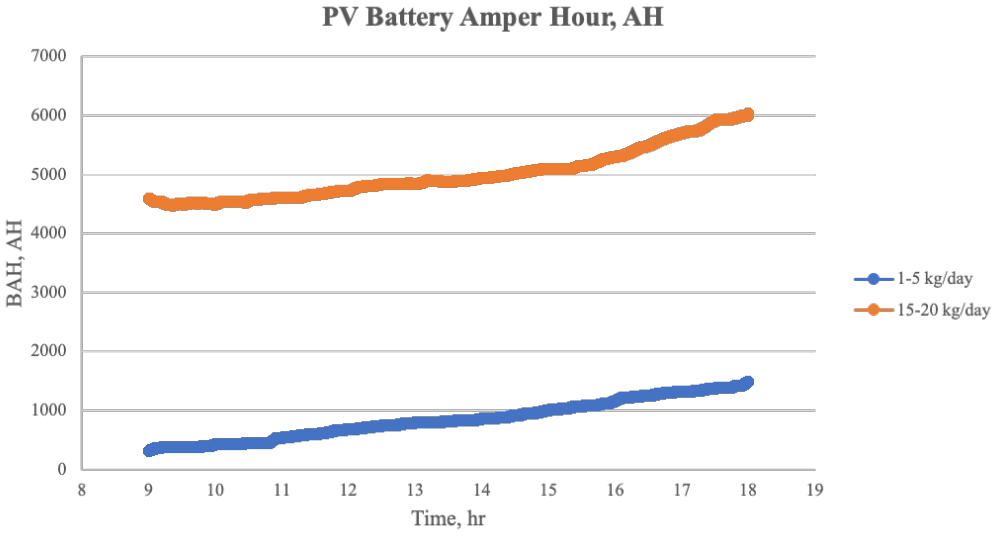
PV Battery Amper Hour, AH
BAH, AH
Time, hr
1-5 kg/day
15-20 kg/day

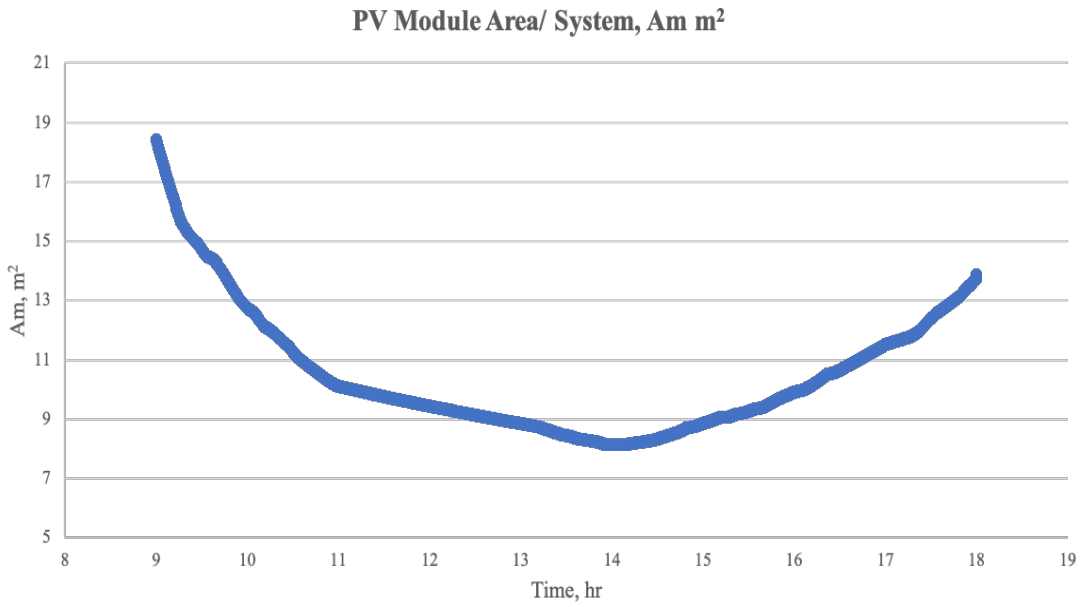
PV Module Area/ System, Am m²
Am, m²
21
19
17
15
13
11
9
7
5
8
9
10
11
12
13
14
15
16
17
18
19
Time, hr

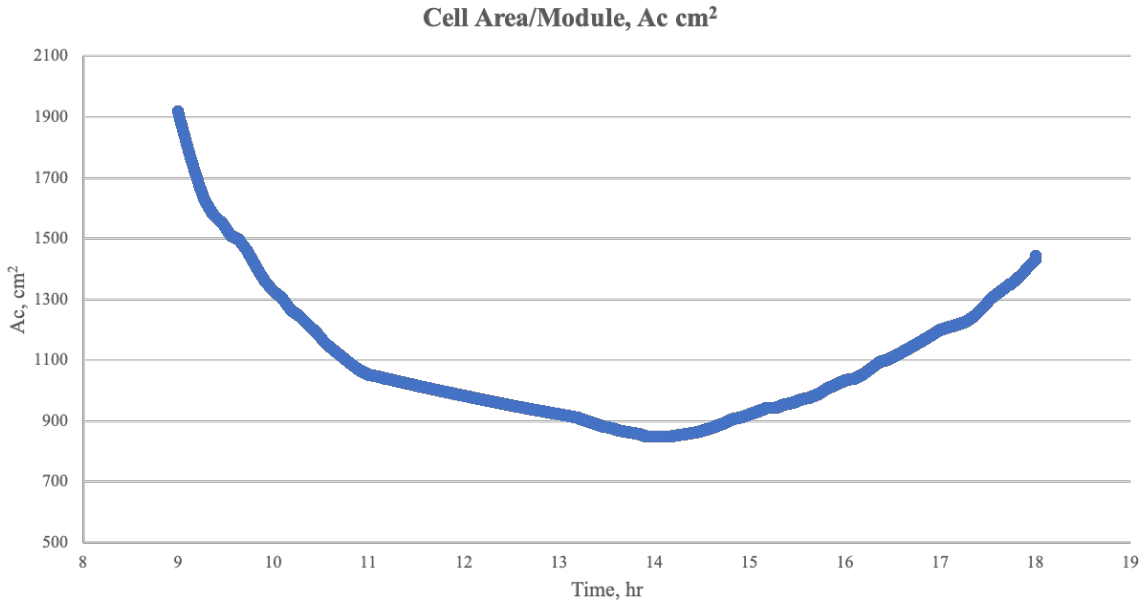
Cell Area/Module, Ac cm²
Ac, cm²
2100
1900
1700
1500
1300
1100
900
700
500
8
9
10
11
12
13
14
15
16
17
18
19
Time, hr

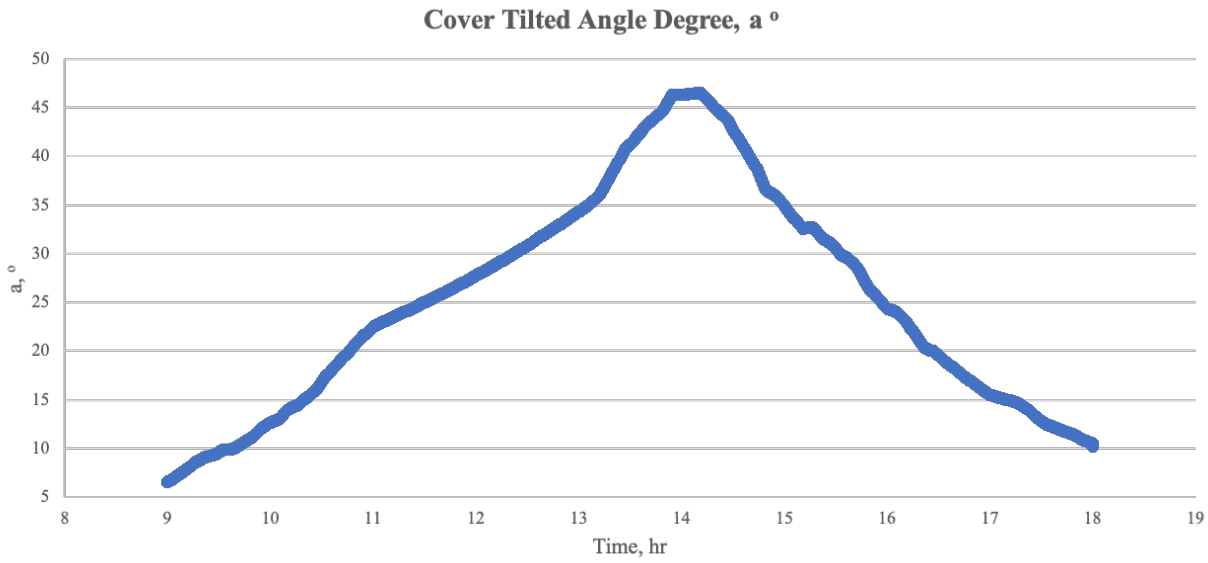
Cover Tilted Angle Degree, a º
50
45
40
35
30
25
20
15
10
5
a, º
8
9
10
11
12
13
14
15
16
17
18
19
Time, hr

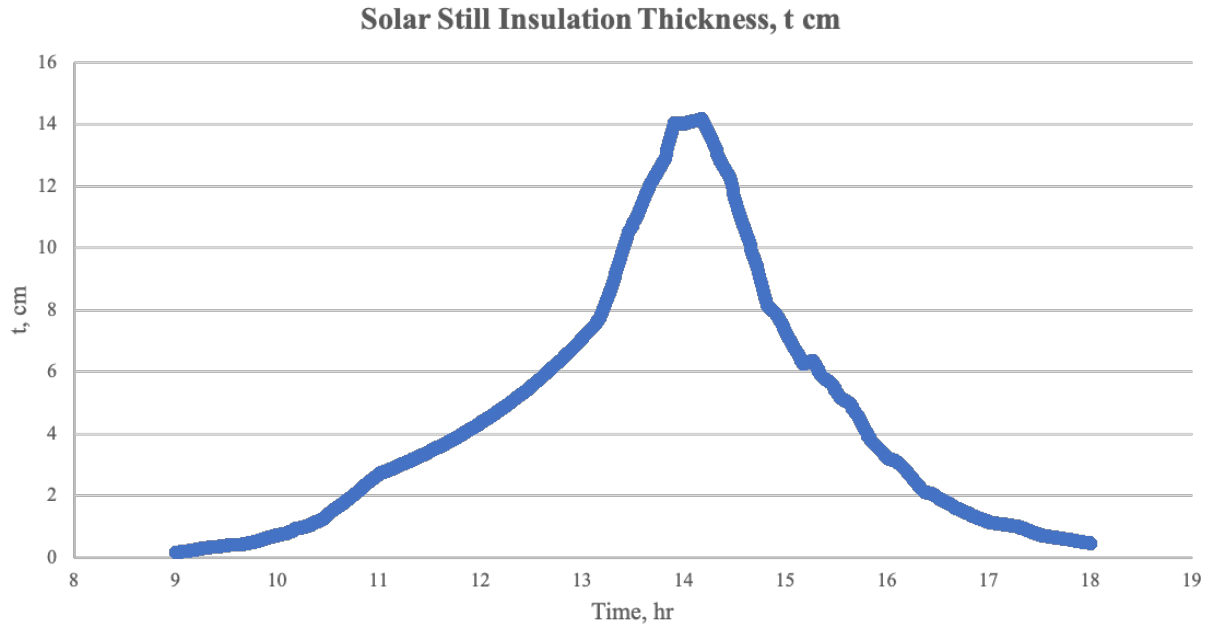
Solar Still Insulation Thickness, t cm
16
14
12
10
8
6
4
2
0
t, cm
8
9
10
11
12
13
14
15
16
17
18
19
Time, hr